"IMMOBILIZATION OF HORSERADISH PEROXIDASE ENZYME ONTO POLYMERIC MICROBEADS AND ITS USAGE IN DYE DECOLORIZATION"

Altynay ZHUMABEKOVA

T.C.
BURSA ULUDAĞ UNIVERSITY
GRADUATE SCHOOL OF NATURAL AND APPLIED SCIENCES

IMMOBILIZATION OF HORSERADISH PEROXIDASE ENZYME ONTO POLYMERIC MICROBEADS AND ITS USAGE IN DYE DECOLORIZATION

Altynay ZHUMABEKOVA
0009-0006-4332-8868

Prof. Dr. Bilgen OSMAN
(Supervisor)

MSc THESIS
DEPARTMENT OF CHEMISTRY

THESIS APPROVAL

This thesis titled "IMMOBILIZATION OF HORSERADISH PEROXIDASE ENZYME ONTO POLYMERIC MICROBEADS AND ITS USAGE IN DYE DECOLORIZATION" and prepared by Altynay ZHUMABEKOVA has been accepted as an **MSc THESIS** in Bursa Uludağ University Graduate School of Natural and Applied Sciences, Department of Chemistry following a unanimous vote of the jury below.

Supervisor: Prof. Dr. Bilgen OSMAN

Head: Prof. Dr. Asım OLGUN   Signature
0000-0002-0657-334X
Bursa Uludag University,
Faculty of Arts and Sciences,
Department of Chemistry

Member: Prof. Dr. Bilgen Osman   Signature
0000-0001-8406-149X
Bursa Uludag University,
Faculty of Arts and Sciences,
Department of Chemistry

Member: Assoc. Prof. Dr. Emel Tamahkar Irmak   Signature
0000-0002-5913-8333
Bursa Technical University,
Faculty of Engineering and Natural Sciences,
Department of Bioengineering

I approve the above result

Prof. Dr. Hüseyin Aksel EREN
Institute Director
../../….

I declare that this thesis has been written in accordance with the following thesis writing rules of the U.U Graduate School of Natural and Applied Sciences;

- All the information and documents in the thesis are based on academic rules;
- Audio, visual and written information and results are in accordance with scientific code of ethics;
- In the case that the works of others are used, I have provided attribution in accordance with the scientific norms;
- I have included all attributed sources as references;
- I have not tampered with the data used;
- I do not present any part of this thesis as another thesis work at this university or any other university.

08/06/2023
Altynay ZHUMABEKOVA

TEZ YAYINLANMA
FİKRİ MÜLKİYET HAKLARI BEYANI

Enstitü tarafından onaylanan lisansüstü tezin/raporun tamamını veya herhangi bir kısmını, basılı (kâğıt) ve elektronik formatta arşivleme ve aşağıda verilen koşullarla kullanıma açma izni Bursa Uludağ Üniversitesi'ne aittir. Bu izinle Üniversiteye verilen kullanım hakları dışındaki tüm fikri mülkiyet hakları ile tezin tamamının ya da bir bölümünün gelecekteki çalışmalarda (makale, kitap, lisans ve patent vb.) kullanım hakları tarafımıza ait olacaktır. Tezde yer alan telif hakkı bulunan ve sahiplerinden yazılı izin alınarak kullanılması zorunlu metinlerin yazılı izin alınarak kullandığını ve istenildiğinde suretlerini Üniversiteye teslim etmeyi taahhüt ederiz.

Yükseköğretim Kurulu tarafından yayınlanan "**Lisansüstü Tezlerin Elektronik Ortamda Toplanması, Düzenlenmesi ve Erişime Açılmasına İlişkin Yönerge**" kapsamında, yönerge tarafından belirtilen kısıtlamalar olmadığı takdirde tezin YÖK Ulusal Tez Merkezi / B.U.Ü. Kütüphanesi Açık Erişim Sistemi ve üye olunan diğer veri tabanlarının (Proquest veri tabanı gibi) erişimine açılması uygundur.

Prof. Dr. Bilgen Osman   Altynay Zhumabekova
08/06/2023   08/06/2023

İmza   İmza
Bu bölüme kişinin kendi el yazısı ile okudum   Bu bölüme kişinin kendi el yazısı ile okudum
anladım yazmalı ve imzalanmalıdır.   anladım yazmalı ve imzalanmalıdır.

ÖZET

Yüksek Lisans Tezi

YABANTURPU PEROKSİDAZ ENZİMİNİN POLİMERİK MİKROKÜRELERE İMMOBİLİZASYONU VE BOYA GİDERİMİNDE KULLANIMI

Altynay ZHUMABEKOVA

Bursa Uludağ Üniversitesi
Fen Bilimleri Enstitüsü
Kimya Anabilim Dalı

Danışman: Prof. Dr. Bilgen OSMAN

Bu çalışmada, yaban turpu peroksidaz (HRP) enzimi poli(etilen glikol dimetakrilat-N-metakriloil-amido-L-triptofan-metil ester) [PEDMT] mikroküreler üzerine adsorpsiyon yöntemi ile immobilize edilerek Kongo kırmızısı (CR) ve Reaktif Siyah 5 (RB5) boyalarının renk gideriminde kullanıldı. Sentezlenen mikroküreler Brunauer-Emmett-Teller (BET) analizi, Fourier Dönüşüm kızılötesi spektroskopisi (FTIR) ve taramalı elektron mikroskobu-enerji dağılımlı X-ışını (SEM/EDX) analizi ile karakterize edildi. İmmobilizasyon verimi, aktivite verimi ve immobilizasyon etkinliği parametreleri sırasıyla %84.86 ± 2.06, %73.78 ± 5.91 ve %86.95 ± 6.92 olarak belirlendi. Serbest ve immobilize enzimlerin göreceli aktiviteleri karşılaştırıldı ve optimum reaksiyon koşulları pH 6.0, %3 H_2O_2 derişimi ve immobilize HRP (PEDMT-HRP) için 50 °C, serbest HRP için 40 °C sıcaklık olarak belirlendi. Metal iyonlarının ve organik çözücülerin enzim aktivitesi üzerindeki etkileri araştırıldı. Serbest HRP ve PEDMT-HRP'nin termal stabilitesi ve depolama stabilitesi incelendi. PEDMT-HRP, aktivitesini %55 oranında koruyarak on kez tekrar kullanıldı. Serbest HRP ve PEDMT-HRP ile renk giderme çalışmaları yapıldı. pH, boya derişimi, mikroküre miktarı ve enzim derişimi, H_2O_2 derişimi ve temas süresinin CR ve RB5'in renk giderimi üzerindeki etkileri belirlendi. Serbest HRP ve PEDMT-HRP ile pH 6.0, 25 mg/L boya derişimi, %3 H_2O_2 derişimi ile 2 saatte en iyi renk giderim değerleri elde edildi. PEDMT-HRP'nin renk giderimindeki tekrar kullanılabilirliği araştırıldı. PEDMT-HRP, CR ile on döngüden sonra aktivitesinin %44'ünü ve RB5 ile beş döngüden sonra %17'sini koruyabildi. Renk giderimi HPLC analizi ile takip edildi. Elde edilen sonuçlar, PEDMT-HRP'nin iki boyanın rengini aynı anda %94 (CR) ve %29 (RB) oranında, serbest enzimin ise %4,5 oranında giderdiğini gösterdi.

Anahtar Kelimeler: Yaban turpu peroksidazı, enzim immobilzasyonu, boya renk giderimi, polimerik mikroküre

2023, IX + 99 sayfa.

ABSTRACT

MSc Thesis

IMMOBILIZATION OF HORSERADISH PEROXIDASE ENZYME ONTO POLYMERIC MICROBEADS AND ITS USAGE IN DYE DECOLORIZATION

Altynay ZHUMABEKOVA

Bursa Uludag University
Graduate School of Natural and Applied Sciences
Department of Chemistry

Supervisor: Prof. Dr. Bilgen OSMAN

In this study, horseradish peroxidase (HRP) enzyme was immobilized onto poly(ethylene glycol dimethacrylate-N-methacryloyl-amido-L-tryptophan methyl ester) [PEDMT] microbeads by adsorption method and used in decolorization of Congo red (CR) and Reactive Black 5 (RB5) dyes. The microbeads were characterized by Brunauer–Emmett–Teller (BET) analysis, Fourier Transform infrared spectroscopy (FTIR), and scanning electron microscopy with energy dispersive X-ray analysis (SEM/EDX). Immobilization yield, activity yield, and immobilization efficiency were determined and had a value of $84.86 \pm 2.06\%$, $73.78 \pm 5.91\%$, and $86.95 \pm 6.92\%$, respectively. Relative activities of free and immobilized enzymes were compared, and optimum reaction conditions were determined as pH 6.0, 3% H_2O_2 concentration, and temperature of 50 °C for PEDMT-HRP and 40 °C for free HRP. The effect of metal ions and organic solvents, thermal and storage stability of enzymes were estimated. Also, it was possible to reuse PEDMT-HRP for ten cycles with 55% of the remaining activity. The decolorization studies were performed and the effects of pH, microbeads amount and enzyme concentration, H_2O_2 and dye concentration, and contact time were indicated. The best decolorization was obtained at pH 6.0, 25 mg/L dye concentration, 3% H_2O_2 concentration, and 2 h of contact time for both enzymes. PEDMT-HRP preserved 44% of activity after the ten cycles with CR and 17% after the five cycles with RB5. Moreover, decolorization was followed via HPLC analysis. The results revealed that PEDMT-HRP could simultaneously decolorize both dyes with 94% (CR) and 29% (RB) efficiency, but the free enzyme displayed 4.5% decolorization.

Keywords: Horseradish peroxidase, enzyme immobilization, dye decolorization, polymeric microbeads

2023, IX + 99 pages.

PREFACE AND/OR ACKNOWLEDGMENT

CONTENTS

SYMBOLS and ABBREVIATIONS

Symbols	Definition
A_i	Activity of immobilized HRP
A_f	Activity of free HRP
C_i	Enzyme's initial concentration
C_s	Enzyme's total concentration in supernatant and washing solutions
Km	Michaelis constant
$[S]$	Concentration of substrate
$Vmax$	Maximum velocity
V_o	Initial velocity

Abbreviations	Definition
AIBN	Azobisisobutyronitrile
BET	Brunauer–Emmett–Teller
CR	Congo Red
DDE	Diethylene glycol diglycidyl ether
EDTA	Ethylene diamine tetraacetate
EGDMA	Ethylene glycol dimethacrylate
FTIR	Fourier Transform infrared spectroscopy
GA	Glutaraldehyde
HPLC	High-performance liquid chromatography
HRP	Horseradish peroxidase
MATrp	N-methacryloyl-amido-L-tryptophan methyl ester
MO	Methyl Orange
PEDMT	Poly(ethylene glycol dimethacrylate-N-methacryloyl-amido-L-tryptophan methyl ester)
PEDMT-HRP	HRP immobilized on PEDMT
PVA	Polyvinyl alcohol
RB5	Reactive Black 5
SEM-EDX	Scanning Electron Microscopy with Energy Dispersive X-Ray

FIGURES

vii

TABLES

1. INTRODUCTION

The rapid increase in population and industrial development has been a big concern in the last century because it causes water pollution. The large amount of hazardous industrial effluent is discharge into natural water reservoirs without appropriate treatment. Synthetic dyes and phenolic compounds are toxic, carcinogenic, mutagenic, and non-biodegradable wastes of pharmaceutical, textile, plastic and food industries that play an essential role in pollution of the environment (Zare et al., 2015; Husain et al., 2011). Dyes are complex aromatic compounds used for coloring purposes. They negatively affect the photosynthetic function of aquatic life and turn into poisonous products when they are released into the environment (Cano et al., 2017). According to chromophore groups, synthetic dyes can be categorized as azo, heterocyclic, anthraquinone, triphenylmethane, or phthalocyanine dyes. Among them, azo dyes are known to be non-degradable, very stable, and resistant to microbial attacks. Therefore, removing them from wastewater by conventional biological processes is difficult. Different physicochemical methods, such as coagulation, adsorption, ozonation, photocatalysis, membrane treatment, and precipitation were investigated to eliminate toxins and dyes from wastewater. However, expensiveness limits applications of these methods (Faryadi et al., 2016).

In recent years, enzymatic methods have attracted significant attention. Enzymes are green biocatalysts with a high potential in various fields, including industrial and biotechnological applications (Wu et al., 2012). Enzymatic treatment is more cost-effective and efficient than conventional treatment due to its environmental friendliness, biodegradability, ability to perform in mild conditions, high specificity and selectivity, remarkable efficiency, and no toxic by-products during wastewater treatment (Bilal et al., 2017a). Among the different enzymes applied for decolorizing and degrading dyes, peroxidases are promising candidates for industrial wastewater treatment due to their stability, low cost, and tolerance to wide temperature and pH ranges (Lai et al., 2005). They can convert harmful compounds into harmless and environmentally safe products under mild reaction conditions. Peroxidases can oxidize many aromatic pollutants such as dyes, phenols, anilines, xenobiotics, and heavy metals (Patel and Day, 1999). Also, peroxidases are used as antioxidants, indicators in the food industry, in the synthesis of

conductive materials and bioelectrodes, in polymer synthesis, paper, and pulp industry, in biosensor development, and in diagnostic kits (Valderrama et al., 2002).

Horseradish peroxidase (HRP; EC 1.11.1.7) is receiving significant attention as a result of its easy availability, broad substrate specificity, and high inhibition resistance over a wide concentration range (Kawakita et al., 2012). HRP is one of the important peroxidase enzymes used in various applications such as biosensors, food processing, immunoassay, dye removal, and bioremediation of environmental pollutants. It catalyzes the oxidation reaction of different substrates by degrading hydrogen peroxide (H_2O_2) (Onder et al., 2011). However, HRP has disadvantages that limit its techno-commercial application, such as deactivation in extreme pH or temperature values, expensive cost, and reusability problem. The enzyme immobilization process can overcome these disadvantages and improve enzyme's properties and application potentials. The support material to be used in enzyme immobilization should be nonpoisonous and prevent denaturation without disrupting the natural conformation of the enzyme (Vineh et al., 2018).

The thesis aimed to immobilize HRP enzyme on poly(ethylene glycol dimethacrylate-N-methacryloyl-amido-L-tryptophan methyl ester) [PEDMT] microbeads by adsorption and use them for decolorization of Congo red (CR) and Reactive Black 5 (RB5) dyes. In the synthesis of microbeads, ethylene glycol dimethacrylate (EGDMA) was used as a crosslinker, and N-methacryloyl-amido-L-tryptophan methyl ester (MATrp) as a monomer. The efficiency of the free and immobilized enzymes was compared by investigating the parameters affecting the immobilization. The effects of pH, temperature, substrate concentration, metal ion, organic solvent, and H_2O_2 concentration on the enzyme activity and the thermal and storage stability of the free and immobilized enzyme were determined. Then, the effects of pH, dye concentration, microbeads amount and enzyme concentration, H_2O_2 concentration, and contact time on the decolorization of CR and RB5 were investigated. In addition, the reusability of the immobilized HRP in dye decolorization was tested.

2. THEORETICAL BASICS and LITERATURE REVIEW

2.1. Horseradish Peroxidase

Plant peroxidases are frequently encountered in research on the biodegradation of manufactural waste. They are divided into three subclasses according to their source and structure. The first peroxidase class is intracellular; cytochrome c, ascorbate, and bacterial catalase peroxidases belong to this group. The second class is extracellular secretory fungi; lignin and manganese peroxidases relate to this class. And third class is secretory plant peroxidases, consisting of peroxidases like bitter gourd peroxidase, turnip peroxidase, and HRP (Jun et al., 2019; Sharma et al., 2018; El-Nahass et al., 2018).

Horseradish (*Armocia rusticana*) is a resistant perennial herb grown mainly in warm regions of the world, especially in some parts of Europe and Asia, as well as in the north-temperate regions of North America due to the nutritional value of its roots (Figure 2.1). The thick yellow fleshy root of *Armoracia rusticana* with a spicy taste has antibiotic and anti-inflammatory properties. Also, it contains calcium, magnesium, sodium, and vitamin C (Sarika et al., 2015). In 1810, Louis Antoine Planche observed that soaking a horseradish root in a tincture of guaiacum resin caused an intense color change. Presumptively, the peroxidase enzyme has oxidized 2,5-di-(4-hydroxy-3-methoxyphenyl)-3,4-dimethylfuran, a compound in resin and produced the blue product, bis-methylenequinone. Since then, HRP has become a valuable tool in biotechnology (Veitch, 2004).

Figure 2.1. Horseradish (*Armoracia rusticana*) (Sarika et al., 2015)

HRP is one type of oxidoreductase peroxidase enzyme that is applied in the treatment of azo dyes, anilines, phenols, and other organic aromatic compounds (Jin et al., 2018; Bayramoglu et al., 2012). HRP can be isolated from various microorganisms, plants, and animals. Its primary source is horseradish plant root (it enables this plant to grow and develop) (Mohan et al., 2005). It is generally extracted as a combination of acidic (A), neutral (C), and basic (E) isoenzymes, but the most prevalent and explored form is isoenzyme C (Wang et al., 2020; Janović et al., 2017; Shakerian et al., 2020). The isoenzyme C HRP exhibits the best degradation activity at pH 7 and 25-40 °C temperature (Shakerian et al., 2020).

A group of researchers revealed the crystal structure of HRP by X-ray in 1997 (Gajhede et al., 1997). There are three α-helical and one β-plated structure in its three-dimensional structure (Figure 2.2) (Gajhede et al., 1997; Veitch, 2004; Zhu et al., 2015). HRP is a glycoprotein metalloenzyme with 18% N-linked oligosaccharides and a molecular weight of approximately 40.000 Da or 44 kDa (Yapaoz and Attar, 2020; Varamini et al., 2021). The HRP's overall carbohydrate amount varies from 18 to 22% based on its origin. It contains four disulfide bridges, 308 amino acids, ferroporphyrin, and two seven-coordinate calcium atoms, stabilizing its structure and property (Jankowska et al., 2021; Wang et al., 2020). One calcium atom is located in the distal (near) region, while another is in the proximal (far) region. The disulfide bridges are placed among 11–91, 44–49, 97–301, and 177–209 cysteine residues; also, there is a hidden salt bridge in the middle of Arg 123 and Asp 99. In the center of the protoporphyrin IX, a heme-cofactor is located being HRP's active site; therefore, HRP belongs to the heme peroxidases group (Figure 2.3) (Hollmann et al., 2004). The heme complex consists of 4 porphyrin rings, pyrrole, iron, and histidine group (His170), and it is bound to the enzyme from the proximal histidine side via the coordinate bond. And histidine itself is also connected with iron through the covalent coordinate bond. Heme's distal side is vacant in the resting condition and ready for H_2O_2 to link (Veitch and Smith, 2000). However, some molecules/ions like CO, CN^-, F^-, and N^{3-} can also bond to the heme and form a six-coordinate complex. Moreover, HRP has six lysine residues that conjugate to target substrates or solid supports (Bayramoglu et al., 2021). HRP enzyme gives maximum absorbance at 403 nm other than 280 nm (Fraguas et al., 2004).
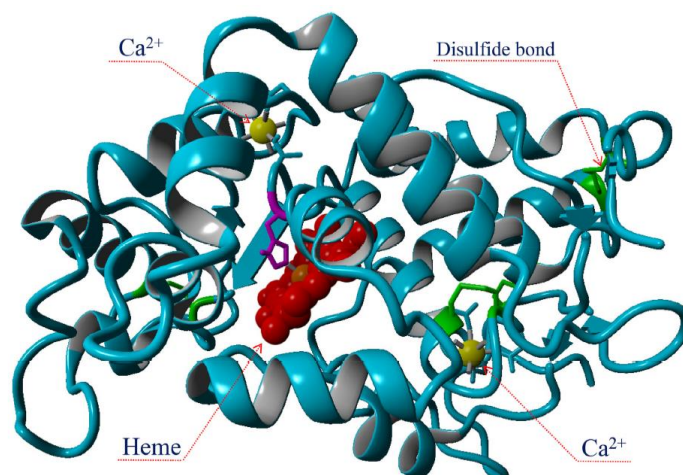
Figure 2.2. X-ray crystal structure of the HRP C isoenzyme (Zhu et al., 2015)
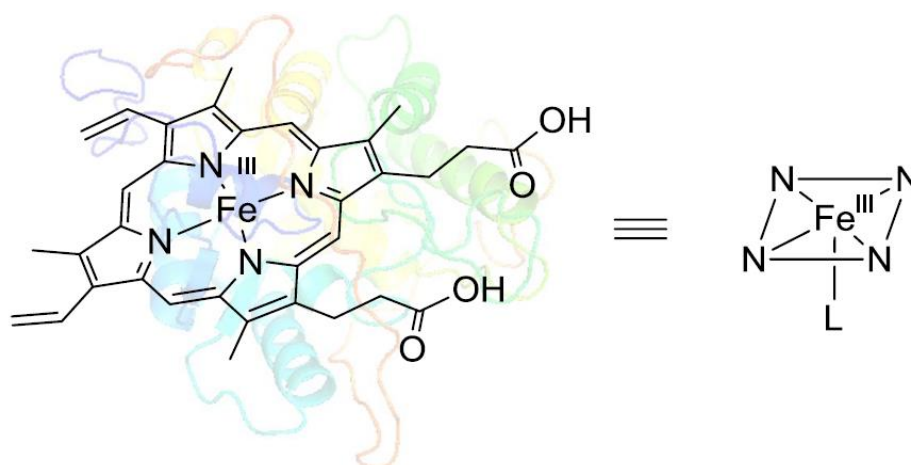
Figure 2.3. Structure of heme complex (Hollmann et al., 2004)

HRP, like other peroxidases, reduces H_2O_2 in its catalytic degradation processes (Bilal et al., 2016). To start reacting with pollutants, HRP must be oxidized and transformed into an active catalytic structure by H_2O_2. However, studies showed that excess H_2O_2 acts as an inhibitor and decreases HRP's activity (Wong et al., 2019). The enzymatic activity of HRP is due to the oxidation and reduction of the iron ion in the heme group. To be more detailed, the catalytic reaction has two stages. As can be seen in Figure 2.4, in the first stage, H_2O_2 replaces the water ligand. Heterolytic break of the oxygen O-O bond, allows H_2O_2 to react with the iron ion (Fe^{3+}) and form three products: H2O, Fe^{4+} oxoferryl center (compound I), and a positively charged radical based on porphyrin. In the second stage, the positively charged porphyrin radical undergoes one-electron reduction or one-electron transfer reaction with chosen substrate: Fe^{4+} oxoferryl species (so-called compound II),

and the first radical of the substrate is obtained. Consecutive compound II undergoes a reduction reaction with the substrate and returns to the initial form of the enzyme (Fe^{3+}); here, the second radical of the substrate is obtained. The obtained free-radical compounds of the substrate tend to polymerize, which is an advantage of the process. Because it is easier to remove polymers from wastewater as they are insoluble in the aqueous phase (Wong et al., 2019; Preethi et al., 2013; El-Nahass et al., 2018; Al-Maqdi et al., 2021; Hollmann et al., 2004). These radical species may also turn into dimers, trimers, or oligomers, which reduce substrates in the following reactions (Veitch, 2004). So, HRP converts toxic compounds into more harmless products or makes them more suitable for further treatment (Šekuljica et al., 2016a). Namely, it is compound II that plays a prominent role in the decontamination of the pollutant. Compound I and II are strong oxidants that probably have +1 V redox potentials. The oxidation reaction of HRP with aromatic compound (AH$_2$) in the attendance of H$_2$O$_2$ is $H_2O_2 + 2AH_2 \xrightarrow[\cdot]{HRP} > 2H_2O + 2AH^{\cdot}$ (Veitch, 2004).
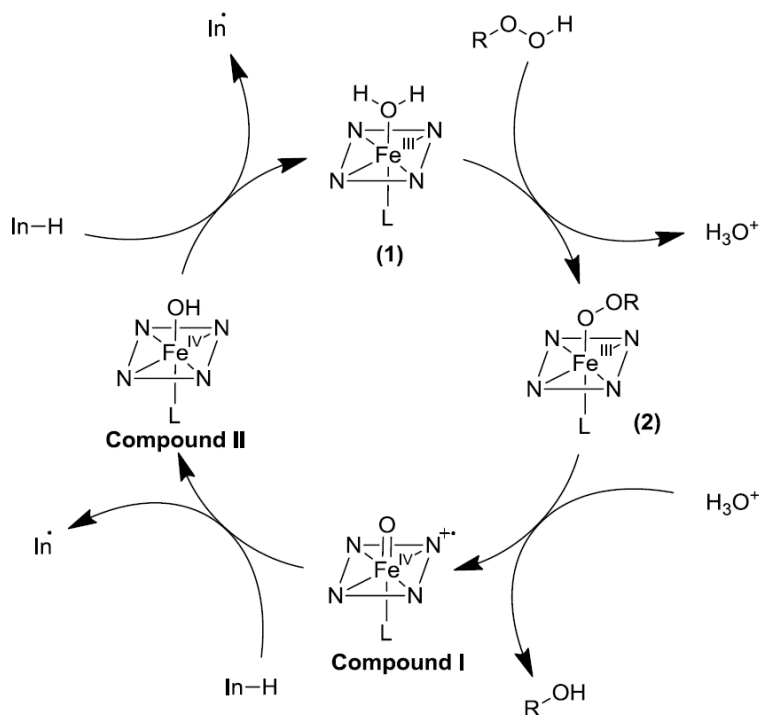
Figure 2.4. Catalytic mechanism of HRP oxidation reaction (Hollmann et al., 2004)

HRP's main task is not to obtain water from peroxide: it is about getting radical products because the production of free radicals makes it possible to form dityrosine and diferulate

linkages, to synthesize lignin and suberin by cross-linking reactions (Kawaoka, et al., 1994). HRP can oxidate indoles, aromatic phenols (i.e., pyrogallol and bisphenols), phenolic acids, and non-aromatic amines (i.e., 4-aminoantipyrine) (Zdarta et al., 2018). It is widely used in biochemistry as it can intensify weak signals so that labeled particles can easily be detected. It is also broadly used in analytics, biotransformation, biosensors, immunoassays, chemiluminescent analysis, organic and polymer synthesis due to its broad substrate specificity, selectivity, affordable price, high activity in different pH and temperature, and extraction convenience (Bayramoglu et al., 2012; Gholami-Borujeni et al., 2011; Keshta et al., 2022). Lately, HRP has been used to decontaminate hazardous compounds such as pharmaceuticals, xenobiotics, dyes, etc. (Bilal et al., 2019a). In medicine and diagnostics, it is applicated to H_2O_2 detection (Šekuljica et al., 2016b). Another field of HRP is biomedical application. For example, in cancer treatment, cancerous cells are transfected into cDNA with HRP. Lately, research works with HRP are generally concerned with recombinant production and enzymatic characterization in various expression systems (Barnard, 2012).

2.2. Enzyme immobilization methods

Enzymes have attracted attention from different fields owing to its easy manufacture, substrate specificity, and sustainability. However, contamination of the final product, low stability, short shelf life, and high price complicate their use. In addition, since enzymes are highly soluble in water, separating them from the reaction medium and reusing them is difficult (Kotwal and Shankar, 2009). Enzyme immobilization is an effective solution for these problems (Lima-Ramos et al., 2014). The term "immobilized" means restricted or limited in movability. Immobilization can be applied to microbial cells, cellular organelles, enzymes, etc. Enzyme immobilization can be described as the binding or trapping of free liquid enzymes inside or on the surface of a solid carrier matrix, resulting in decreased mobility (Garcia-Galan et al., 2011). Chibata et al. (1967) reported the first industrial application of an immobilized enzyme where immobilization of aminoacylase (EC 3.5.1.14) isolated from *Aspergillus oryzae* was carried out. Immobilized enzymes are preferred in many fields, such as biodiesel production, biosensor, bioremediation, analytics, drug metabolism, pharmaceutical, cosmetics, food, and agriculture. Today's usages of immobilized enzymes include:

- Manufacture of important compounds by stereospecific or regiospecific biological transformations

- Energy generation with biological techniques

- Treatment of certain pollutants

- Continuous analysis of various compounds with high sensitivity and high specificity

- Medical applications including new drug types or artificial organs for enzyme therapy

An important products manufactured via immobilized enzymes are given below in Table 2.1.

Table 2.1. Products manufactured via immobilized enzymes (Brena and Batista-Viera, 2006; Krajewska, 2004)

Enzyme	Product
Penicillin acylase	Semi-synthetic penicillins
β-Galactosidase	Hydrolyzed lactose
Nitrile hydratase	Acrylamide
Glucose isomerase	High-fructose corn syrup
Lipase	Cocoa butter equivalents

Immobilization is especially profitable for the following situations:

- For expensive enzymes (such as penicillin acylase)

- For low molecular weight substrates (such as sugar and amino acids)

- For processes where microbial contaminations may occur. In this condition, a sterile substrate or a temperature higher than 60 °C will help

- In cases where the product must be completely enzyme-free (such as allergy-free diets)

Some usage areas of immobilized enzymes are summarized in Table 2.2.

Table 2.2. Some usage areas of immobilized-enzymes (Brena and Batista-Viera, 2006; Öztop et al., 2010; Krajewska, 2004)

Enzyme	Carrier Matrix	Usage Area
L-Asparaginase	Polyethylene glycol	Medicine and drug metabolism
Penicillin acylase	Polyacrylamide gel	Antibiotic production
Trypsin	Cellulose	Food industry
Lipase (Rhizopus)	Polyurethane	Biodiesel production
Acetylcholinesterase	Polyvinyl alcohol (PVA)	Biosensor
Lipase (C. rugosa)	Polypropylene membrane	Bioremediation

Immobilized enzymes have advantages and disadvantages over free (aqueous) enzymes (Çelebi et al., 2009). Some advantages are given below (Cowan and Fernandez-Lafuente, 2011; Sassolas et al., 2012):

- Product formation can be kept under control
- They are more stable and resistant to different external parameters such as pH, temperature, and denaturing organic solvents; therefore, enzyme activity can be maintained longer
- They are less costly than aqueous enzymes
- They reduce side effects in clinical applications

The disadvantages are:

- There is a loss in enzyme activity compared to free enzyme
- The amount of the enzyme consumed during its repeated use is limited
- The carrier materials are quite expensive

The essential privileges of immobilization are summarized in Table 2.3.

Table 2.3. Comparison of free and immobilized enzyme properties (Eş et al., 2015)

Free enzyme	Immobilized enzyme
It is difficult to remove them from the reaction environment due to product /enzyme/substrate mixture	They are easily separated from the environment by simple methods such as filtration and centrifugation
They may contaminate the products	If they are completely separated, there is no contamination in the products
They are more easily affected by environmental conditions; therefore, they are unstable	They are more resistant to environmental conditions and more stable
They are used once and for a short time	They can be reused many times and for a longer time
They can self-destruct	Self-destruction is reduced to a minimum

The immobilization methods can be grouped as physical and chemical methods in accordance with the type of interaction between enzyme and matrix (Figure 2.5). Examples of physical method are entrapment and adsorption, and examples of chemical method are covalent attachment and cross-linking. The difference is that in chemical method enzyme covalently bonds to the matrix, while in physical method covalent bond is not used. But in some situations, enzyme can be immobilized to the support via different interactions.
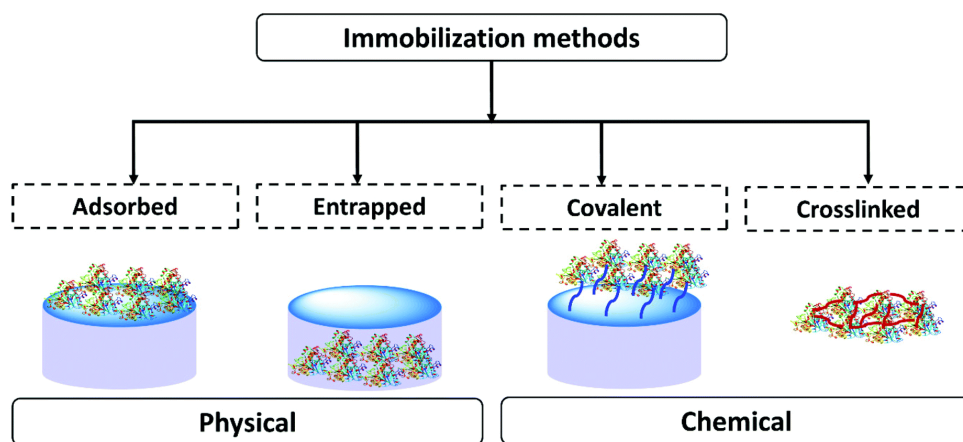
Figure 2.5. Classification of immobilization methods (Imam et al., 2021)

According to reversibility, immobilization techniques are divided into reversible and irreversible methods. Reversibly immobilized enzymes can be separated from the carrier under mild conditions due to the weaker enzyme-carrier bond. When the enzyme's activity decreases, the carrier can be regenerated and rebind with the fresh, unused enzyme. Adsorption belongs to the reversible method. In irreversible immobilization methods, if the enzyme is separated from a carrier, it loses biological activity. Common irreversible techniques are covalent bonding, entrapment, and cross-linking.

During the immobilization process, it must be considered whether the enzyme's activity to be applied is high or low and whether the carrier material to be used is suitable for the applied enzyme and immobilization technique (Figure 2.6). The thermal stability of the enzyme is affected by some factors. These factors include buffer conditions, disulfide bridges, and glycosylation. The critical control points to be considered during this process are the maximum temperature limit and the specified pH range. These factors ensure enzyme stability during the process (Barnard, 2012).
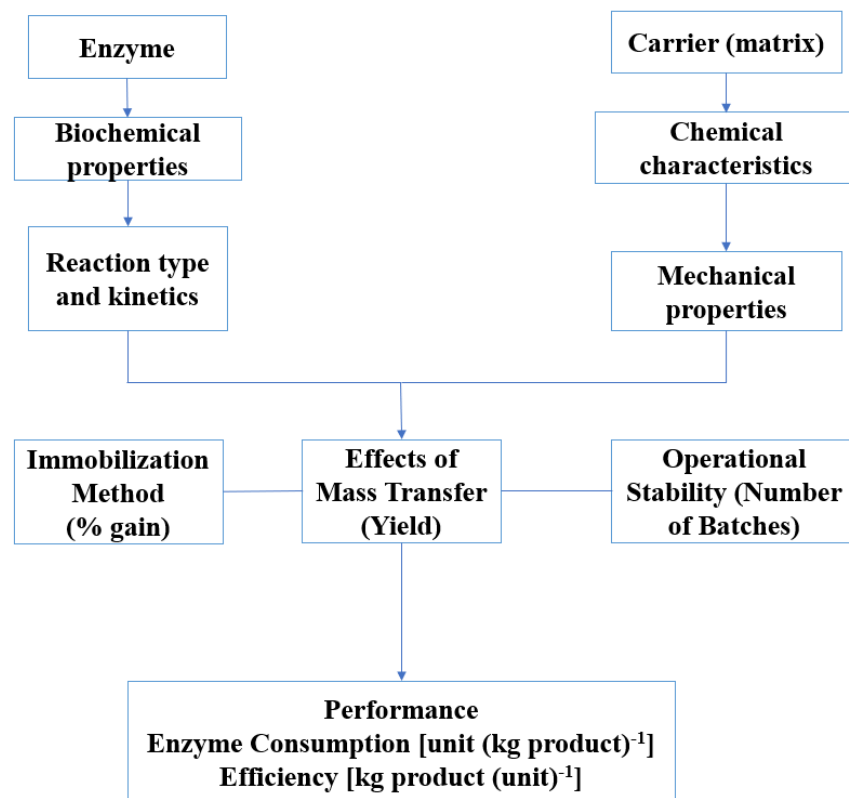
Figure 2.6. Properties of immobilized enzyme resulting from the interaction of enzyme and matrix (Uludağ, 2000)

Different factors can affect the immobilized enzyme's stability, including the chemical and physical structure of the matrix, the microenvironment of the enzyme, the interaction type between enzyme and matrix, the binding position and number of bonds, the flexibility of conformational change in the matrix, and the conditions under which the enzyme was immobilized. Choosing a suitable immobilization method is very important to prevent activity loss. The immobilization process shouldn't modify the active site's chemical structure and reactive groups, so it is crucial to learn the nature of the active site before choosing the method. The specific protective groups can protect enzyme's active site from different modifications. Later these groups are easily removed without affecting enzyme activity. A substrate or a competitive inhibitor can fulfill the function of this protective group in some situations (Sheldon, 2007). Possible effects of immobilization on enzyme activity are given in Figure 2.7.
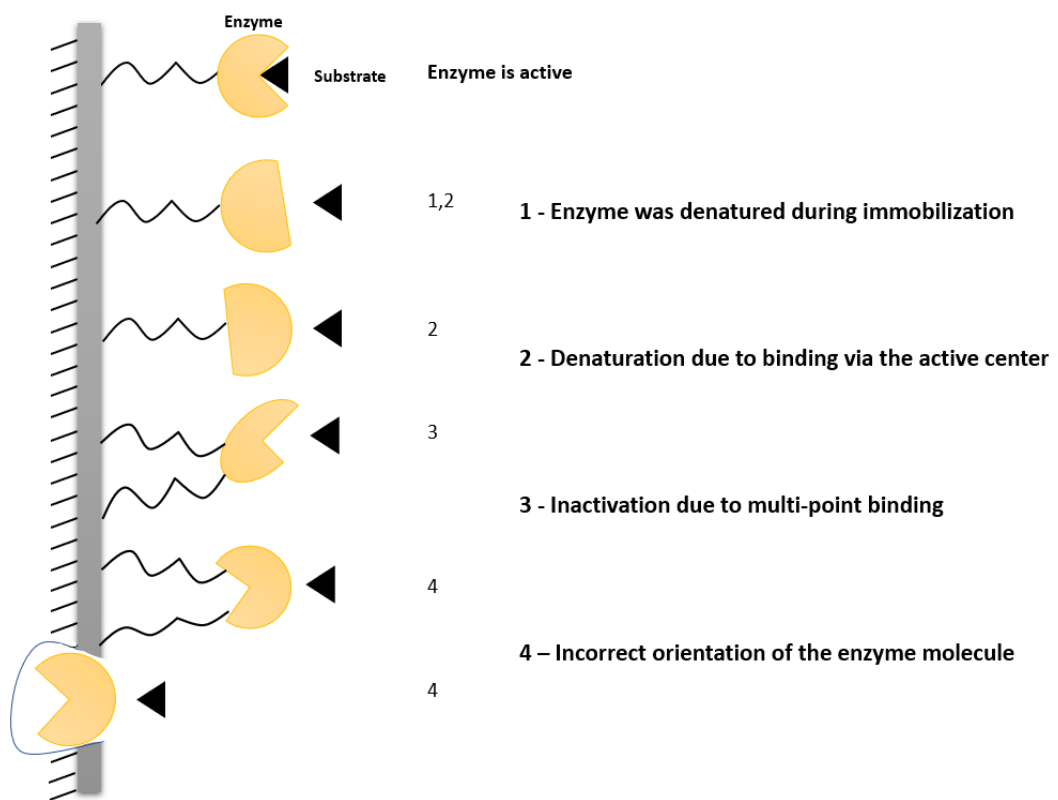
Figure 2.7. Possible effects of immobilization on enzyme activity (Sambamurthy, 2006; Bonnet et al., 2003)

To improve the immobilization process, the following factors should be considered (Hoffmann et al., 2017):

- The enzyme must be stable under immobilization conditions
- If the immobilized enzyme is to be used as a catalyst in a chemical reaction, the nature of the reaction should be considered before choosing the immobilization method
- Attaching free enzyme to the surface rather than entrapping it inside the matrix is preferred
- Immobilized enzyme leaves the matrix through the pores during or after immobilization. The pore width of the support should be considered
- The active ends of the enzyme should be protected so that it does not react with crosslinking reagents. The crosslinking reagent should be as large as possible so that it does not penetrate the active end
- While immobilizing enzymes with high activity, the amount of loading enzyme should be reduced
- The washing process to remove the unbound enzyme should not affect the enzyme
- The mechanical properties of the support material, especially its physical form and mechanical stability should be evaluated.

2.2.1. Adsorption

Adsorption is the oldest and simplest immobilization method with wide application in which enzyme gets adsorbed to carriers with high surface tension. The most popular adsorbents are starch, ion exchange resins, bentonite, activated charcoal, gluten, porous glass, etc. Enzymes attach to the surface of the support or the pores of mesoporous material by H-bonds, van der Waals forces, and electrostatic or hydrophobic interactions. Adsorption is accomplished by mixing a water-insoluble adsorbent with an enzyme solution under appropriate conditions for a certain incubation period. At the end, the immobilized enzyme is washed with a buffer to clear away unbound enzymes. Adsorption has many advantages over other methods: enzymes save their initial catalytic activity because the immobilization conditions are mild, no additional binding agents or modification steps are required, it has a high enzyme loading capacity, and carriers can be easily reused later by removing (desorption) the enzyme. Therefore, it is a low-cost and easy-to-implement method. However, because of the weak interaction, adsorbed enzymes are usually less stable and more sensitive to environmental changes (pH, ionic

strength, temperature, and solvent polarity). Consequently, immobilized enzymes may easily be desorbed from the support. The adsorption method is divided into three mechanisms: physical adsorption, electrostatic bonding, and hydrophobic adsorption (Figure 2.8) (Hoffmann et al., 2017). The physical adsorption strategy is the most common and widely used to develop enzymatic biosensors. It has some benefits due to simplicity, cost-saving, and resurfacing features, but at the same time, it's a time-taking method which consumes high amount of reagent. In addition, as the enzyme cannot be homogeneously immobilized to the carrier, access of the substrate to the enzyme's active site may be interrupted (Junior et al., 2016; Brady and Jordan, 2009).

The electrostatic bonding method depends on the solution's pH, temperature, enzyme's isoelectric point, and concentration. It is based on the protein-ligand interaction used in chromatography. The surface of an enzyme can carry a positive or a negative charge, and it can be immobilized to the oppositely charged matrix through the ionic or strong polar bond. Commonly used support materials are synthetic polymers, polysaccharide derivatives, and inorganic materials. Here, the immobilization efficiency depends on the support's surface charge density; high surface charge density allows high amount of enzyme to bind. This method causes minimal changes in the structure of the enzyme. Extreme or suboptimal conditions may cause enzyme leakage, therefore it is important to carry out the reactions under proper conditions (pH, temperature, ionic strength, etc.). Layer-by-layer deposition and electrochemical doping are essential techniques in electrostatic bonding immobilization (Kumar et al., 2009; Neto et al., 2011; Nisha et al., 2012).

Another immobilization approach is hydrophobic adsorption. Hydrophobic interactions occur by the displacement of water molecules emerging due to entropy gain during immobilization. The bond strength depends on the hydrophobicity of the adsorbent and the enzyme. It can be regulated by parameters such as pH, temperature, salt concentration, and the size of the hydrophobic ligand molecule. β-amylase and amyloglucosidase were reversibly immobilizied on hexyl-agarose via hydrophobic adsorption (Liu et al., 2018; Hartmann and Kostrov, 2013).
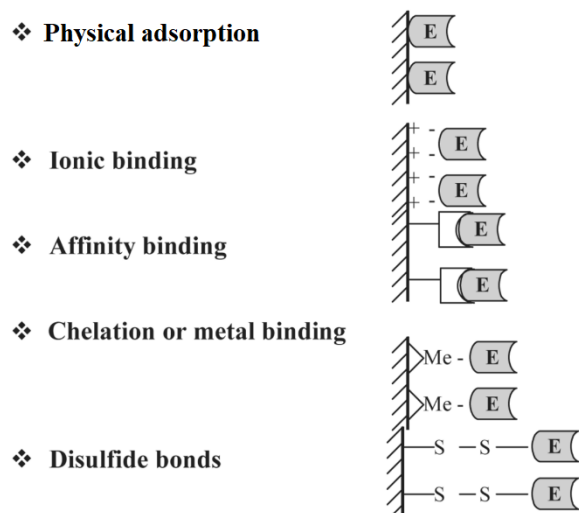
Figure 2.8. Reversible immobilization methods (Brena and Batista-Viera, 2006)

2.2.2. Chelation

Chelation is a physical immobilization method mainly applied as a chromatographic method. Here, the metal legands that are weakly linked to the matrix's transition metal ions are replaced by enzyme molecules during the immobilization process. The metal ions make a coordination bond with enzyme's charged amino acids such as cysteine, histidine, and tyrosine. A competing ligand with a high concentration or with a higher affinity towards metal ions (such as ethylene diamine tetraacetate (EDTA)) can reverse the bonding (Wu et al., 2009). Reversibility of binding allows to effortlessly regenerate the matrix with high yield, but at the same time, the binding stays reasonably strong, as enzyme release is maximally restricted. Before addition of enzyme, it is possible to temporarily bond chelating anions to the surface of the matrix. However, these chelating reagents are not safe for food production and may cause health hazards. This method is not preferred in some industries because of high cost and reliability problems. Another important disadvantage of the method is the decrease in enzyme activity which is a consequence of the fact that the active site binds to metal ions (Afaq et al., 2001).

2.2.3. Entrapment

It is the method where the enzyme does not straightly interact with the matrix. It gets inserted into a polymeric network (polyacrylamide, alginate, kappa carrageenan, etc.) or in semi-permeable membranes that release only substrate and products but hold the enzyme. It ensures continuous substrate conversion (Figure 2.9). This method also allows

to to encapsulate several enzymes within the same membrane. It falls into five different categories: lattice type, microcapsule type, liposome type, hollow-fiber type, and membrane type (Aehle, 2004). The entrapment process is carried out in two steps: first, the enzyme is added to a monomer solution; second, the monomer solution is polymerized by a chemical reaction. Although the enzyme is confined within a polymer lattice, it does not react with the polymer. Since chemicals are not used in entrapment method, the enzyme does not undergo major changes and saves its properties. The other advantages of entrapment are simpleness and soft reaction conditions. Also, entrapment sets up the enzyme's unique optimum microenvironment by providing favorable pH, polarity, and amplitude. It increases the enzyme's stability and minimizes denaturation. However, an important disadvantage is the mass transfer resistance that prevents the substrate from fully reaching the active site. Also, due to the polymerization procedure, the carrier matrix may deteriorate and misfunction. Another disadvantage is that if the pore size of the carrier is too large, the entrapped enzymes may leak and cause low immobilization efficiency. Therefore, entrapment is not recommended if the size of the enzyme and substrate is similar (Nguyen and Kim, 2017; Nakarani and Kayastha, 2007; Krishnamoorthi et al., 2015; Brena and Batista-Viera, 2006).
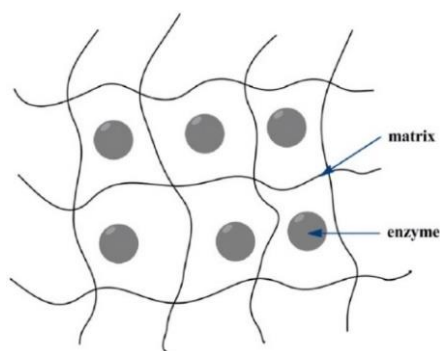
Figure 2.9. Immobilization of enzyme molecules through entrapment (Liu and Chen, 2016)

2.2.4. Covalent bond

Covalent immobilization is accomplished by forming a covalent bond between the enzyme and support material's functional groups (Figure 2.10) (Hoffmann et al., 2017). Mostly used enzymes in this method include lysine, cysteine, aspartic acid, and glutamic acid. Mainly used carriers are agarose, cellulose, polyvinylchloride, and porous glass. The

carrier's critical functional groups are -S-, -SH-, -OH, -COO-, and -NH$_3$. Depending on functional groups, different mechanisms can be applied (Figure 2.11).
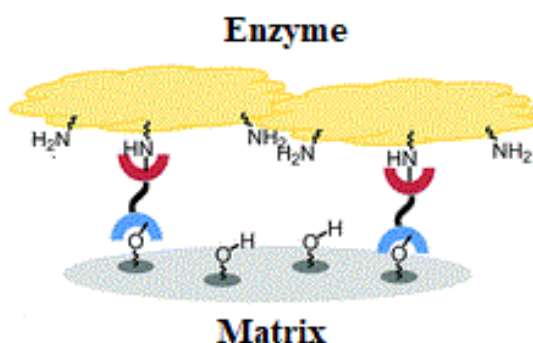
Figure 2.10. Example of covalently immobilized enzyme (Sim et al., 2018)

For covalent immobilization, the support must be activated with binding molecules that covalently connect the carrier and enzyme (Figure 2.12) (Cao, 2005). Different binders such as glutaraldehyde (GA), carbodiimide, dicyclohexylcarbodiimide, and cyanogen bromide can be applied for different matrices (Nguyen and Kim, 2017; Liu et al., 2018). Carbodiimide (RN=C=NR) is a functional group that provides the bonding between carrier's carboxyl group and enzyme's amino group or vice versa. For example, to increase the immobilization efficiency of N-hydroxysuccinimide, it can be derivatized with carbodiimide. GA is another common binding agent. The first aldehyde group of the GA undergoes a Schiff-base reaction with the carrier, and the second group makes a covalent bond with the enzyme. Enzymes, such as isomerases and oxidoreductases can be bonded to the matrix through thiol groups in their structure, For example, thiol groups can make a strong bond with gold particles due to their high affinity. Alternatively, those enzymes can be immobilized on thiol-containing matrices by building disulfide bonds (S-S) (Hanefeld et al., 2009).

- Epoxidation method

$$CH_2 - CH - CH_2$$
$$\diagdown \diagup$$
$$O$$
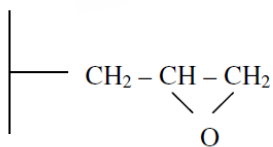
- Carbodiimide method

$$COOH + RN = C = NR$$

- Silanization method

$$OCH_3$$
$$|$$
$$Si - OH + CH_3O - Si - CH_2 - CH_2 - CH_2 - NH_2$$
$$|$$
$$OCH_3$$
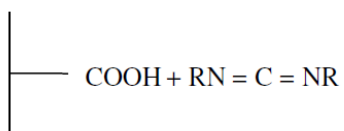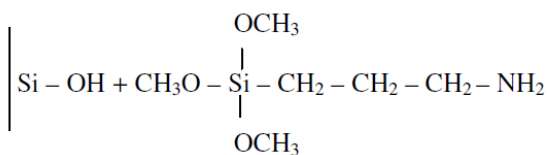
- Glutaraldehyde (cross-linking)

$$NH_2 + O=C-CH_2-CH_2-CH_2-C=O$$
$$| \qquad\qquad\qquad |$$
$$H \qquad\qquad\qquad H$$

- Cyanogen bromide

$$OH$$
$$+ Br - C \equiv N$$
$$OH$$
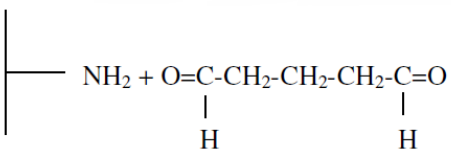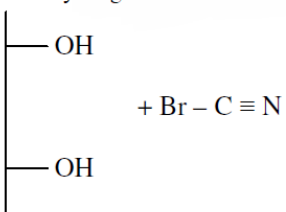
- Tresil chloride method

$$OH + Cl - S - CH_2 - C - F$$
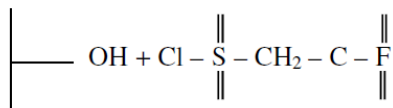
Figure 2.11. Activation methods for carriers (Petri et al., 2004)
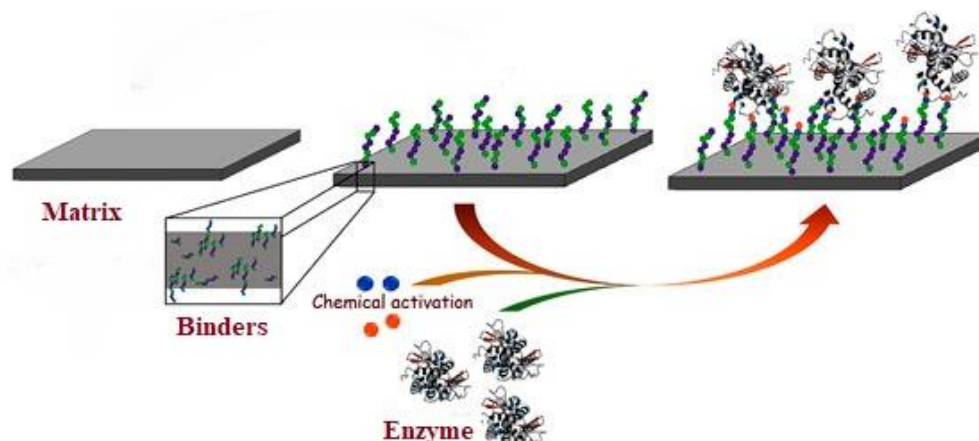
Figure 2.12. Covalent immobilization process (Flores-Rojas et al., 2017)

In covalent immobilization, the bond between enzyme and matrix is quite robust. Thus, the immobilized enzyme shows high resistance to extreme physical or chemical conditions, and the enzyme does not easily leak from the matrix. The convenience of the covalent bonding method depends on the enzyme's binding site. If an enzyme binds to the carrier via its active site, an inevitable loss in activity can be observed. A common procedure to prevent covalent binding from the active site is to saturate the active site with a competitive inhibitor. Also, covalent immobilization causes partial modification of amino acids in the active site due to the harsh immobilization conditions (Calleri et al., 2012; Zhang et al., 2012; Pierre et al., 2006; Sambamurthy, 2006).

2.2.5. Cross-linking

Cross-linking is a method based on the covalent cross-linking of enzyme particles within themselves to build insoluble, very high molecular weight three-dimensional enzyme aggregates without using any support matrices (Figure 2.13). Chemicals with high functional properties, such as GA, diazobenzidine, diisothiocyanotoluene bisisocyanate, transition metal ions, bovine serum albumin, and dextran are used as crosslinkers, but mainly used one is GA due to its low cost, high efficiency, and stability (Figure 2.14) (Górecka and Jastrzębska, 2011). GA has two aldehyde groups that interact with enzyme's amino acids (Bilal et al., 2017d; Brady et al., 2008).
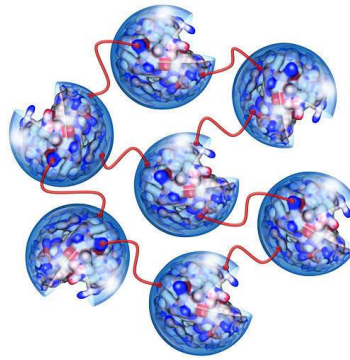
Figure 2.13. Cross-linked enzymes (CLEA Technologies, 2023)

Since the chemical bond between cross-linked enzyme biomolecules is irreversible and strong, the obtained aggregate is stable, and enzyme leakage is minimal. It is an easy technique to apply and allows immobilizing free enzymes using bi- or multiple functional groups. However, GA can negatively affect the structure and activity of the enzyme, therefore, inert proteins need to be added to reduce its effect (Sheldon, 2007). Moreover, the cross-linking process is quickly affected by external factors, and it is challenging to keep the formed aggregates under control (Hoffmann et al., 2017). This method is convenient for combination with other support-dependent immobilization methods, such as minimizing the loss of enzymes in adsorption immobilization.
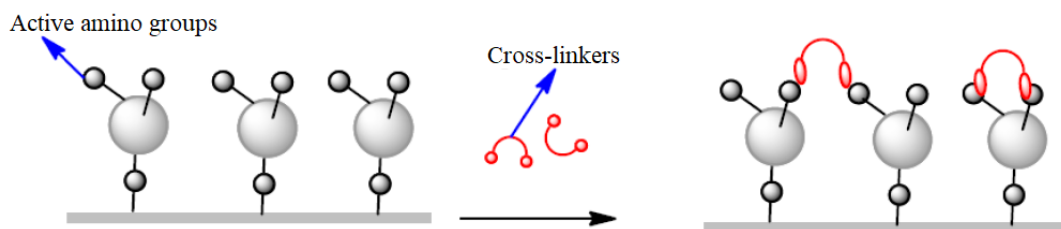
Figure 2.14. Schematic representation of cross-linking process (Cao et al., 2006)

2.2.6. Support Matrices

The carrier or support matrices are critical in operating successful enzyme immobilization. Therefore, when choosing suitable matrix materials, it is necessary to consider their properties and advantages (Sirisha et al., 2016).

According to their nature, support matrices are categorized as organic and inorganic, then further divided into subclasses (Figure 2.15).
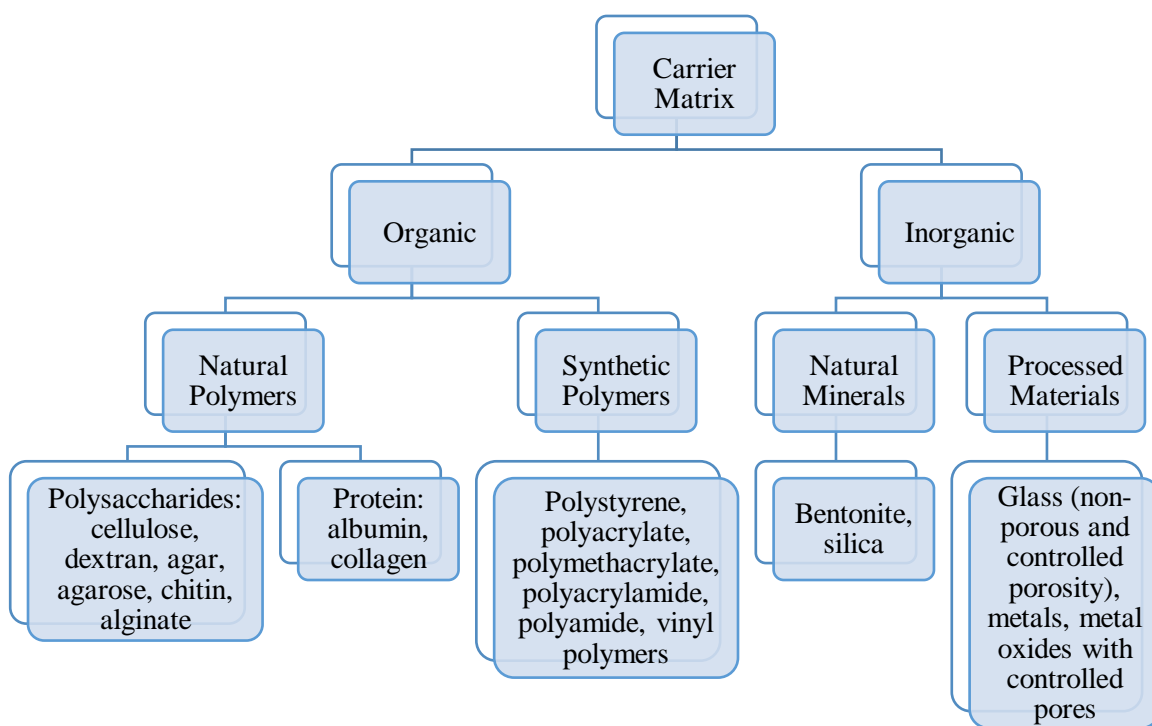
Figure 2.15. Classification of carriers (Brena and Batista-Viera, 2006)

An ideal matrix must have the following characteristics:

▪ It should be cost-effective, non-toxic, and biodegradable

▪ It should be completely inert after immobilization and not interfere with a catalytic reaction

▪ It should be resistant to various thermal and mechanical conditions

▪ It should be chemically, physically, and biologically stable

▪ It should ensure that the immobilized enzyme is highly reusable

▪ It should increase the specificity of the enzyme

▪ It should have suitable functional groups

▪ It should be insoluble in water

▪ It should have a high capacity so that the maximum amount of enzyme can be immobilized.

▪ It should have pores with an appropriate diameter

▪ It should have antimicrobial and non-specific adsorption properties

▪ It should be biocompatible with clinical applications (Tran and Balkus, 2011; Magner, 2013; Hartmann and Kostrov, 2013; Brady and Jordaan, 2009).

2.3. Synthetic dyes

2.3.1. Reactive Black 5

RB5, also called Remazol Black B, was launched in 1957 by Hoechst as part of the original Remazol line (Fergusson and Padhye, 2019; Lewis, 2011). RB5 is one of the most widely used synthetic reactive dyes in the dyeing industry. Its global production is over 46,000 tons per year (Glover, 2004). It is highly preferred because it gives bright and permanent color, binds easily to cellulose, and has less color loss during dyeing. Also, its production is economical and consumes small energy (Adnan et al., 2015; Jalali and Doroudi, 2020). The molecular formula of RB5 is $C_{26}H_{21}N_5Na_4O_{19}S_6$, and the molecular weight is 991.82 g/mol (Jalali and Doroudi, 2020). It is greatly water-soluble and occurs in anionic form due to the existance of sulfonic acid groups (Demiray et al., 2021).

While structurally classifying the dyes, the chromogen and coloring part of the molecule should be considered, as well as the basic structure. According to structure, dyes are divided into seven groups: azo, nitro and nitroso, polymethine, arylmetin, azo (18) annulen, carbonyl, and sulfur dyes (Christie, 2014). RB5 is classified as an anthraquinone azo dye (Figure 2.16). It is characterized by the azo (-N=N-) group, the chromophore group in its structure. They are not found in natural substances, so all azo dyes are obtained synthetically (Kaykıoğlu and Debik, 2006; Sun et al., 2017a).
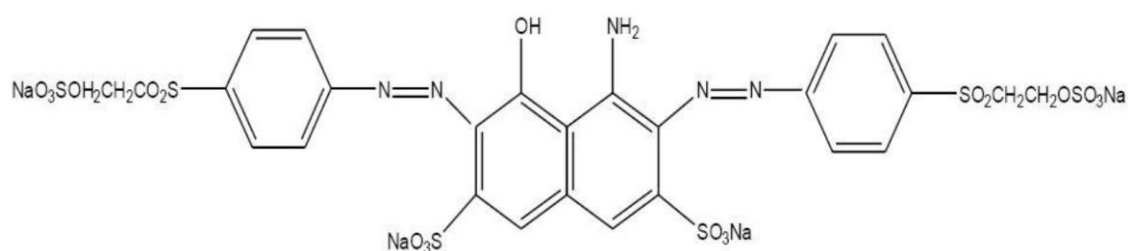
Figure 2.16. Chemical structure of RB5 (Fergusson and Padhye, 2019)

RB5 has wide color gamuts and strong color rendering capabilities, and it is inexpensive to obtain. The most straightforward representation of azo dyes, aromatic rings B and D, are presented in Figure 2.17. Azo chromophore group B shows the electron-accepting

side, and the D group shows the electron-donating side. If there is one azo group in the dye structure, it is called monoazo dye; if there are two azo groups, it is called diazo dye; and if there are three azo groups, it is called triazo dye (Majumdar et al., 2022).
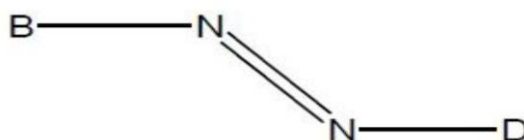
Figure 2.17. Azo chromophore group (El Sikaily et al., 2012)

Dyes are classified as basic, acidic, direct, mordant, reactive, metal-complex, disperse, pigment, and chrome mordant dyes according to their dyeing properties (Mahapatra, 2016). RB5 is in the reactive dye class. These dyes are used for dyeing textiles, papers, fibers, carpets, leathers, wools, plastics, silk, and polyamide; they are also widely applied in cosmetic, ink, and electroplating industries (Kyzas, 2014; Eren and Acar, 2006; Jalali and Doroudi, 2020). RB5 is also applied as a mixture with other dyes (Fergusson and Padhye, 2019).

Reactive dyes show a similar structure to other dye classes but contain a different reactive group that forms a covalent bond with functional groups of the fiber (Chakraborty, 2015). In order of importance, the functional groups can be given as follows: chromophore group, reactive group, bridge group, and solubilizer group (Figure 2.18). The bridge connects the reactive and the chromophore group; the –NH– group is the most preferred bridge as it is more suitable for synthesis (Hunger, 2007; Chinta and VijayKumar, 2013). According to their solubility, synthetic dyes are divided into water-soluble and water-insoluble. Water-soluble dyes are divided into three groups according to the character of the salt-forming group: anionic, cationic, and zwitterion. Water-insoluble dyes, on the other hand, are classified as dyes that dissolve in the substrate, dyes that dissolve in organic solvents, dyes that have temporary solubility, dyes that are formed in the fiber and by polycondensation, and dyes that are pigments. RB5 is included in the water-soluble anionic dye group. Anionic water-soluble dyes contain mostly sulfonic ($-SO_3^-$) and partially carboxylic ($-COO^-$) salts of sodium ($-SO_3Na$ and $-COONa$) as a water-soluble group (Hameed et al., 2007; Öz et al., 2021).
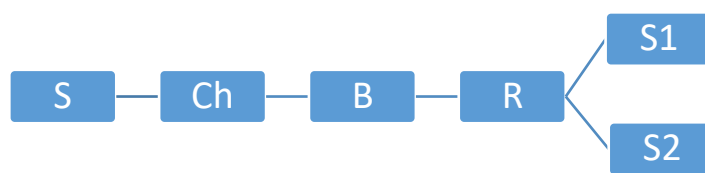
Figure 2.18. Chemical structure of reactive dyes (S: Solubility group, Ch: Chromophore group, B: Bridge group, R: Reactive group, S1: Substituent displaced during substitution reaction, S2: Other substituents) (Wang et al., 2020)

2.3.2. Congo Red

Acidic or anionic dyes are water-soluble dyes containing one or more anionic groups (usually $-SO_3H$) that are particularly applied to wool and polyamides. Their employment is carried out in acidic baths, and almost all of them are salts of organic acids. Metal complex and reactive dyes containing sulfonic acid groups belong to this class. Many acid dyes are sodium salts of sulfonic acids. These dyes are used for dyeing silk, cationic-modified acrylonitrile fiber, paper, leather, and food materials (Dizge et al., 2008). One of the acidic dyes, CR was first mentioned in 1883 by Paul Botiger, who worked for the Bayer company in Germany. He discovered this dye while trying to obtain an acid-base indicator. However, since the company did not like the dye's light and bright red color, Botiger patented it himself and sold it to Aktien-Gesellschaft für Anilin-Fabrikation in Berlin. They started to sell this substance as "Congo Red." The name "Congo" was given in 1885 during the Berlin West Africa Conference (Steensma et al., 2001; Yakupova et al., 2019; Frid et al., 2007).

CR is the sodium salt of the acid called benzidinediazo-bis-1-naphtylamine-4-sulphonic acid and belongs to the secondary diazo dye group (R-N=N-R bond) (Jalandoni-Buanet et al., 2010). It has a symmetrical linear structure with a molecular diameter of 21 Å; two phenyl rings in its structure (located in the hydrophobic center) are connected with two charged terminal naphthalene fragments via diazo bonds. Terminal naphthalene fragments include amine groups and sulfonic acid (Figure 2.19) (Romhányi, 1971; Frid et al., 2007).

Terminator-Connector-Linker-Connector-Terminator

Sulphonazo form - red

Chinone form - blue
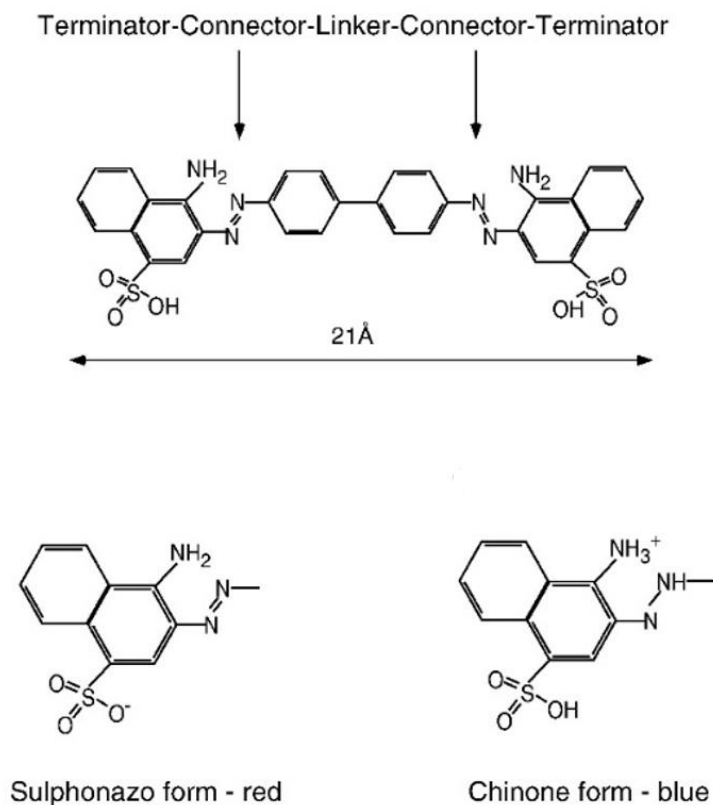
Figure 2.19. Chemical structure of CR (Romhányi, 1971)

CR refers to the direct dye class and is the first synthetic dye to stain the fiber directly without additional chemicals. Table 2.4 shows the chemical and physical properties of CR. The 3D structure is shown in Figure 2.20.

Carbon Hydrogen Oxygen Nitrogen Sodium Sulfur
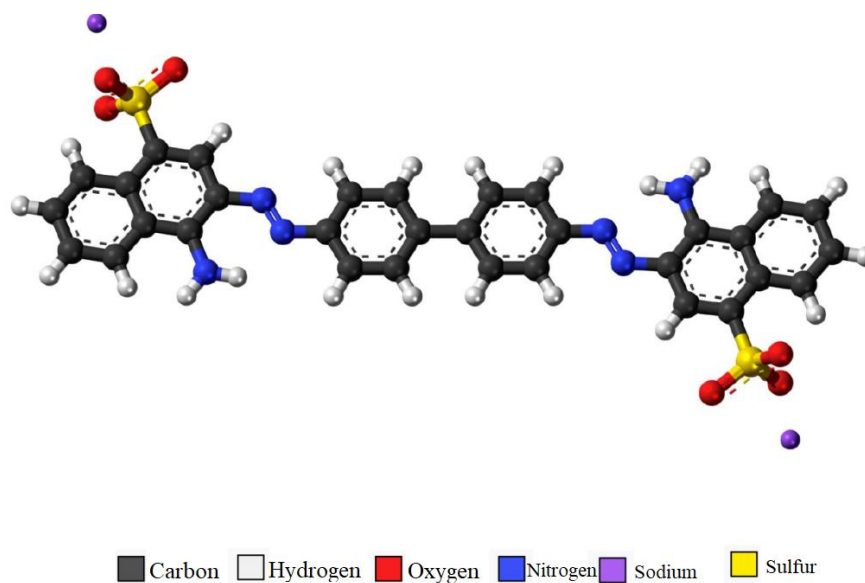
Figure 2.20. 3D structure of CR (Ali et al., 2020)

Table 2.4. Main properties of CR (Abbas and Trari, 2015; Chatterjee et al., 2007)

Name	Congo red (Disodium 4-amino-3-[4-[4-(1-amino-4-sulfonato-naphthalen-2yl)diazenylphenyl]phenyl]diazenyl-naphthalene-1-sulfonate)
Chemical formula	$C_{32}H_{22}N_6Na_2O_6S_2$
Molecular weight	696.663 g/mol
pKa	4
Composition	(%) C:55.0; N:12.06; O:13.78; H:3.18; Na:6.77; S:9.21
Wavelength (λ_{max})	498 nm, 488 nm, 595 nm
Appearance	Brownish red powder
Melting point	360 °C
Boiling pressure	760 mmHg
Solubility in water	25 g/L (20 °C)
Solubility	Soluble in ethanol; insignificantly soluble in acetone
Density	0.995 g cm^{-3} at 25 °C

CR is soluble in water but dissolves better in organic solvents such as ethanol. It resembles cellulose fibers due to its strong and rigid structure. CR is prone to clumping in solutions: hydrophobic interaction between the dye molecules causes aggregation. This aggregation is more common in concentrated, high salt, and/or low pH CR solutions (Alver et al., 2017; Sarsik et al., 2009). CR has important spectrophotometric properties. It is blue-violet at pH=3 (sulphonazo form) and red at pH=5 (chinone form). Due to its color change between pH 3.0-5.2, this substance is used as an acid-base indicator (Horobin and Kiernan, 2020; Romhányi, 1971; Frid et al., 2007). As a result of delocalized electrons in the benzene and azo groups that form the conjugated system, CR can conduct electricity and therefore be used in semiconductor technology (manufacture of display devices, optical layers, grain-optic sensors) (Chatterjee et al., 2007). It is also used in plastic, textile, paper, and rubber manufacturing (Vimonses et al., 2009; Purkait et al., 2007); in the determination of free HCl in gastric juice analysis; in detecting bacteria and protein disorders; in vivo vitalization (Naseem et al., 2018); in biochemistry and histology to stain microscopic environments (liposome, cytoplasm, fungi, bacteria, red blood cells, amyloid-β protein, collagen) (Michels and Büntzow, 2010; Alturkistani

et al., 2016; Yakupova et al., 2019; Frid et al., 2007; Chatterjee et al., 2007). The use of CR in some sectors (cotton, pulp, etc.) has already been abandoned: when touched with sweaty hands, the clothes with CR change color, creating a poisonous effect (Hunger et al., 2000). Although it has carcinogenic and mutagenic properties, it is still widely used in the textile, printing, paper, and plastic industries (Chakraborty, 2015; Jalandoni-Buanet et al., 2010).

2.3.3. CR and RB5 as environmental pollutants

The discharge of dye-containing textile wastewater into water reservoirs has always been a serious problem, as synthetic dyes are incredibly toxic to aquatic life. They are remarkably soluble in water, carry double bonds, different functional groups, and long and multiple aromatic rings; consequently, they are durable, persistent and have low biodegradability (Xu et al., 2011; Qiu et al., 2009; Namal, 2017; Chatterjee et al., 2010). Some dyes that are not treated adequately can remain in the environment long. For example, the half-life hydrolyzed Reactive blue 19 dye has a half-life of approximately 47 years at pH 7 and 25 °C. Yet the decomposition products of dyes themselves are genotoxic, carcinogenic, and mutagenic to life forms because they contain benzidine, naphthalene, and other aromatic compounds.

Over 1000 tons of synthetic dyes are released to water sources annually by different manufactories as wastewater; 45% of them are reactive dyes (Nadaroglu et al., 2015; Dursun et al., 2013). RB5's nature is extremely teratogenic, mutagenic, and poisonous (Umpuch and Sakaew, 2015). Since it has a complicated structure, it is not simply eliminated from wastewater (Hamzeh et al., 2012). A very small quantity of RB5 can reduce oxygen concentration under water and inhibit the growth of plants, thus damaging the ecosystem and food chain (Qureshi et al., 2017; Bazrafshan et al., 2015). It enhances the overall dissolved and suspended solids percentage, raises the chemical and biological oxygen demand, and changes the wastewater's salinity, pH, and color (Hassan and Carr, 2018; Jafari et al., 2014). Also, soil contamination with RB5 negatively affects carbon and nitrogen cycles (Rathi and Kumar, 2022). In humans, RB5 can initiate bladder cancer, asthma, blindness, skin rashes, end-stage kidney disease, chrosomal abnormality, and heart failure (Deng et al., 2019; Jafari et al., 2016; Chang and Shih, 2018).

CR has been broadly used in the industry; however, it is risky to living beings and can introduce numerous health hazards due to benzene and naphthalene rings in its structure (Munagapati and Kim, 2016; Waheed et al., 2019; Afkhami and Moosavi, 2010; Kamal et al., 2016). Firstly, CR-including effluent, is hardly degraded and requires high chemical oxygen demand (Borthakur et al., 2017; Wang et al., 2018). The color of CR itself frustrates the reoxygenation of water and reduces the transmittance of light when they are above a specific concentration, causing a severe decrease in the photosynthetic and biological activity of the aquatic flora and fauna (Namal, 2017; Raval et al., 2016). CR was reported to affect the metabolism, respiration, and development of green algae, which in turn triggers eutrophication (Oladoye et al., 2022). The nature of the dye is allergic, carcinogenic, mutagenic, and poisonous. If the dye comes into contact with human skin, it may cause skin and eye irritation (Zaini et al., 2014; Sarkar et al., 2014; Swan and Zaini, 2019). Human beings take a vital dose of protein from aquatic plants and animals, but it was reported that CR bioaccumulates in them. Thus, consuming contaminated aquatic creatures may lead to diseases such as cramps, hypertension, and fever (Amer et al., 2022; Sharma et al., 2022). When the dye penetrates the body, it can create thrombocytopenia, decrease total serum protein, provoke the aggregation of platelets, and initiate urothelial and hepatocellular carcinoma. Besides, it came out that CR has teratogenic effects: 20 mg/100 g of the dye activated anophthalmia, hydronephrosis, and hydrocephalus in pregnant rats, while 40 mg/100 g led to death (Frid et al., 2007). Secondly, when CR is degraded, carcinogenic compounds are formed. Azo bond in CR gets broken reductively and produces toxic amines. Amines immediately metabolize to red colloidal benzidine solutions which are poisonous to human (Chen et al., 2018; Song et al., 2016; Miandad et al., 2018; Zeng et al., 2014; Oladoye et al., 2022; Swan and Zaini, 2019). Therefore, CR and RB5-containing wastewater must be efficiently treated with environmentally-safe methods (Naseem et al., 2018).

2.4. The application of immobilized HRP in dye decolorization

When the studies related to the application of immobilized HRP are examined, it can be seen that there are many reports on dye decolorization with HRP immobilized onto different materials, mainly by covalent and cross-linking methods. The studies are summarized in Table 2.5.

Karim et al. (2012) immobilized HRP on a β-cyclodextrin (CD)-chitosan complex and compared its efficiency with the water-soluble enzyme in decolorization of azo dyes (0.5% Cypress Green, 1.5% Sultan Red) at pH 8.0 with 0.6 mM H_2O_2 and 0.2 U/mL enzyme. The optimum temperature was 40 °C, and the optimum reaction time was 2 h. The cross-linked enzyme was more stable and active than the free enzyme. Also, the cross-linked enzyme showed 69% efficiency even after five reuse cycles.

Bayramoglu et al. (2012) improved HRP characteristics by immobilizing HRP on the polyaniline (PANI) grafted polyacrylonitrile (PAN) films using GA to decolorize Direct Blue-53 and Direct Black-38. The thermal, pH, and storage stabilities, activity, and reusability of the immobilized HRP increased compared to free enzyme. The HRP-immobilized PAN-g-PANI removed 91% and 95% of Direct Blue-53 and Direct Black-38 at 10 mg/L dye concentration, whereas the free enzyme removed 73% and 81% of dyes, respectively. Moreover, immobilization improved the reusability of HRP as 83% of initial activity was retained after eight weeks at 4 °C when the free enzyme lost its original activity after three weeks.

In work by Šekuljica et al. (2016a), HRP was cross-linked onto kaolin via GA to improve the potential of C.I. Acid Violet 109 decolorization. After one hour of incubation at pH 4.0, 0.1 U enzyme, 0.6 mM hydrogen peroxid H_2O_2, and 30 mg L^{-1} dye, the cross-linked HRP showed 76.5% decolorization, while the free enzyme displayed 92.3%. Nevertheless, with the dye concentration of 100 mg L^{-1}, free HRP retained 23%, whereas the kaolin-HRP retained 92% of the activity. Moreover, kaolin cross-linked HRP was reapplied four times in the decolorization reaction and preserved 15% of its activity.

In the report of Bilal et al. (2018), the polyacrylamide was fabricated by cross-linking approach and used as a matrix for HRP immobilization to. Polyacrylamide based gel immobilized horseradish peroxidase (PAG-HRP) demonstrated the highest relative activity at 10 mg/L dye concentration and pH 6.

Table 2.5. Comparison of the effectiveness of different immobilized HRP enzymes for use in dye decolorization

Immobilization method/support	Applications	Optimum pH	Optimum dye concentration, mg/L	Optimum enzyme dose	Optimum H_2O_2 concentration	Optimum contact time	Reusability	References
Cross-linking/ β-CD-chitosan complex	0.5% Cypress Green, 1.5% Sultan Red	8.0	-	0.2 U/mL	0.6 mM	2 h	69% efficiency after 5 reuse	Karim et al. (2012)
Acrylamide gel and alginate	Acid Black 10 BX	2.0	30	2.205 U/mL	0.6 μL/L	45 min	-	Mohan et al. (2005)
Entrapment and cross-linking/Na-alginate	Acid Yellow 11	5.0	-	0.0033 mg/mL	0.3 mM	12 min	74% efficiency after 10 reuse	Yapaoz and Attar (2020)
Encapsulation/ calcium alginate gel beads	Acid Orange 7 and Acid Blue 25	7.4	-	0.8 U/g	1.25/1 ratio of H_2O_2/dye	90 min	10% efficiency after 10 reuse	Gholami-Borujeni et al., 2011
Cross-linking/kaolin	C.I. Acid Violet 109	4.0	30	0.1 U	0.6 mM	-	15% efficiency after 4 reuse	Šekuljica et al. (2016a)
Covalent bonding/two ReliZyme™ supports (HFA 403 and EP 403)	Amido Black 10, Acid Orange 7, Direct Green, Methylene Blue, Acid Red, Neutral Grey	5.0-6.0	-	-	1.43 mM	30 min	80% efficiency after 10 reuse	Borza et al. (2020)
Encapsulation/ calcium alginate gel beads	Reactive Blue 221/Reactive Blue 198	5.5	-	0.120 g	43.75 μM/37.5 μM	180 min/240 min	15% efficiency after 3 reuse	Farias et al. (2017)
Adsorption/kaolin	C.I. Acid Violet 109	5.0	40	0.1 IU	0.2 mM	40 min	35% efficiency after 7 reuse	Šekuljica et al. (2016b)

Table 2.5. Comparison of the effectiveness of different immobilized HRP enzymes for use in dye decolorization (continued)

Adsorption/amine-functionalized superparamagnetic iron oxide	Acid Black-HC	2.5	1.6×10^{-4} mol/L	-	0.32 mol/L	-	-	Keshta et al. (2022)
Cross-linking/ ZnO nanowires/macro porous SiO_2 composite	Acid Blue 113/Acid Black 10 BX	3.0/7.0	50	107.5 mg/g-support	-	35 min	79.4% efficiency after 12 reuse	Sun et al. (2017b)
Adsorption/UiO-66-NH$_2$	Methylene Blue and Methyl Orange (MO)	9.0	10		3%	60 min		Kurtuldu et al. (2022)

To upgrade the dye decolorization performance, HRP was cross-linked onto ZnO nanowires/macroporous SiO_2 composite through diethylene glycol diglycidyl ether (DDE) and was employed for the decolorization of Acid Blue 113 and Acid Black 10 B.X. by Sun et al. (2017b). The maximum decolorization ratio was achieved at 50 mg/L of initial dye concentration and 35 min of contact time. It was 95.4% and 90.3% for Acid Blue 113 and Acid Black 10 B.X., respectively. Stability and reusability of the immobilized enzyme were tested with Acid Blue 113. It recovered 79.4% of initial activity after 12 recycling and 80.4% after storing at 4 °C for 60 days. Additionally, cross-linked HRP had much better temperature and pH resistance set side by side with free HRP.

The study by Bilal et al. (2017b) determined the use of the HRP cross-linked onto PVA-alginate beads by sodium nitrate in MO decolorization. The authors determined that immobilization improved the storage stability and reusability of the natural enzyme. Namely, after 180 min at 60 °C, the activity of free HRP was only 4.21%, while immobilized HRP so far preserved 49.82% of its initial activity. After ten continuing reaction runs, immobilized HRP held 64.14% of efficiency, whereas the free HRP could be applied once only. In the dye decolorization study, a considerable drop in spectral shift proved the complete decolorization of MO by PVA-alginate immobilized HRP.

In the report of Vineh et al. (2020), the immobilization of HRP onto a functionalized reduced graphene oxide-SiO_2 by the covalent bonding using GA as a cross-linker was discussed. The efficiency of RGO-SiO_2/HRP in removing the 2500 mg/L of phenolic compounds and in dye decolorization was studied. The immobilization improved the reusability, storage stability, pH, and temperature resistance of HRP. Free and RGO-SiO_2/HRP had 50% and 100% of phenol removal, respectively. Also, 100% of MO decolorization was observed with SiO_2/HRP, while with the free enzyme, it was only 7%.

In the study of Celebi et al. (2013), HRP was immobilized onto two different polysulfone support materials (bisphenol A and bisphenol AF-based polysulfone support) and the decolorization efficiency of Acid Black 1 and Reactive Blue 19 dyes was studied. The thermal and storage stabilities of the immobilized HRP expanded compared with the free enzyme. Immobilized enzymes were reused for seven cycles with various intervals after

storage at 4 °C. Besides, bisphenol AF-based polysulfone support had more favorable pH stability than bisphenol A-based polysulfone support materials.

In the study by Borza et al. (2020), HPR was covalently immobilized on two ReliZyme™ supports containing active epoxy groups (HFA 403 and EP 403 carriers) to be used in decolorizing seven textile dyes. The maximum dye decolorization was achieved for Amido Black 10. Dye decolorizations of the immobilized systems remained high (80%) even after reusing them ten times. During the experiments, the immobilized HRPs were stable over a broader pH range and temperature than the free HRP. After incubation at 55 °C for 30 min, the HFA 403 immobilized HRP retained 90% of the initial activity, while free HRP retained only 40%.

The study of Bilal et al. (2016) provided a method for the covalent immobilization of HRP on the calcium-alginate by applying GA in the role of cross-linking reagent and using it for the decolorization of Reactive Red 120, Reactive Blue 4 and Reactive Orange 16. The highest relative activity was obtained for Reactive Blue 4 (87.23%). The decolorization efficiencies of Reactive Red 120 and Reactive Orange 16 reached over 72.39% and 79.57%, respectively. The immobilized HRP could be reused for seven cycles retaining over 40% of its initial activity.

Arslan (2011) fabricated 1,6-diaminohexane-glycidyl methacrylate-poly(ethylene terephthalate) (HMDA-GMA-g-PET) fibers by grafting poly (ethylene terephthalate) fibers using glycidyl methacrylate and initiator benzoyl peroxide, with the following covalent linkage of 1,6-diaminohexane. It was observed that these fibers could be activated with GA, and HPR can successfully be immobilized on them. The author applied the immobilized enzyme to 50 mg/L MO decolorization. After 45 min, maximum dye decolorization of 98% and 79% with the immobilized and free HRP, respectively, were obtained.

Crestini et al. (2011) aimed to co-immobilize laccase and HRP enzymes onto alumina particles followed by layer-by-layer coating with polyelectrolytes and use it for cascade oxidation of lignin. Multienzyme biocatalysts showed a higher lignin conversion because of its stability, while free enzymes were depolymerized.

Jin et al. (2018) studied the co-immobilization of chloroperoxidase and HRP on ZnO nanowires/macroporous SiO_2 composite by in situ cross-linking. The co-immobilized biocatalyst showed high catalytic activity in removing Acid Black 120 and Direct Black 38 over broad H_2O_2 concentration, pH, and temperature ranges. In addition, the co-immobilized enzyme kept its high activity after 60 days of storage and was reused 20 times.

In the study of Mohan et al. (2005), two types of immobilization of HRP were implemented: acrylamide gel and alginate immobilization. The activity of free and immobilized enzymes in Acid Black 10 BX dye decolorization was compared. HRP immobilized onto acrylamide gel exhibited better performance than others with 79% of dye decolorization. Alginate immobilized and free enzyme decolorized 54% and 67%, respectively.

In the study by Gholami-Borujeni et al. 2011, Acid Orange 7 and Acid Blue 25 were chosen to study the use of encapsulated HRP in decolorizing azo dyes. HRP was immobilized on calcium alginate gel beads. Favorable conditions for decolorization of Acid Orange 7 and Acid Blue 25 were tested, and 25-50 °C temperature, 90 min contact time, 0.8 U/g enzyme amount for 500 American Dye Manufactures Institute color, 1.25/1 ratio of H_2O_2/dye were found to be the most suitable. About 75% and 84% of Acid Orange 7 and Acid Blue 25 decolorization were observed. Reusability studies demonstrated that immobilized HRP showed more than 82% decolorization after four batches, and HRP could be used for ten batches.

Farias et al. (2017) reported that HRP could be immobilized on Ca-alginate beads and successfully used in the decolorization of Reactive Blue 221 and Reactive Blue 198. The greatest decolorization (93%) for Reactive Blue 221 was obtained after 180 min at pH 5.5, 30 °C, and 43.75 μM H_2O_2 concentration. For Reactive Blue 198, the maximum decolorization was 75%, reached after 240 min, at 30 °C, pH 5.5, and 37.5 μM H_2O_2. The capsules were reusable for three cycles.

In the report of Jiang et al. (2014), the encapsulation of HRP in phospholipid-templated titania particles and using it in the treatment of wastewater polluted with phenol, 2-chlorophenol, and Direct Black-38 were discussed. The encapsulated HRP showed

effective performance in a broad range of temperatures and pHs, also even in the presence of inhibitors (barium chloride, copper(II) chloride, calcium chloride, manganese(II) chloride, H_2O_2, methanol, and acetone). The immobilized HRP removed phenol, 2-chlorophenol, and Direct Black-38 with an efficiency of 92.99%, 87.97%, and 79.72%, respectively. In addition, it was productively reused five times with the remaining efficiency of 51.58%.

Yapaoz and Attar (2020) aimed to monitor the decolorization of Acid Yellow 11 by free, entrapped, and crosslinked-entrapped enzymes. HRP was immobilized by two approaches: Na-alginate entrapment and GA cross-linking before Na-alginate entrapment. Experimental data revealed that the immobilization method of cross-linking before entrapment gave the best results as the total decolorization of 100% was achieved after 12 min at 30 °C temperature, pH value 5.0, 0.3 mM H_2O_2, and 0.0033 mg/mL enzyme. Also, crosslinked-entrapped HRP demonstrated 74% of dye decolorization after ten batches.

The aim of Jankowska et al. (2021) was to develop a procedure for adsorption and the covalent immobilization of HRP on polyamide six electrospun fibers and to apply the synthesized biocatalysts for the decolorization of RB5 and Malachite Green from solutions imitating contaminated sea waters. It was observed that a larger quantity of HRP was linked to the support by covalent immobilization using GA rather than the adsorption method. However, the most effective decolorization was achieved after one hour with HRP absorbed into PA6 support (69% and 83% decolorization ratio for RB5 and Malachite Green, respectively).

The report by Šekuljica et al. (2020) purposed to immobilize HRP on the carrier Purolite®A109 through covalent (with 2% GA) as well as adsorption mechanisms and to examine them in the removal of C. I. Acid Violet 109 dye from fabricated wastewater. Covalently immobilized HRP had less enzyme activity than adsorbed HRP but exhibited better operational and storage stability. Besides, HRP adsorbed on Purolite®A109 resulted in more effective dye decolorization (75%) compared to the covalently bonded one (70%).

Šekuljica et al. (2016b) found that kaolin has excellent features for being an advantageous matrix in the enzyme immobilization process. For this reason, HRP was immobilized onto kaolin through the adsorption method and involved in CI Acid Violet 109 decolorization. Under favorable conditions (pH 5.0, 0.2 mM H_2O_2 concentration, 40 mg/L dye concentration, 24 °C temperature, and 0.1 IU HRP-kaolin), 87% of decolorization was achieved in 40 min. The reusability research represented that kaolin immobilized HRP could be reused seven times in the demanded reaction with the remaining $35 \pm 0.9\%$ decolorization percentage.

The study of HRP immobilization on amine-functionalized superparamagnetic iron oxide by adsorption technique and its usage in oxidative degradation of Acid Black-HC was investigated by Keshta et al. (2022). *Km* and *Vmax* of free and immobilized HRP were evaluated and confirmed the greater substrate affinity of amine-functionalized superparamagnetic iron oxide immobilized HRP (Fe_3O_4@NH_2-HRP) compared to free enzyme. Immobilization positively impacted the HRP's operational, thermal, and storage stability. The experiments revealed that the specific activity of Fe_3O_4@NH_2-HRP was 1.2 times higher than free HRP's. Also, it can be concluded that under optimal conditions (pH 2.5 and 37 °C, H_2O_2 0.32 mol/L, and dye concentration 1.6×10^{-4} mol/L), the immobilized biocatalyst displayed remarkably high catalytic activity in the decolorization of Acid Black-HC dye.

Wang et al. (2020) fabricated active heterologous HRP C1A from *Armoracia rusticana* by expressing it in *Escherichia coli* and immobilized the synthesized material on an agarose-chitosan hydrogel matrix. Immobilization improved some HRP characteristics like pH and temperature stability. Moreover, immobilized-recombinant HRP C1A kept over 80% of its initial activity after six reaction cycles. The immobilized HRP was then successfully applied in decolorizing textile dyes like Acid Blue 129, Methyl Blue, Methyl Red, and Trypan Blue. The maximum decolorization of 76% was realized with Acid Blue 129. In addition, the authors suggested a possible model scheme for the decolorization mechanism.

The efficiency of HRP immobilization on three different carriers (magnetite-activated carbon, activated carbon, and chitosan) was examined by Pirillo et al. (2012). Magnetite-

activated carbon and activated carbon were excluded from further studies because they had a high adsorption capacity. HRP was immobilized on chitosan covalently via GA and applied as a biocatalyst to remove Alizarin Red and Eriochrome Blue Black R dyes. HRP immobilized on chitosan via GA (CS–GA–HRP) demonstrated significant activity (89%) in decolorization of Alizarin Red but low activity with Eriochrome Blue Black R (barely 27%). According to the results of reusability experiments with Eriochrome Blue Black R, the enzyme was deactivated after the second cycle.

The aim of the study by Janović et al. (2017) was to research the different immobilization techniques of HRP on different supports: encapsulation in calcium alginate capsules, immobilization on chitosan beads, immobilization on calcium alginate fibers, and immobilization on aluminum oxide. Immobilized enzymes were used to decolorize Reactive Blue 52. The authors preferred three biocatalysts with the best activity results and continued further studies (Chitosan-HRP, Aluminum oxide-Gelatin-HRP (Al-Gel-HRP), and Aluminum oxide-HRP-Gelatin (Al-HRP-Gel)). The H_2O_2 concentration's effect on the decolorization process was studied with Chitosan-HRP, and results revealed that H_2O_2 concentrations between 0.22 to 4.4 mM do not significantly affect the enzyme's dye decolorization performance. Furthermore, Chitosan-HRP was involved in the decolorization of dyes, and the maximum decolorization (68%) was obtained with Remazol Brilliant Blue R, while the minimum decolorization (28%) was with acridine dye. Reusability study with Reactive Blue 52 presented that the synthesized biocatalysts can be applied seven times. Even after seven cycles Al-HRP-Gel, Al-Gel-HRP, and Chitosan-HRP still saved 53%, 78%, and 67% of activity, respectively.

Aldhahri et al. (2021) reported the immobilization of HRP on an innovative 2D copper oxide nanosheet (CuONS) and following encapsulation in poly (methyl methacrylate) (PMMA). The effective usage of CuONS-PMMA was fulfilled (72.8% activity), and the enzyme's properties were notably improved. The optimum pH was widened from 7 to 7.5, the optimum temperature has improved from 40 °C to 40–50 °C, and resistance to metal ions was achieved. Also, the immobilization process enhanced the enzyme's reusability. After ten reuses, enzyme conserved 52% of its activity. CuONS-PMMA immobilized enzyme was used to decolorize Crystal Violet, Methyl Green, and Malachite Green, with results of 83%, 76%, and 70%, respectively.

Bilal et al. (2019b) reported establishing support from agarose–chitosan hydrogel with N-hydroxysuccinimide cross-linker and immobilizing HRP. ACH–HRP displayed high efficiency under both acidic and alkaline environments, also at 70 °C temperature. Due to immobilization, the enzyme could preserve 60% of initial activity even after ten repeated uses. Besides, the authors investigated ACH–HRP's good potential for removing Reactive Blue 19.

In the study by Satar et al. (2009), white radish peroxidase was adsorbed on Celite and used for Reactive Red 120 and Reactive Blue 171 treatment. The authors analyzed the impact of different redox mediators on dye decolorization and revealed that 1-hydroxybenzotriazole is the most successful mediator. The highest decolorization grade was obtained at pH 5.0 and 40 °C temperature after 1 h. The results showed that Celite-adsorbed white radish peroxidase has a higher affinity for Reactive Red 120; also, it was stable towards sodium azide, organic solvents, and mercuric chloride.

The chitosan-immobilized HRP (CTS-HRP) by Bilal et al. (2017c) was synthesized via entrapping HRP in chitosan beads. After the immobilization, the optimum temperature and pH were changed from pH 7.0 and 30 °C to pH 7.5 and 70 °C. CTS-HRP had better thermostability and stability against heavy metals, urea, EDTA, cysteine, 1, 4-dithiothreitol, and Triton X-100. Furthermore, immobilized enzyme presented high decolorization ratio of Remazol Brilliant Blue R (82.17%), RB5 (97.82%), CR (94.35%), and Crystal Violet (87.43%). A recyclability study showed that after six reaction runs, CTS-HRP kept 64.9% of dye decolorization capacity.

Li et al. (2020) encapsulated HRP in highly ordered macro–micropore zeolitic imidazolate framework-8. Immobilized enzyme's storage stability was evaluated. After four weeks of storage at room temperature in phosphate buffer, activity decreased only by 10%. Also, HRP encapsulated in single-crystal ordered zeolitic imidazolate framework-8 (HRP@SOM-ZIF-8) was reused in reaction five times and still had about 85% of activity. Besides the excellent storage stability and reusability, HRP@SOM-ZIF-8 had remarkable stability against chelating compound. After the incubation in 1 wt% EDTA for 40 min, it still preserved 96% of initial activity. HRP@SOM-ZIF-8 was also applied to decolorize MO, CR, rhodamine B, and rhodamine 6G. It immediately

eliminated dyes in 2 min, demonstrating a specific high removal capability for rhodamine B. The immobilized HRP displayed admirable reusability with CR. The dye removal efficiency after five reactions remained more than 90%.

Herein, incubation and immobilization of HRP onto zirconium(IV)-based metal–organic frameworks formed by terephthalate and 2-aminoterephthalate ligands (UiO-66-NH$_2$) with an adsorption mechanism was actualized by Kurtuldu et al. (2022). The authors observed that HRP@UiO-66-NH$_2$ could productively be applied to eliminate Methylene Blue and MO. Significant parameters in the decolorization of Methylene Blue and MO, including pH, temperature, the concentration of H$_2$O$_2$ and dye were researched to describe free and immobilized enzyme activities. HRP@UiO-66-NH$_2$ could retain its activity at raised temperatures and biodegrade Methylene Blue and MO to 60% and 45% under favorable conditions (pH 9.0, 50 °C temperature, 3% H$_2$O$_2$, 60 min contact time).

The application of an HRP immobilized on calcium alginate beads was reported by Urrea et al. (2021) for the productive decolorization of Orange II. The H$_2$O$_2$ concentration's effect on the Orange II decolorization reaction was investigated. Results demonstrated that H$_2$O$_2$ increases the decolorization rate (90 ± 2%) while absence does the opposite (3 ± 1%). The initial Orange II oxidation rates at pH values 7 and 9 were calculated (0.65 and 7.3 μM/min), and pH 9 was 11 times more beneficial than pH 7. Also, alginate/HRP beads illustrated the best initial II oxidation rate at 30 min of contact time. Orange II consumption rate was measured under different amounts of beads. The higher the amount of beads, the higher the Orange II consumption rate. Regarding recyclability, alginate/HRP beads were reasonably deactivated in the fifth reuse.

Sun et al. (2018) used zinc oxide (ZnO) nanowires/macroporous silicon dioxide composite as a matrix to cross-link HRP by in-situ approach. Three cross-linkers were evaluated: ethylene glycol diglycidyl ether, DDE, and trimethylolpropane triglycidyl ether. Among these cross-linkers, DDE had the highest enzyme loading amount (118.1 mg/g), excellent specific activity (14.9 U/mg-support), minimal mass loss of HRP (after 48 hours of leaching, 94.6% of original loading HRP amount was saved) and the best thermal stability (above 75.3% of leftover activity after 2 hours of incubation at 60 °C temperature). Immobilized HRP treated two anthraquinone dyes, Reactive Blue 19 and

Acid Violet 109 (95.9% and 94.3% of dye decolorization in 30 min were observed, respectively). Also, after 2 h, 100% decolorization of both dyes was achieved. The optimum pH for decoloring anthraquinone dyes was tested; pH 4.5 for Acid Violet 109 and pH 5.0 for Reactive Blue 19 were the most efficient. In particular, DDE cross-linked HRP displayed excellent reusability. Even after 12 times of reuse in the decolorization of Reactive Blue 19 and Acid Violet 109, the cross-linked peroxidase saved 79.6% and 76.8% of the initial activity, respectively.

The purpose of Mohamed et al. (2021) was to immobilize the HRP on cationic maize starch (CMS) (a positively charged and modified natural polymer) via electrostatic adsorption. The catalytic efficiency of immobilized HRP was estimated by using guaiacol as a substrate. Results revealed that the immobilization decreased the pH and temperature sensitivity of the enzyme. The optimum pH broadened from 7 to 6-7 and the optimum temperature switched from 30 °C to 50 °C. In addition, compared to the soluble form, CMS-HRP did not lose its activity even at 80 °C. Reusability study exhibited that CMS-HRP saved 65% of its activity even after ten reuses. The CMS immobilized enzyme demonstrated remarkably high resistance toward heavy metals and denatured compounds. Some metals (Co^{2+}, Fe^{2+}, Ni^{2+}, Ca^{2+}, and Mg^{2+}) and trypsin improved the immobilized enzyme's activity. Moreover, the biocatalyst's ability to remove MO was assessed, and due to the results, after 60 min of contact, 97% of the dye was decolorized.

Preethi et al. (2013) applied free and immobilized HRP to decolorize CI Acid Blue 113. To detect the enzyme's most favorable activity conditions, experiments of parameter optimization were carried out. It was concluded that the free HRP demonstrates the best activity at 20 °C temperature; 45 min of interaction time; 0.08 U enzyme dosage; 14 μL H_2O_2; pH 6.6, and 30 mg/L dye concentration. Further, HRP was immobilized on Ca alginate beads, and process parameters were optimized. Compared with free HRP, immobilized HRP showed the highest decolorization at a higher reaction time (240 min) and lower temperature (4 °C). The re-utilization studies proved that immobilized enzymes could be reapplied for three cycles. Also, free HRP's decolorization effectiveness was analyzed, and the results were satisfying.

Bayramoglu et al. (2021) published the appliance of an immobilized HRP on the poly(2-hydroxyethyl methacrylate-glycidyl methacrylate) [p(HEMA-GMA)] cryogel to decolorize Direct Blue-6. Optimum temperature and pH were identified (35 °C and pH 5.5), *Km* and *Vmax* values were determined (295 mmolL^{-1} and 197 U mg^{-1}), thermal and storage stabilities were examined (45% of activity at 65 °C; more than 78% of activity after eight-week storage at 4 °C). The Direct Blue-6 decolorization performance of the HRP-p(HEMA-GMA) cryogel was examined at various conditions. Results revealed that the maximum decolorization rate could be obtained at pH 6.0, 5.0 mmol/L H$_2$O$_2$, and 20 mgL^{-1} of dye concentration. Also, the toxicity evaluations with *D. magna* and *C.vulgaris* were accomplished.

Gul and Ocsoy (2021) observed that nanocomposite containing horseradish peroxidase–laccase nanoflower and iron oxide nanoparticles decorated with magnetic carbon nanotube (HRP-Lac NF@mCNT NC) can excellently be used as a nanocatalyst for decolorization of Malachite Green and Acid Orange 7. The maximum decolorization of dyes was achieved after 60 min of operation at pH 7.4. Around 99% of dye decolorization was observed with Malachite Green, while with Acid Orange 7, it reached 100%. The re-utilization studies demonstrated that it is possible to recycle HRP-Lac NF@mCNT NC for 16 times, and it still maintains above 95% and 85% of the initial activity with Malachite Green and Acid Orange 7, respectively.

Farhina and Uzma (2019) reported an article explaining the immobilization of HRP on two supports (alginate and acrylamide). The efficiency of the two immobilization methods and their Acid Black 10 BX decolorization efficiencies were measured. The acrylamide gel immobilized HRP had a more excellent decolorization capability (80%) than the alginate immobilized enzyme (55.5%). Due to recyclability results, authors could reuse immobilized enzymes (alginate and acrylamide immobilized) 5 times. After five cycles, alginate-immobilized HRP retained 22.2% of its activity, while acrylamide gel-immobilized HRP retained only 15%.

3. MATERIALS and METHODS

3.1. Materials

Table 3.1. List of chemicals used in experiments

Reagent	Manufacturer	Catalog number
Polyvinyl alcohol	Aldrich	363081
L-tryptophan methyl ester hydrochloride ($C_{12}H_{14}N_2O_2 \cdot HCl$)	Aldrich	364517
Sodium sulfate (anhydrous)	Acros Organics	196640010
Methacryloyl chloride (C_4H_5ClO)	Fluka	64120
Ethyl alcohol (C_2H_5OH)	Merck	1.00986
Hydrochloric acid (HCl)	Merck	1.00317
Dichloromethane (CH_2Cl_2)	Merck	1.06054
Triethylamine ($K_6H_{15}N$)	Across Organics	157910010
N,N'-azobisisobutyronitrile (AIBN)	Merck	8.01595
Toluene (C_7H_8)	Riedel-de Haën	24529
Ethylene glycol dimethacrylate (EGDMA) ($[H_2C=C(CH_3)CO_2CH_2]_2$)	Sigma-Aldrich	33568-1
Ethylene glycol	Sigma-Aldrich	324558
Dimethyl sulfoxide (DMSO)	Merck	S5604824
Ethyl alcohol (C_2H_5OH)	CarloErba	4146082
O-Dianisidine	Sigma	D9143-5G
Hydrogen peroxide 30%	Merck	K41143697
Peroxidase from Horseradish	Sigma	P-8250
Sodium phosphate dibasic dihydrate	Sigma-Aldrich	04272
Sodium phosphate monobasic dihydrate	Sigma-Aldrich	04269
Sodium hydroxide	Sigma-Aldrich	06203
Sodium acetate trihydrate	Riedel-de Haen	25022
Acetic acid (glacial) 100%	Merck	K2856
Tris(hydroxymethyl)-aminomethane	Merck	1.08387.0500

Table 3.1. List of chemicals used in experiments (continued)

Magnesium sulfate heptahydrate	Merck	1.05886
Calcium hydride	Merck	8.02100
Copper (II) chloride	Merck	8.18247
Iron (III) chloride	Merck	8.03945
Cobalt (II) chloride hexahydrate	Sigma-Aldrich	255599
Scandium (III) oxide	Sigma-Aldrich	307874-5G
Dichloromethane	Merck	1.06054
Toluene	LACHEMA	510390800
Ethanol	Merck	1.11727.2500
Diethyl ether	Merck	1.00921
Benzene	Merck	1.01782
Chloroform	Riedel-de Haen	34854

3.2. Method

3.2.1. Synthesis of PEDMT microbeads

PEDMT microbeads were synthesized using the suspension polymerization method reported by Osman et al., 2013. MATrp was used as a monomer, EGDMA as a crosslinker, and azobisisobutyronitrile (AIBN) as an initiator. PVA was a stabilizer, and toluene was a pore former. First of all, the MATrp monomer was prepared (Figure 3.1). Hydroquinone and L-tryptophan methyl ester were dissolved in 100 mL of methylene chloride, and the solution was cooled to 0 ºC. To the cooled mixture, triethylamine and 5 mL of methacryloyl chloride were gradually added; then, the mixture was agitated with a magnetic stirrer at room temperature under the nitrogen atmosphere for 2 h. After completion of the reaction, the mixture was treated with 10% NaOH solution to remove unreacted methacryloyl chloride. The methylene chloride phase was eliminated with a rotary evaporator, and the remaining solid (MATrp) was dissolved in ethanol and used as a monomer.
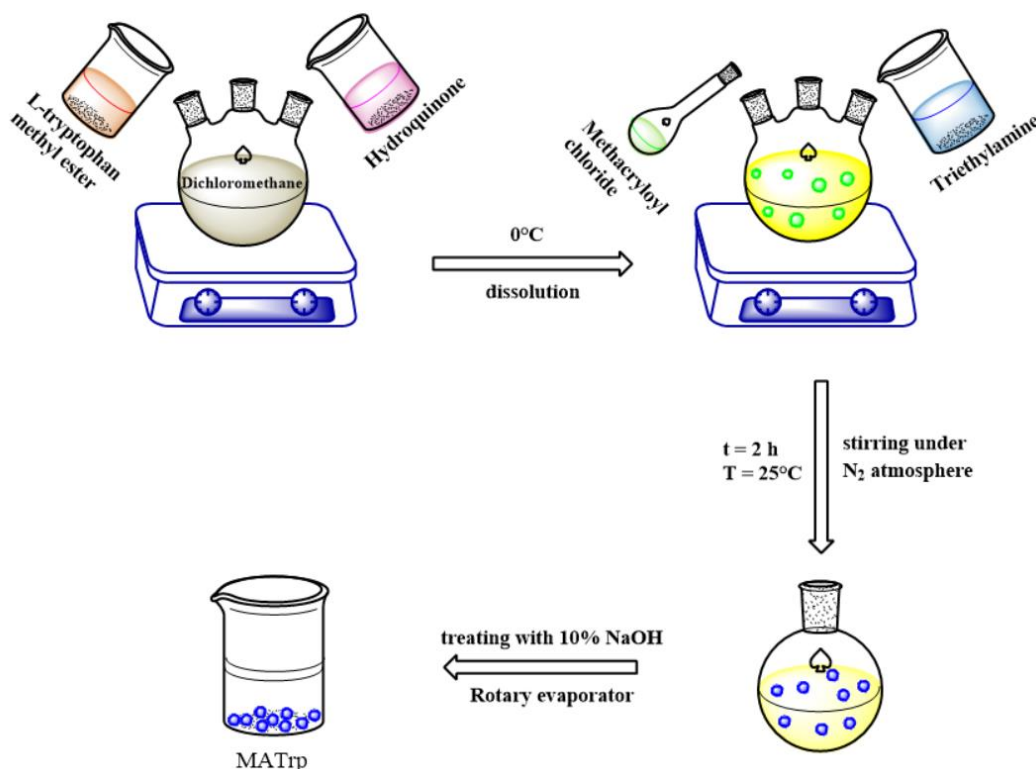
Figure 3.1. Preparation of MATrp monomer

To prepare the polymerization mixture, the organic phase (MATrp, EGDMA, AIBN, and toluene) was added to the water phase including PVA and mixed in a reactor for 4 h at 65 °C and then for 8 h at 80 °C. The synthesized PEDMT microbeads were washed with ethanol and distilled water to remove unreacted monomers. Subsequently, microbeads were dried at 50 °C in a vacuum oven (Figure 3.2).
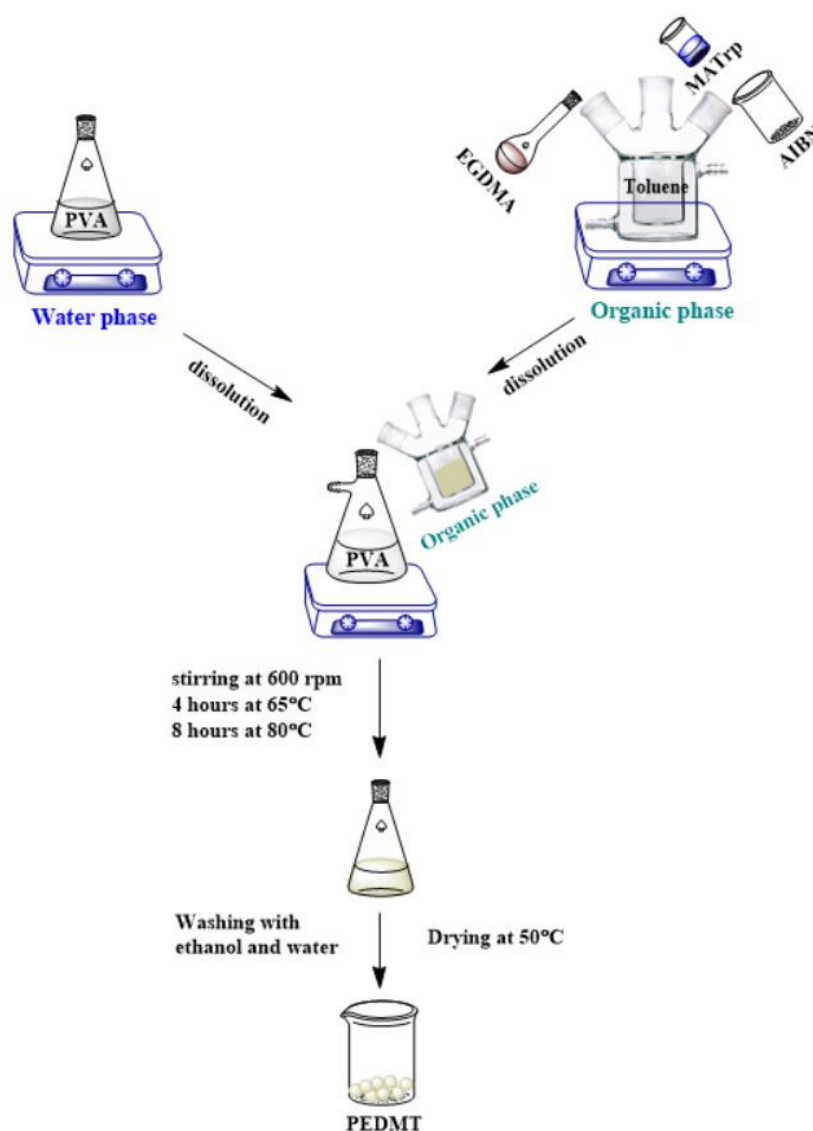
Figure 3.2. Preparation of PEDMT microbeads

3.2.2. Characterization of PEDMT microbeads

The dimensions of the obtained microbeads were examined with the optical microscope (Zeta Instrument). The microbeads were also characterized using Scanning Electron Microscopy with Energy Dispersive X-Ray Analysis (SEM-EDX), Fourier Transform

infrared spectroscopy (FTIR), and Brunauer–Emmett–Teller (BET) analysis. FTIR analysis was performed with Perkin Elmer Spectrum 100 FTIR. SEM-EDX (Carl Zeiss Gemini 300) was used to determine microbeads' surface morphology and test for the presence of the HRP enzyme. The microbead's average pore size (nm), specific surface area (m^2/g), and total pore volume (cm^3/g) were determined by BET analysis with an ASAP2000 instrument (Micromeritics). P/P°-V(cc/g) and pore diameter (A°)-dV(d)(cm^3/A°/g) graphs were prepared by using N_2 adsorption-desorption data obtained under vacuum at 77 K.

3.2.3. Immobilization of HRP on PEDMT microbeads

To immobilize HRP on microbeads, 100 mg of the obtained PEDMT microbeads was weighed and mixed with 1U of HRP enzyme solution (pH 6.0), then the resulting mixture was incubated and stirred at 4 °C for 24 h. After that, the mixture was centrifuged at 8000 rpm at 4 °C to separate and store the supernatant for the following experiments. The solid part (HRP immobilized on PEDMT microbeads or PEDMT-HRP) was washed three times with pH 6.0 buffer (phosphate) to exclude free enzymes not attached to microbeads. Ultimately, it was left to dry overnight at room temperature, then kept in the refrigerator at 4 °C until subsequent application (Figure 3.3).
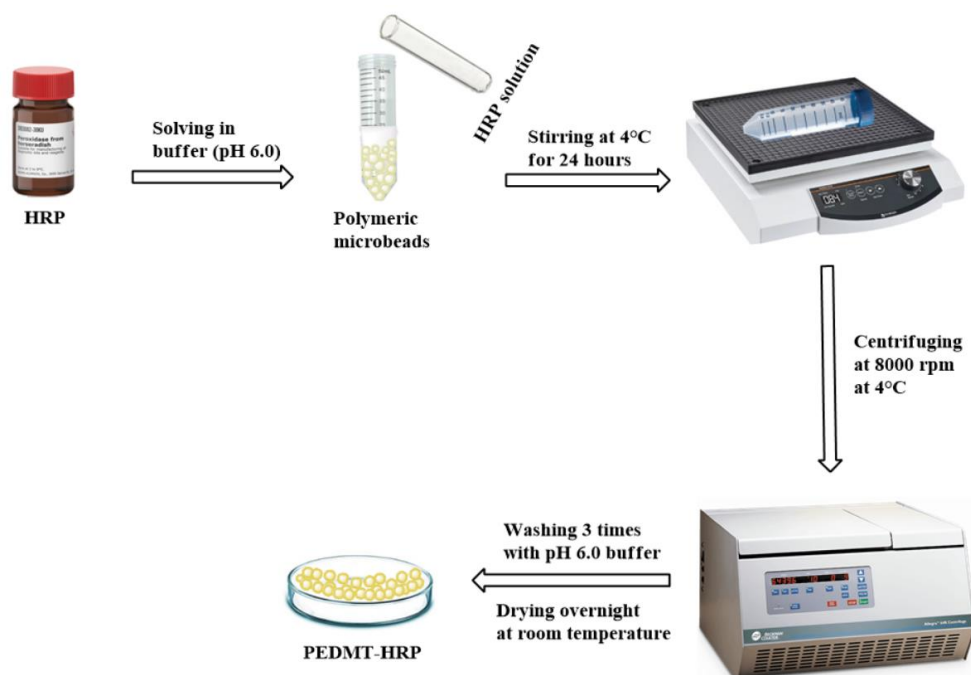
Figure 3.3. HRP immobilization procedure

3.2.4. Determination of immobilization parameters

To quantitatively describe the effectiveness of immobilization, immobilization yield (I.Y) (%) in Equation 3.1, activity yield (A.Y) (%) in Equation 3.2, immobilization efficiency (I.E) (%) in Equation 3.3, and HRP enzyme activity (%) were determined (Bindu et al., 2018).

$$\text{Immobilization yield (\%)} = \frac{C_i - C_s}{C_i} * 100 \tag{3.1}$$

Here, C_i − is the initial concentration of enzyme, C_s − is the total concentration of unbound enzyme in the supernatant and washing solutions.

$$\text{Activity yield (\%)} = \frac{A_i}{A_f} * 100 \tag{3.2}$$

Here, A_i – is the activity of immobilized HRP, and A_f – is the activity of free HRP.

$$\text{Immobilization efficiency (\%)} = \frac{Activity\ yield}{Immobilization\ yield} * 100 \tag{3.3}$$

The total peroxidative activity of the free and immobilized HRP was measured colorimetrically by using o-dianisidine as a substrate (Altikatoglu et al., 2009). The assay mixture contained 5 mg of PEDMT-HRP or an equal amount of free HRP, o-dianisidine (6 mM, 2 mL) dissolved in phosphate buffer (pH=6.0, 50 mM), and H_2O_2 (75 μL, 3%). The mixture was incubated in a water bath for 10 min at 40 °C, then NaOH solution (1.5 M, 75 μL) was added to stop the reaction. HRP activity was evaluated by measuring the increase in absorbance of bisazobiphenyl that occurs due to oxidation and polymerization of o-dianisidine at (460 nm). One unit (1.0 U) of peroxidase activity is described as the amount of enzyme that catalyzes the oxidation of 1.0 μmol of o-dianisidine to the colored product in 1 minute. All experiments were done in triplicate, and mean ± SD (standard deviation) values were calculated. The highest activity value was assumed as 100%, the results were relatively evaluated and given as relative activity.

3.2.5. Stability studies of HRP and PEDMT-HRP

To compare the stability of free and immobilized HRP, the effects of pH, temperature, substrate concentration, metal ion, organic solvent, and H_2O_2 concentration on the activity

were investigated. *Km* and *Vmax* values of free HRP and PEDMT-HRP were calculated and compared. The reusability and thermal and storage stability were determined.

3.2.5.1. Effect of pH

To find the optimum pH values of free and immobilized enzymes, the substrate was dissolved in different buffer solutions (pH 2.0–pH 10.0), and activities were measured. Three types of buffers were used: 50 mM acetate buffer for pH 2.0 to 5.0, 50 mM phosphate buffer for pH 6.0 to 7.0, and 50 mM Tris-HCl buffer for pH 8.0 to 10.0. The pH with the highest enzyme activity was defined as the optimum pH value.

3.2.5.2. Effect of temperature

The effect of temperature on the free HRP and PEDMT-HRP activity was examined at different temperatures in the range of 25 and 70 °C. The enzymes were incubated at different temperatures for 30 min, and then their activities were assayed using a substrate solution prepared at the optimum pH value. The temperature with the highest enzyme activity was determined as the optimum temperature.

3.2.5.3. Effect of H_2O_2 concentration

To determine the optimum H_2O_2 concentration, enzyme activities were measured at various H_2O_2 concentrations (1-5%). Enzyme activity measurements were performed as previously described: free and immobilized HRP were incubated with o-dianisidine (6 mM, 2 mL) and 75 μL of H_2O_2 solution (1-5% v/v) at optimum pH and temperature. The reactions were stopped by adding NaOH solution (1.5 M, 75 μL) to the reaction medium. Results were given as relative activity, assuming the highest activity as 100%.

3.2.5.4. Thermal stability

Enzymes were kept in a water bath at 50 °C for 3 h. Aliquots were taken at different time intervals (0-180 min), and the activities were measured at optimum conditions. The remaining activities were calculated by assuming the initial activity as 100%.

3.2.5.5. Effect of metal ions and organic solvents

Free HRP and PEDMT-HRP were pre-incubated in different metal ion solutions (5 mM, 1 mL) (Ag^+, Ca^{2+}, Co^{2+}, Cu^{2+}, Mg^{2+}, Ni^{2+}, Sc^{3+}, Zn^{2+}, Pb^{2+}, and Fe^{3+}) at 25 °C for 24 hours, and then their activities were measured under optimum conditions. Organic solvents, 1-pentanol, 2-propanol, acetonitrile, chloroform, ethanol, ethyl acetate, n-hexane, isoamyl alcohol, dichloromethane, dimethyl formamide, dimethylsulfoxide, tetrahydrofuran, were used. Free HRP and PEDMT-HRP were agitated with organic solvents (%5 v/v, 1 mL) at room temperature for 24 h, and their enzymatic activities were measured. The activity in the absence of these compounds (metal ion solution and organic solvent) was assumed to be 100%.

3.2.5.6. Effect of metal ion concentration

Free and immobilized enzymes were kept in calcium hydride and iron (III) chloride solutions of different concentrations (5, 10, 15 and 20 mM). After 24 h of incubation, their activities were assayed under optimum conditions. The activity of the control solution including no metal ion was accepted as 100%, and other activities were calculated relatively.

3.2.5.7. Storage stability

To analyze the storage stability, both free and immobilized HRP were stored at room temperature (~25 °C) for 4 weeks, and residual activities were measured weekly. Initial enzyme activity was considered 100%, and activities were calculated relatively.

3.2.5.8. Reusability of PEDMT-HRP

To investigate the reusability of PEDMT-HRP, the enzyme activity was measured repeatedly under optimum conditions. After each cycle, PEDMT-HRP was separated from the reaction medium by centrifugation and washed with phosphate buffer (pH 6.0). The reaction was repeated with a fresh substrate solution ten times under the same conditions. Initial enzyme activity was defined as 100%, and the following activities were measured relatively.

3.2.5.9. Determination of *Km* and *Vmax* values

Michaelis–Menten constant (*Km*) and maximum reaction rate (*Vmax*) were determined for free and immobilized HRP. For this purpose, the Lineweaver-Burk equation given in Equation (3.4) was used.

$$\frac{1}{V_0} = \frac{K_m}{V_{max}} \frac{1}{[S]} + \frac{1}{V_{max}}$$

(3.4)

In the equation, *Vo* – is the initial velocity; [S] – is the molar concentration of substrate (o-dianisidine); *Vmax* – is the maximum reaction rate; and *Km* – is the Michaelis-Menten constant (mM). Initial velocities were measured by varying the substrate concentration (0.25, 0.5, 1, 2, 3, 4, 5, and 6 mM).

3.2.6. Dye decolorization studies

To evaluate the efficiency of free HRP and PEDMT-HRP in dye decolorization, CR and RB5 dyes were used as model dyes. Stocks (500 mg/L) of dye solutions were prepared and used for further experiments by diluting. The maximum wavelengths were detected by preparing UV-spectra for dye solutions using a UV-VIS spectrophotometer (Shimadzu UV-1700). Calibration plots were prepared and used to determine the dye concentration during decolorization studies. The decolorization efficiency was calculated by Equation (3.5).

$$Decolorization\ (\%) = \frac{Initial\ absorbance - Final\ absorbance}{Initial\ absorbance} * 100$$

(3.5)

3.2.6.1. Determination of decolorization pH

The effect of pH on dye decolorization was examined with free and immobilized HRP. 20 mg/L solutions of CR and RB5 were prepared with three different buffers: acetate buffer (50 mM, pH 3.0, 4.0, and 5.0), phosphate buffer (50 mM, pH 6.0 and 7.0), and Tris-HCl buffer (50 mM, pH 8.0, pH 9.0 and pH 10.0). The process was carried out in a beaker, and the reaction mixture consisted of 10 mL dye solution, 75 μL H_2O_2 (3 %), and PEDMT-HRP (50 mg) or an equal amount of free HRP (150 μL). Decolorization was assessed by mixing the enzymes with textile dyes at 25 °C for 2 h and measuring the

decrease in absorbance with UV–visible spectrophotometer at the specific λ_{max} of CR and RB5. The highest decrease in the dye absorbance was accepted as 100%.

3.2.6.2. Determination of dye concentration

The effect of dye concentration on decolorization was studied using (5, 10, 25, 50, 75, and 100 mg/L) of CR and RB5 solutions. The process included mixing 10 mL of dye solution with a constant H_2O_2 concentration (3%) and a constant amount of enzymes (50 mg for PEDMT-HRP; 150 μL for HRP) at a fixed temperature (25 °C). The experiments were performed at the optimum pH value. The dye concentration in which maximum decolorization obtained was considered 100%.

3.2.6.3. Determination of microbead amount and enzyme concentration

The experiment was conducted at optimum pH and dye concentration, at constant temperature (25 °C) and H_2O_2 concentration (3%) with different amounts of microbeads (10, 25, 50, 75, and 100 mg) and enzyme solution volume (50, 100, 150, 200, and 300 μL). The amount of free and immobilized HRP with the highest decolorization efficiency was accepted as 100%.

3.2.6.4. Determination of H_2O_2 concentration

The optimum H_2O_2 concentration was investigated by performing decolorization experiments with H_2O_2 solutions at different concentration (75 μL) (1-5%). H_2O_2 was added to the reaction mixtures containing 20 mg/L of CR and RB5 solution with optimum pH and a fixed amount of free and immobilized HRP enzyme. The highest decolorization was accepted as 100%.

3.2.6.5. Determination of contact time

The contact time is vital for establishing the optimal decolorization time. The reaction mixture was stirred for different intervals (30, 60, 90, 120, 150, and 180 minutes) on a horizontal shaker to determine optimum contact time. Experiments were performed at optimum pH, constant free and immobilized HRP amount, and fixed H_2O_2 and dye concentration. The decolorization ratios were measured at the end of specified periods.

3.2.6.6. Reusability study

The reusability of PEDMT-HRP was investigated using the enzyme in several sequential decolorization process. After each cycle, PEDMT-HRP microbeads were separated by filtration and washed with phosphate buffer (pH 6.0), then reused with a fresh dye solution. The assay was repeated for ten cycles with CR and five cycles with RB5. The removal efficiency of the immobilized enzyme in the first cycle was considered 100%, and the subsequent activities were calculated relatively.

3.2.7. Chromatographic analyses of dyes

To evaluate the CR and RB5 decolorization by PEDMT-HRP in the presence of two dyes in the same solution, a decolorization study was performed under the optimum conditions via HPLC analysis. A solution containing the mixture of the dyes were prepared, including 20 mg/L CR and 20 mg/L RB5. The concentration of dyes after the decolorization process was determined using the Agilent 1100 model HPLC with photodiode array detector (PDA) available in Bursa Uludağ University Biochemistry Research Laboratory. A gradient elution system was used. HPLC conditions are summarized in Table 3.2.

Table 3.2. HPLC conditions of the decolorization study

Separation	Isocratic elution system (A 60% : B 40%)
Solvent A	Ammonium acetate buffer (10 mM) pH=3.6
Solvent B	Acetonitrile
Mobile Phase Flow rate	1 mL/min
Column to be used for separation	Zorbax C18 (RP18, ODS, Octadecyl)
Particle size	5.0 μ
Inner diameter	4.6 mm
Length	250 mm
PDA	200-800 nm
Column temperature	Room conditions
Injection Volume	5 μL

Table 3.2. HPLC conditions of the decolorization study (continued)

The gradient elution program	0 min 40% solvent B
	7 min 60% solvent B
	17 min 98% solvent B
	24 min 98% solvent B

The wavelengths in which the absorption was maximum were defined, and the calibration graphs for both dyes were prepared with chromatograms. The dye removal ratios of CR and RB5 were calculated through the calibration graphs.

4. RESULTS and DISCUSSION

4.1. Characterization of the PEDMT microbeads

In this study, the HRP enzyme was immobilized on PEDMT microbeads. The microbeads were synthesized by cross-linking MATrp monomer with EGDMA. The polymerization reaction was carried out through the suspension polymerization technique reported by Osman et al., 2013. The suspension polymerization starts with liquid/liquid dispersion and ends with solid/liquid dispersion. Here, MATrp monomer droplets were dispersed in an aqueous phase by adding a stabilizer (PVA). The reaction between EGDMA and MATrp under suitable reaction conditions is given in Figure 4.1. The synthesized microbeads were examined with the optical microscope (Zeta Instrument), and it was determined that they were spherical.

Ethylene glycol dimethacrylate (EGDMA) N-methacryloyl-amido-L-tryptophan methyl ester (MATrp) PEDMT
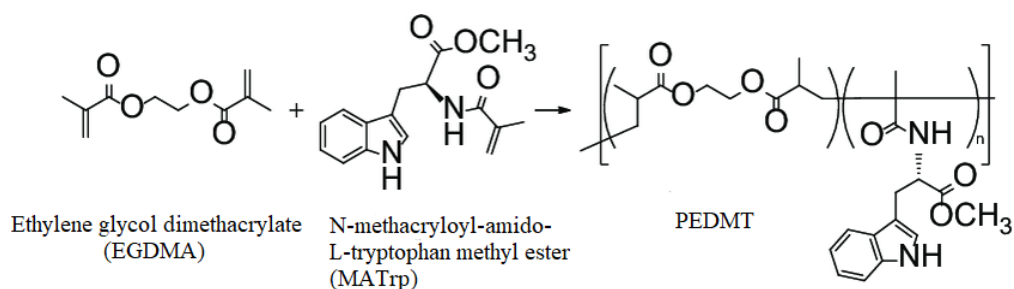
Figure 4.1. Synthesis reaction of PEDMT microbeads

SEM analyses were performed to examine the surface morphology of polymeric microbeads before and after immobilization. SEM images of PEDMT and PEDMT-HRP microbeads obtained at different magnifications are given in Figure 4.2. It can be clearly seen that the prepared microbeads had a highly porous and spherical structure. They were approximately 150 µm in diameter. SEM images taken at higher magnification ratios illustrated that after immobilization, most of the pores were clogged, and there were bumps on the surface of microbeads. It can be assigned to the physical adsorption of HRP inside the pores and onto the surface of microbeads. Consequently, the surface morphology of PEDMT microbeads were changed after immobilization, demonstrating that HRP was successfully immobilized on PEDMT microbeads.
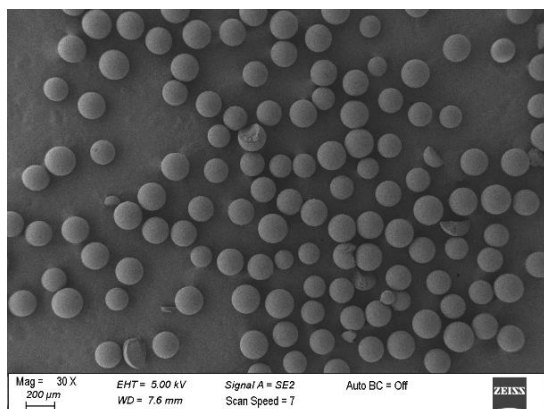
(a)
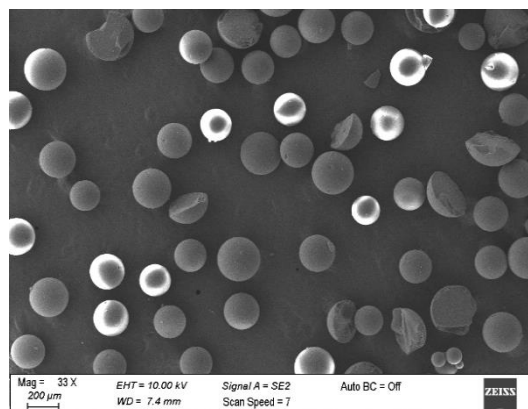
(b)
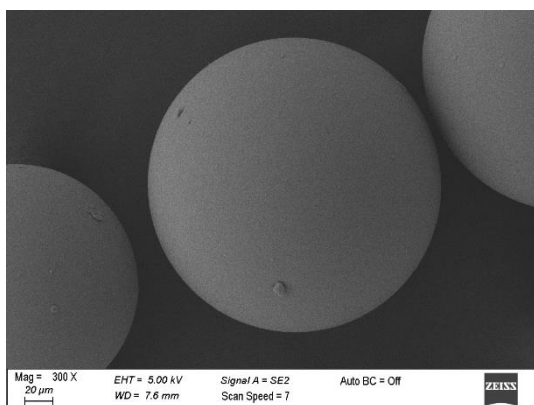
(c)
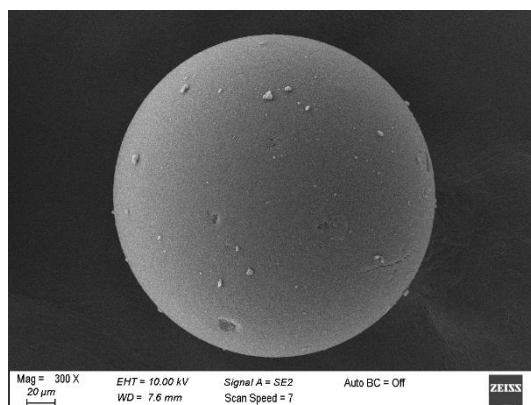
(d)
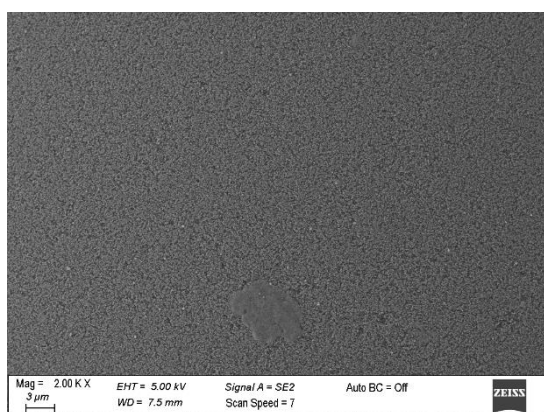
(e)
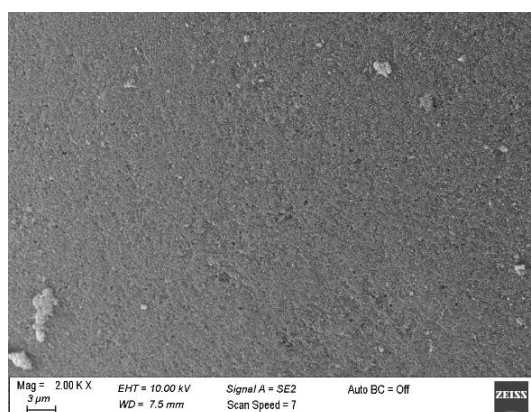
(f)

Figure 4.2. SEM images of PEDMT (a,c,e,g,i) and PEDMT-HRP (b,d,f,h,j) microbeads at different magnification ratios
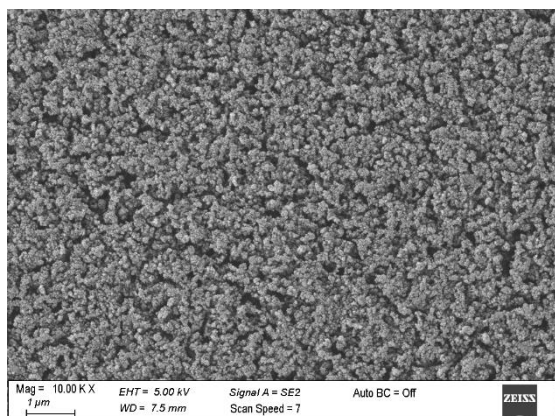
(g)
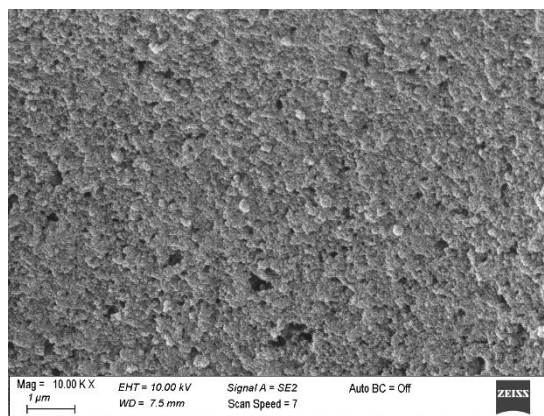
(h)
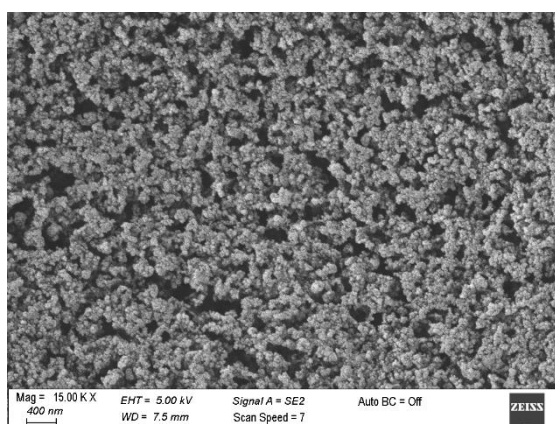
(i)
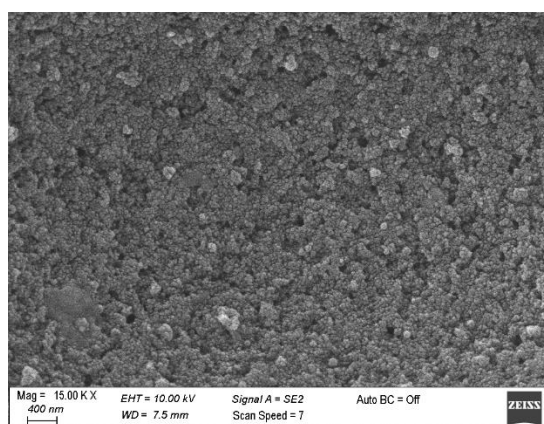
(j)

Figure 4.2. SEM images of PEDMT (a,c,e,g,i) and PEDMT-HRP (b,d,f,h,j) microbeads at different magnification ratios (continued)

PEDMT and PEDMT-HRP microbeads were subjected to EDX analysis to determine their elemental composition (Figure 4.3). The results showed the presence of carbon C, nitrogen N and oxygen O elements in both PEDMT and PEDMT-HRP. However, it is obvious that compared to microbeads, PEDMT-HRP contained another extra element, that is, sulfur (0.43%). Also, after immobilization mass fraction of nitrogen increased from 2.26% to 3.5%. Overall, it can be concluded that immobilization has changed the elemental composition of polymeric microbeads.
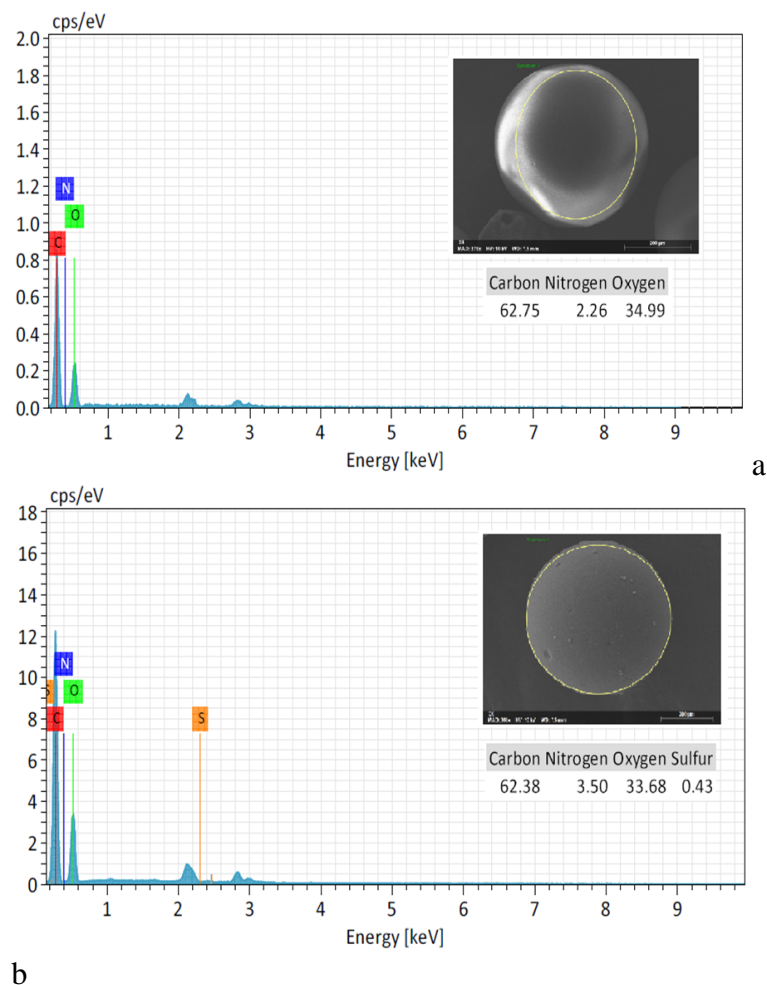
Figure 4.3. SEM-EDX spectra of PEDMT (a) and PEDMT-HRP (b) microbeads

To identify the surface functionalities and demonstrate the presence of HRP bound to the microbeads, FTIR characterization studies were performed in the range of 4000–400 cm^{-1}. FTIR spectra of PEDMT microbeads, HRP enzyme, and PEDMT-HRP are given in Figure 4.4. For the free HRP, the characteristic adsorptions at 1639 cm^{-1}, 1528 cm^{-1}, and 1387 cm^{-1} were attributed to the vibration of (-CONH-) amide I, amide II, and amide III, respectively. The detected peak at 3284 cm^{-1} is related to O–H vibration, and 2934 cm^{-1} is associated with the alkyl group (-CH$_2$). Another absorption band at 1038 cm^{-1} corresponds to the aliphatic amines (C–N stretching mode). In the FTIR spectrum of PEDMT microbeads, absorption bands of the ester carbonyl group (C=O) at 1724 cm^{-1} and repeating aliphatic C-H bonds at 2952 cm^{-1} were observed. In the case of PEDMT-HRP, the spectrum still presented characteristic peaks of microbeads. The ester carbonyl group at 1720 cm^{-1} and aliphatic C-H bond at 2952 cm^{-1} were observed. However,

PEDMT-HRP had an extra absorption band at 1404 cm^{-1} assigned to NH (amide III) vibration. In addition, similar to the free HRP spectrum, PEDMT–HRP had O–H vibrations at 3422 cm^{-1} and C–N at 1022 cm^{-1} (Tavares et al., 2020). All these data proved that HRP was successfully immobilized on PEDMT microbeads.
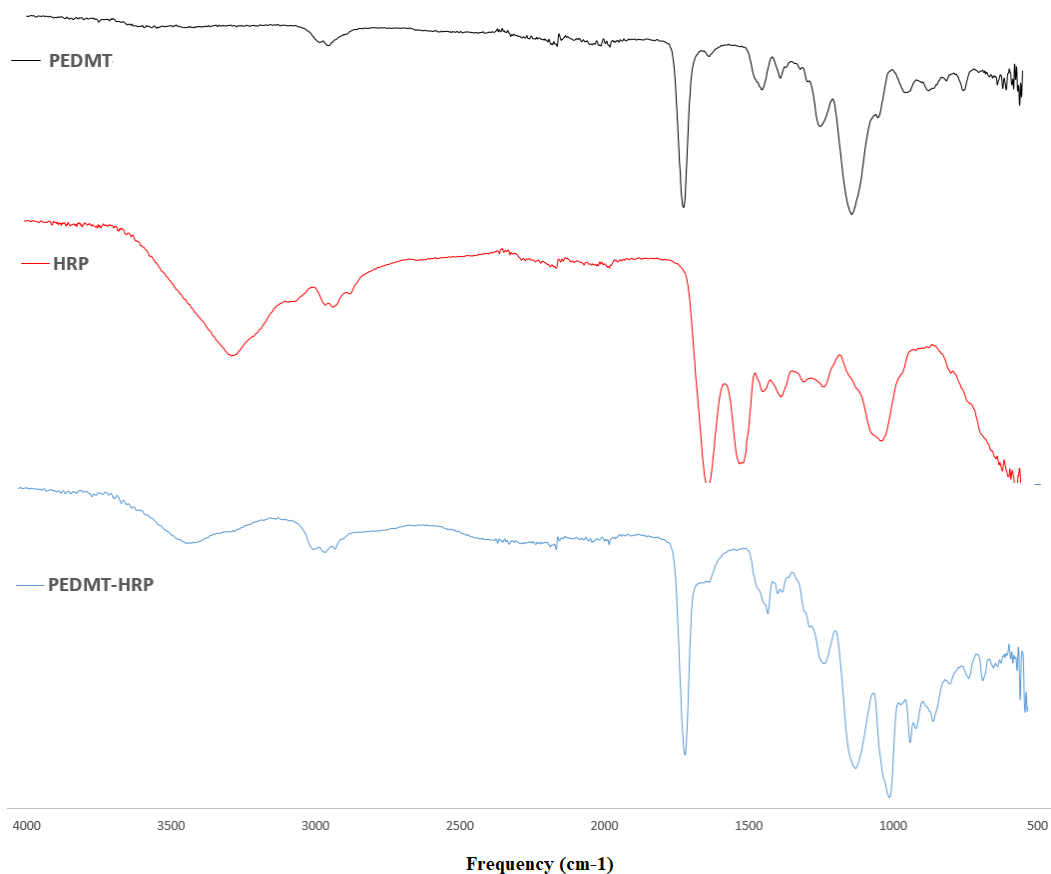
Figure 4.4. FTIR spectra of HRP and PEDMT and PEDMT-HRP microbeads

BET analysis was performed to describe the microbead's surface's physical properties. The specific surface area, pore volume, and pore diameter of microbeads were determined (Table 4.1). The PEDMT has a pore volume and pore size of 1.94 cm^3 g^{-1} and 9.99-55.3 A^0, respectively. It illustrates that microbeads had a highly porous structure and are micro- and mesoporous. The surface area of the PEDMT was found to be very high (1103 m^2 g^{-1}). High porosity and large surface area facilitated better HRP immobilization, which resulted in high enzyme activity. N$_2$ adsorption/desorption isotherms and pore diameter distribution graphs are given in Figure 4.5.

Table 4.1. Surface area, pore volume, and pore size of PEDMT

	Surface area (m^2 g^{-1})	**Pore volume (cm^3 g^{-1})**	**Pore size (A^0)**
PEDMT	1103	1.94	9.99-55.3
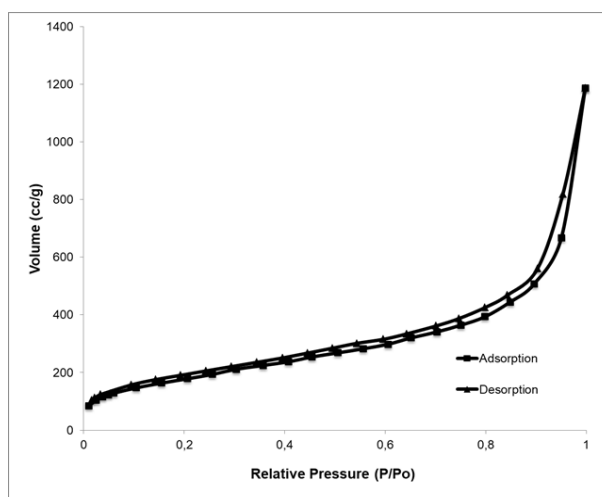
(a)
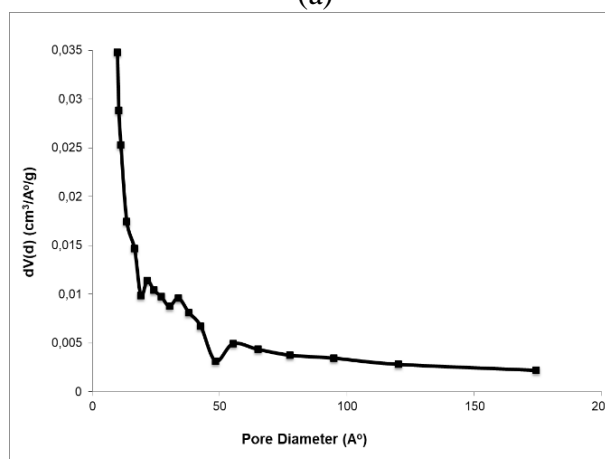
(b)

Figure 4.5. Adsorption/desorption isotherms of nitrogen at 77.40 K (a) and pore size distribution (b) obtained by Dv(d) according to average pore diameter for the PEDMT microbeads

4.2. Immobilization parameters

Determining the optimum enzyme unit is vital to perform the immobilization process effectively (Boudrant et al., 2020). Therefore, immobilization yield (I.Y), activity yield (A.Y), and immobilization efficiency (I.E) were determined for HRP immobilization process. I.Y indicates the enzyme loading capacity and expresses the actual percentage of an enzyme that immobilized on support (Hermanová et al., 2015). A.Y compares the

activity of immobilized and free enzymes. It shows the percentage of activity lost during immobilization. I.E illustrates the amount of enzyme that was immobilized and the activity of the enzyme loaded on the carrier (Bindu et al., 2018). In this work, I.Y was calculated as $84.86 \pm 2.06\%$, A.Y as $73.78 \pm 5.91\%$, and I.E as $86.95 \pm 6.92\%$. Gholami-Borujeni et al. (2011) used calcium alginate gel beads for HRP encapsulation and obtained 90% of I.E. Since the alginate-enzyme solution was utterly turned into beads, the enzyme was encapsulated and stabilized well. It led to lower enzyme leakage and high I.E. It should be noted that although the enzyme was immobilized via physical adsorption, the I.E was almost the same as that of encapsulation reported by Gholami-Borujeni et al. (2011). Sun et al. (2017b) applied ZnO nanowires/macroporous SiO_2 composite to support HRP cross-linking and reported 75.3% of I.E. In the study, the support material was first cross-linked and then the enzyme added. Since the amount of adsorbed cross-linker was low, the amount of bound enzyme was also limited compared to our study. Jiang et al. (2014) encapsulated HRP in phospholipid-templated titania particles. They achieved 70.51% of I.Y as well as 56.31% of A.Y. Abdulaal et al. (2020) immobilized HRP on a Fe_3O_4Np–PMMA film by encapsulation method and observed 88.4% of I.E. As a result, the values of the immobilization parameters for PEDMT-HRP were comparable with other reports. It can be pointed out that obtained I.E was high (86.95%), and it was presumably due to the hydrophobic interactions between the support and HRP molecules. The indole ring in the L-tryptophan methyl ester residue and the porphyrin ring in the structure of the enzyme molecule probably interacted with hydrophobic interactions and Van der Waals bond. The carbonyl groups of HRP have a high potential to make hydrogen bond with the NH group in the PEDMT structure. Also, the microbeads have a highly porous structure and large surface area, increasing the adsorption capacity of HRP to the microbeads. Consequently, the PEDMT microbeads are suitable support for HRP immobilization.

4.2.1. Optimum pH

Enzyme activity is affected by different reaction parameters (Vineh et al., 2020). The pH of the enzyme solution influences the ionization of amino acids, active site conformation, enzyme-carrier interaction, surface charge density, and enzyme-substrate connection (Bilal et al., 2016; Lopes et al., 2021). In some pH values, enzymes may become inactive

and lose activity. Therefore, pH is a vital parameter that must be studied in enzymatic reactions (Arslan et al., 2011). In this work, the enzyme activity was measured in the pH range of 2 to 10 and the results are given in Figure 4.6. As seen in Figure 4.6, the maximum activities of both free and immobilized enzymes were achieved at pH 6.0.
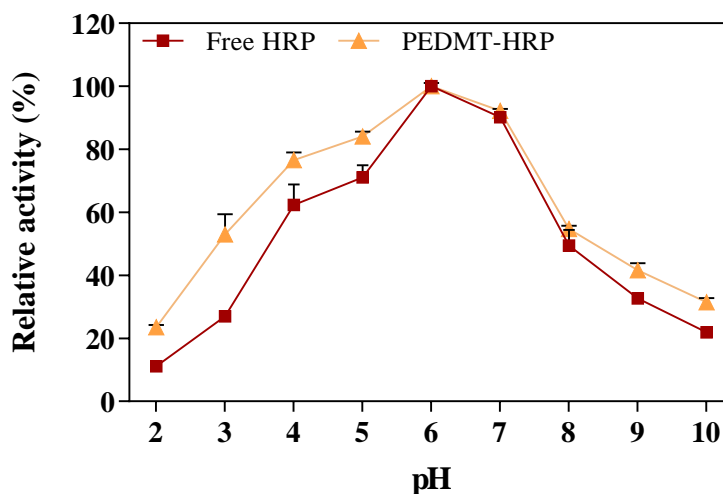
Figure 4.6. Optimum pH for HRP and PEDMT-HRP

Since HRP was immobilized via the adsorption, there was no covalent bond, and the enzyme's active site did not significantly change after immobilization. Šekuljica et al. (2016b) reported that highly acidic condition interrupts the heme molecule's hydrogen bond and causes separation from the enzyme structure. Therefore, acid-induced enzyme denaturation can explain the low activity at pH 2. However, the relative activity of the immobilized enzyme was higher even at pH 2, and it was more stable over a more comprehensive pH range than the free HRP. PEDMT-HRP showed 53% and 42% of activity at pH 3.0 (acidic environment) and pH 9.0 (alkaline environment), respectively, whereas free HRP showed 27% and 33% of activity under the same pH values. Higher pH resistance of PEDMT-HRP is due to the stabilizing and protecting effect of the immobilization (Jiang et al., 2014), which is the main advantage of the immobilization process. Owing to immobilization, the enzyme becomes more stable and is less affected by environmental factors than the free enzyme, making them suitable for use in various fields (Šekuljica et al., 2016b; Keshta et al., 2022). HRP was immobilized on PEDMT at pH 6.0. The isoelectric point (pI) of HRP is 5.5 (Rennke and Venkatachalam, 1979). It means that at pH 6.0, the net charge of enzyme was close to 0. Thus, the hydrophobic interaction between PEDMT and HRP was strong.

61

4.2.2. Optimum temperature

The temperature is another critical parameter that must be evaluated in enzyme activity (Jankowska et al., 2021). It affects the activation energy, the velocity of enzyme and substrate molecules, the enzyme's catalytic activity and thermostability, and energy expense (in industrial applications) (Arslan et al., 2011). The optimum temperatures of free HRP and PEDMT-HRP were investigated between 25-70 °C, and the results are shown in Figure 4.7.
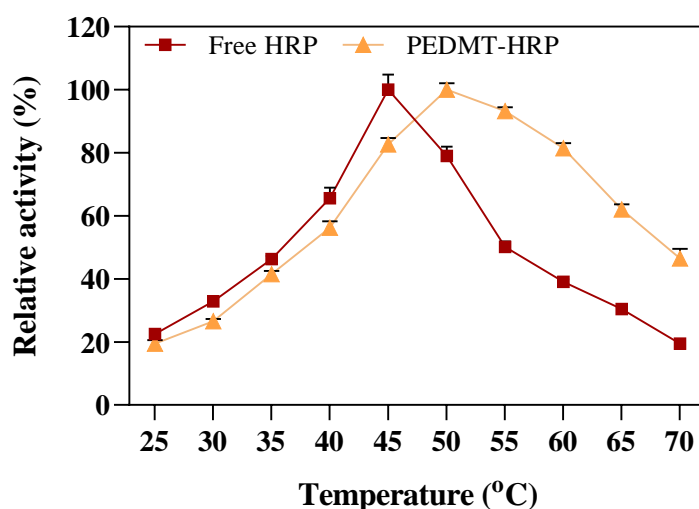
Figure 4.7. Optimum temperature for HRP and PEDMT-HRP

The results showed that there was a rapid activity drop in the free enzyme and an increase in the immobilized enzyme with the temperature rise. The maximum activity of the free enzyme was observed at 45 °C, while the PEDMT-HRP showed maximum activity at 50 °C. Enzyme-support binding causes a decrease in the conformational elasticity of the enzyme and increases activation energy to rearrange the appropriate enzyme-substrate conformation (Aldhahri et al., 2021). Thus, the increase in the optimum temperature may be due to the increase in activation energy. When the temperature was increased to 55 °C, the free enzyme started to denature, whereas the immobilized enzyme retained approximately 95% of relative activity. While the free enzyme was denatured entirely at 70 °C, PEDMT-HRP retained about 50% of its relative activity. These results show that the PEDMT-HRP was stable over a broader temperature range and had a higher thermal resistance than the free HRP. Because immobilization decreases the enzyme's thermal vibrations and stabilizes its conformational structure (Jankowskai et al., 2021).

62

4.2.3. Optimum H_2O_2 concentration

H_2O_2 is an essential co-substrate of the HRP enzyme that initiates a free radical reaction to form reaction intermediates and oxidize the substrate (Mohan et al., 2005). For higher reaction efficiency, determining an optimal H_2O_2 concentration in enzymatic reactions is vital. Because an excess amount of H_2O_2 inactivates the enzyme and an insufficient amount can not provide enough oxidant (Gholami-Borujeni et al., 2011). To find the optimum H_2O_2 concentration, enzyme activities were measured at different H_2O_2 concentrations (1-5%) under constant conditions, and the results are shown in Figure 4.8. The activity of both enzymes was increased with an increasing H_2O_2 concentration. The maximum activity was obtained when the H_2O_2 concentration was 3%. With a further increase in the H_2O_2 concentration, the activity of the free enzyme continued to decrease while the immobilized enzyme's activity was stabilized. The results proved the high stability of immobilized HRP under different conditions.
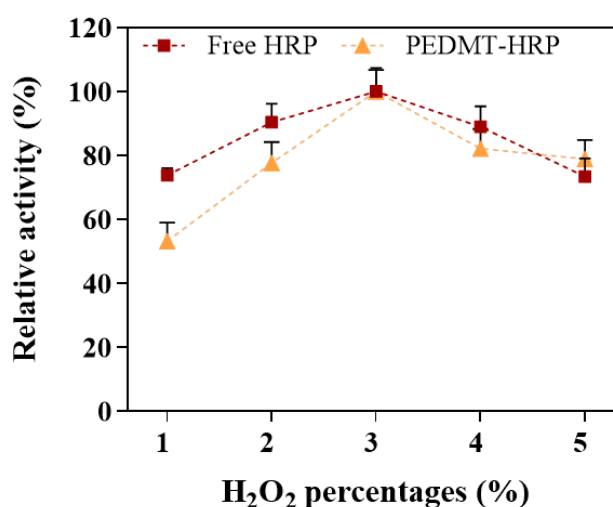
Figure 4.8. Optimum H_2O_2 concentration for HRP and PEDMT-HRP

4.2.4. Thermal stability of HRP and PEDMT-HRP

Enzymes are denatured at high temperatures after a time due to disruption of protein structure. When denaturation occurs, they lose their activity. Thus, their application and storage are restricted (Celebi et al., 2013; Bayramoglu et al., 2012). The immobilization process, on the other hand, makes enzymes more resistant to environmental conditions, including intense heat. It is advantageous for commercial use (Vineh et al., 2020; Altikatoglu et al., 2020). Thermal stability is a parameter that shows the ability of

enzymes to remain active at elevated temperatures. Figure 4.9 shows the thermal stability of both free HRP and PEDMT-HRP. After 3 h at 50 °C, free HRP lost its initial activity (only 28% of activity remained), while the PEDMT-HRP retained 50%. The activity of PEDMT-HRP decreased less and slowly compared to free HRP. The improvement in temperature resistance may be due to the enzyme's reduced molecular mobility and high conformational integrity due to immobilization. Also, owing to the high decomposition temperature of the polymeric microbeads, the free enzyme can protect its active site against temperature (Jankowska et al., 2021; Keshta et al., 2021). The results showed that immobilization significantly improved the thermal stability of the enzyme and protected it from denaturation at high temperatures (Bilal et al., 2016).
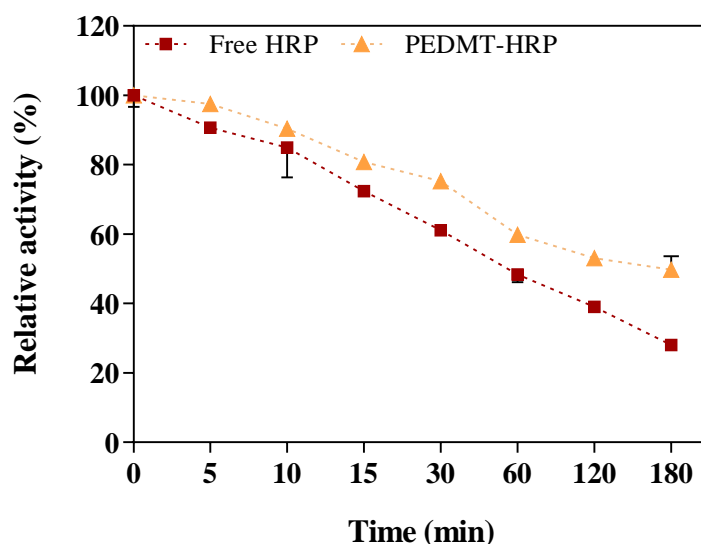
Figure 4.9. Thermal stability of HRP and PEDMT-HRP

4.2.5. Metal ions and organic solvent effect

To evaluate the tolerance of enzymes against metal ions and organic solvents, the enzymes were incubated with different metal ion solutions and organic solvents; then, the enzyme activities (free and immobilized) were measured under optimum conditions. This parameter is essential to ensure the enzyme suits various complex environments. The effect of metal ions is shown in Figure 4.10.
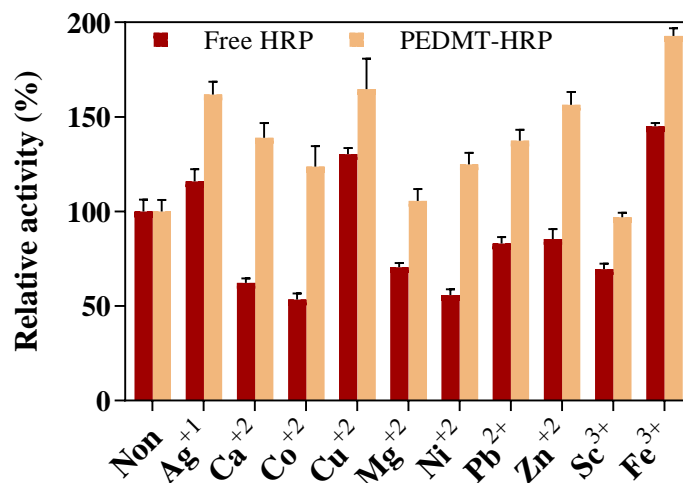
Figure 4.10. Effect of metal ions on the activity of HRP and PEDMT-HRP

It was determined that Ag^+, Cu^{2+}, and Fe^{3+} increased the activity of both free and immobilized enzymes, increasing by 16%, 30%, and 45% with free HRP and by 62%, 65%, and 93% with PEDMT-HRP, respectively. However, in the presence of other metal ions (Ca^{2+}, Co^{2+}, Mg^{2+}, Ni^{2+}, Sc^{3+}, Zn^{2+}, and Pb^{2+}), free HRP lost its activity, while PEDMT-HRP, on the contrary, gained a significant amount of activity. As a result, it can be reported that PEDMT-HRP was not inhibited by any of the metal ions compared to free HRP, and its activity was higher. The effect of organic solvents on enzyme activity is illustrated in Figure 4.11. As a result, both enzymes were not inhibited only by two solvents: ethanol and DMSO. DMSO increased the activity of the free and immobilized enzymes by approximately 4% and 24%, respectively. In comparison, ethanol increased PEDMT-HRP's activity by 14% but did not significantly change the free enzyme's activity (an increase of only 2%). Other solvents (dichloromethane, toluene, diethyl ether, chloroform, and benzene) caused a decrease in the activity of free HRP and PEDMT-HRP. However, the activity of the immobilized enzyme was relatively higher, and it was not affected by these solvents as much as the free enzyme. For example, chloroform inhibited free enzyme's activity by 50%, whereas immobilized enzyme was inhibited only by 8%. The results approved that the PEDMT-HRP has a significantly higher stability against metal ions and organic solvents. This is due to the stabilization effect of immobilization (Lopes et al., 2021).
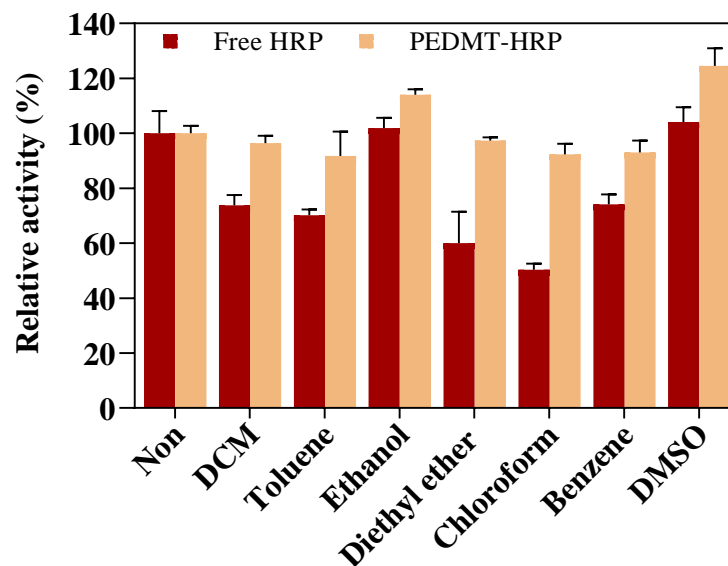
Figure 4.11. Effect of organic solvents on the activity of HRP and PEDMT-HRP

4.2.6. Metal ions concentration effect

HRP enzyme has two calcium ions (Ca^{2+}) between α-helices and one iron ion (Fe^{3+}) in the enzyme's active site. Since these metals are present in the structure of HRP enzyme, it was decided to study the effect of their concentration on the HRP activity. The effect of Ca^{2+} concentration and Fe^{3+} concentration on enzyme activity is given in Figure 4.12 and Figure 4.13, respectively. With an increase in the concentration of Ca^{2+} ions, the activity of the free HRP decreased, but the activity of the PEDMT-HRP increased. At 30 mM Ca^{2+} concentration, free HRP lost half of its activity, while PEDMT-HRP gained 80% of activity. For Fe^{3+} ions, the activity of both enzymes increased with increasing concentration. However, the rise in PEDMT-HRP activity was much higher than the increase in free HRP. 30 mM of Fe^{3+} caused an increase in the free enzyme's activity by 2.5 times and immobilized enzyme's activity by 7.5 times. According to the results, both Fe^{3+} and Ca^{2+} ions did not inhibit PEDMT-HRP either at low or high concentrations but rather increased its activity very well, demonstrating the stability of the immobilized HRP compared to the free HRP.
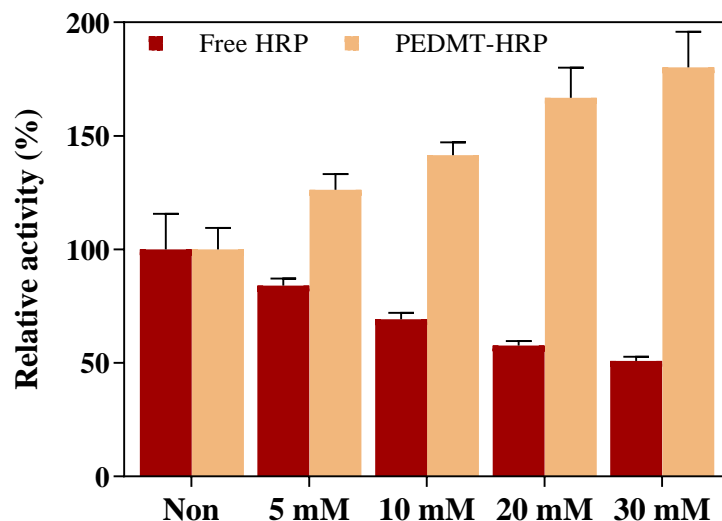
Figure 4.12. Effect of Ca^{2+} concentration on the activity of HRP and PEDMT-HRP
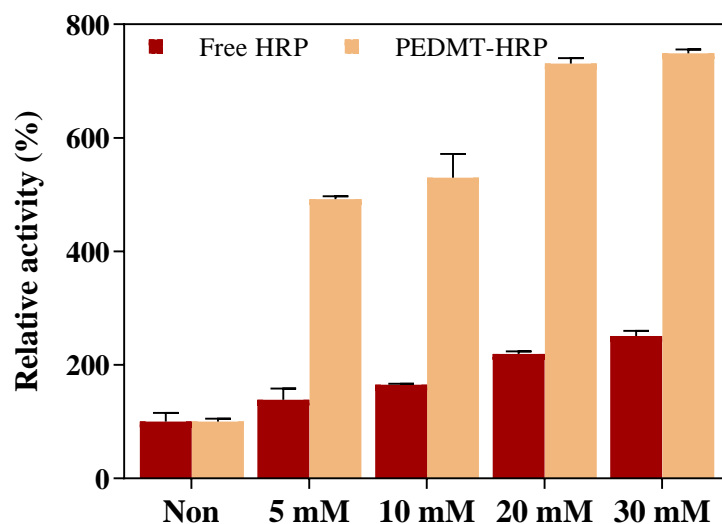
Figure 4.13. Effect of Fe^{3+} concentration on the activity of HRP and PEDMT-HRP

4.2.7. Storage stability of HRP and PEDMT-HRP

Storage stability is a crucial parameter for the commercial-scale application of the enzymes. It is well known that the enzyme in solution is unstable during storage, and its activity decreases spontaneously over time. Therefore, the storage stability of both free HRP and PEDMT-HRP was investigated at room temperature for 4 weeks. As seen in Figure 4.14, free HRP showed a downward trend over time. After 4 weeks, the free enzyme and PEDMT-HRP lost approximately 53% and 33% of their initial activity, respectively. The free enzyme's stability is lower because it is easily affected by environmental factors such as temperature and pH. Due to the protein structure, it can not

67

adapt to environmental changes and may become denatured. However, immobilized enzymes generally adapt to environmental conditions better than free enzymes due to their stable conformational state and strong interactions with the carrier matrix (Noma et al., 2020). The results showed that immobilization of HRP onto the PEDMT microbeads increased the stability of the enzyme.
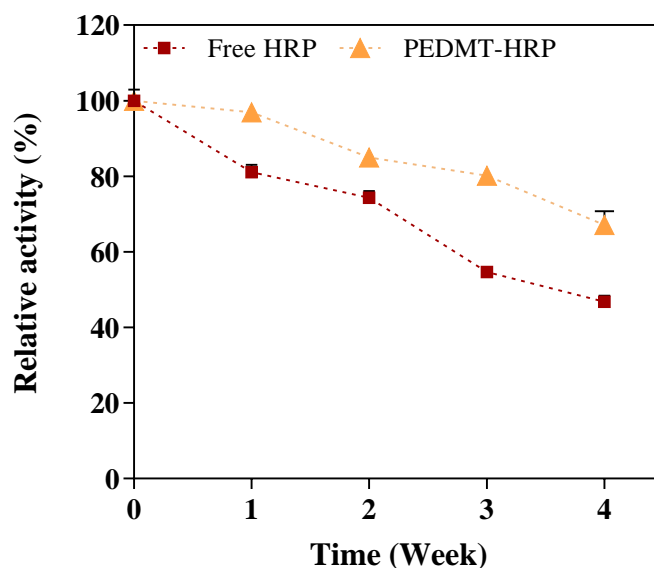
Figure 4.14. Storage stability of free HRP and PEDMT-HRP

4.2.8. Reusability

Reusability is one of the most critical parameters that make immobilized enzymes more advantageous over free enzymes (Vineh et al., 2020). Therefore, the reusability of the PEDMT-HRP was investigated, and the results are shown in Figure 4.15. As can be seen from the results, the immobilized enzyme retained approximately 55% of its initial activity even after the 10th use. It proves that the PEDMT-HRP is suitable for reuse. A decrease in activity may have occurred due to enzyme leakage or disruption of protein conformation (Jankowska et al., 2021). While free enzymes are easily denatured and used only once, immobilized enzymes can be separated from the reaction medium and used many times. Reusability also reduces the cost of immobilized enzymes and prevents the side effects (Ulu et al., 2018; Bayramoglu et al., 2012). As a result, the PEDMT-HRP is effective in reusing many times, which shows that it has potential for application in industry.
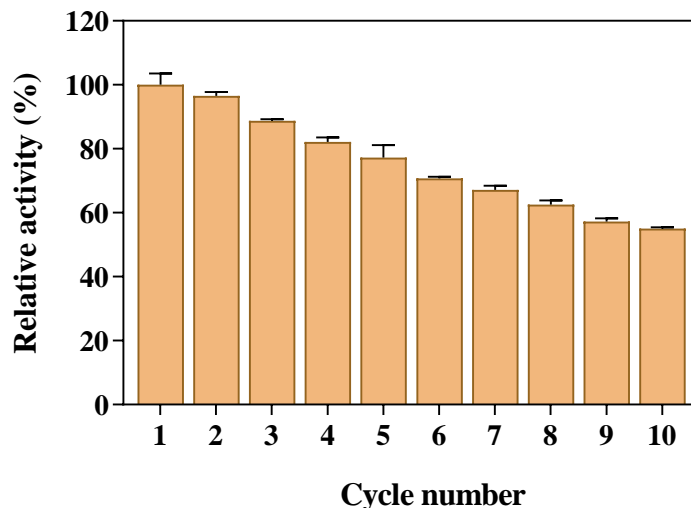
Figure 4.15. Reusability of PEDMT-HRP

4.3. *Km* and *Vmax* values

To investigate the effect of immobilization on enzyme activity, kinetic parameters of free HRP and PEDMT-HRP were calculated through Lineweaver–Burk plot (Figure 4.16). *Vmax* (maximum velocity) is the maximum rate of an enzymatic reaction when it is saturated by the substrate. *Km* (Michaelis constant) is the substrate concentration that allows to reach half of the maximum velocity, and it shows how quickly an enzyme is saturated by the substrate. *Km* values of free and immobilized enzymes were determined as 3.66 mM and 0.76 mM, respectively. PEDMT-HRP's *Km* value was 4.8 times higher than free HRP, indicating that the HRP's affinity for o-dianisidine remarkably increased after immobilization. It can be said that the active site of PEDMT-HRP was efficiently filled and bounded with the substrate. The *Vmax* value of free HRP (0.23 µmol/min) was 4.6 times higher than that of PEDMT-HRP (0.05 µmol/min). Generally, the kinetic parameters displayed that the immobilization of HRP on PEDMT microbeads increased its substrate affinity and enhanced the formation of enzyme-substrate complexes.
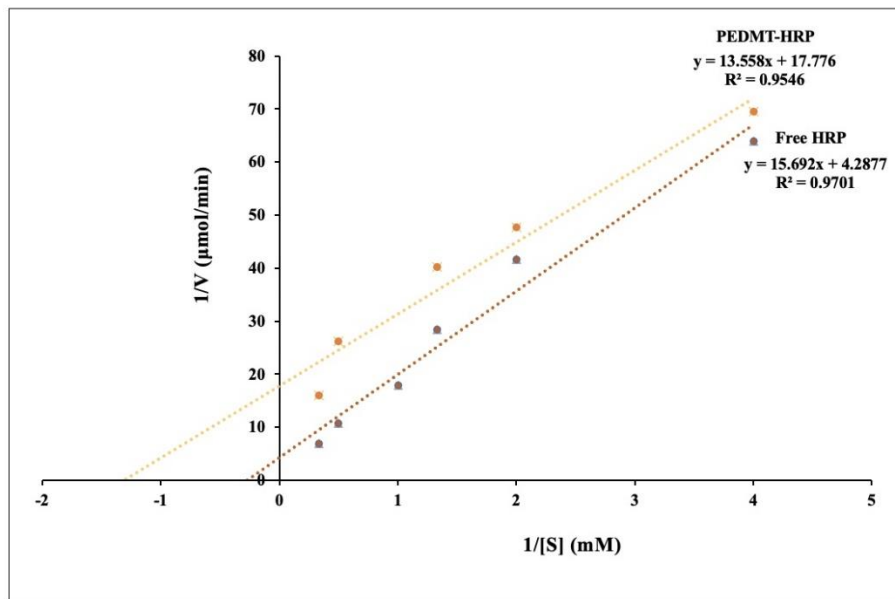
Figure 4.16. Lineweaver–Burk plots for HRP and PEDMT-HRP

4.4. Decolorization of CR and RB5 solutions

HRP is an enzyme with a high biotechnological potential and can oxidize various aromatic pollutants. For this reason, the use of immobilized enzymes in decolorization of CR and RB5 was investigated and compared with the free enzyme. Since the maximum absorbance of some dyes changes with pH, UV-spectra of CR and RB5 were prepared in the wavelength of 200 nm to 800 nm. It was observed that CR has maximum absorbance values between 487-560 nm, while RB5 has only one maximum absorbance value at 598 nm for all pHs.

4.4.1. Decolorization pH

Textile wastewater can have a broad range of pH values. Therefore it is vital to ensure that obtained immobilized enzyme illustrates high activity under acidic, basic, and neutral conditions (Jin et al., 2018). Figure 4.17 shows the impact of pH on the enzymatic decolorization of CR and RB5 solutions. It was found that both free HRP and PEDMT-HRP showed the best decolorization at pH 6.0 with CR and RB5. The highest decolorization percentage for PEDMT-HRP was 89% (CR) and 84% (RB5), whereas for free HRP, it was 48% (CR) and 43% (RB5). As demonstrated, in contrast with free HRP, PEDMT-HRP can decolorize CR and RB5 more efficiently (by 41%) over a broader pH range (from 6 to 8), providing an advantage for the use of PEDMT-HRP in the industry.
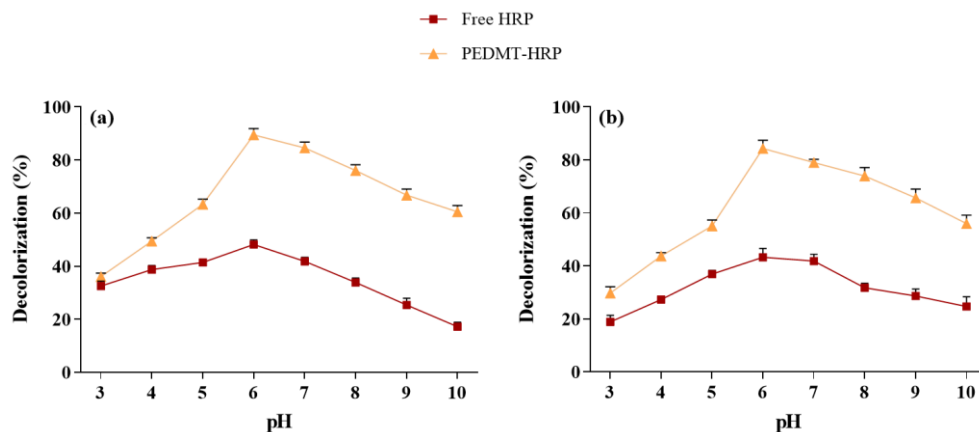
Figure 4.17. Effect of pH on decolorization of (a) CR and (b) RB5 solutions

4.4.2. Decolorization dye concentration

Substrate concentration significantly affects the enzyme's performance. The increase in substrate concentration increases the reaction rate until it achieves its maximum. After the active center is fullfilled with the substrate, further addition of substrate will no longer affect the reaction rate (Mohan et al., 2005). Thus the effect of dye concentration on the enzyme's decolorization ability was investigated and the results were depicted in Figure 4.18. The free HRP and PEDMT-HRP could optimally remove the color of CR and RB5 at a concentration of 25 mg/L (PEDMT-HRP removed the color of CR at 25 mg/L and 50 mg/L with very close efficiency). It was observed that as the dye concentration increased, the color removal decreased. As a result, 25 mg/L is the limiting dye concentration value for optimal decolorization under established experimental conditions.
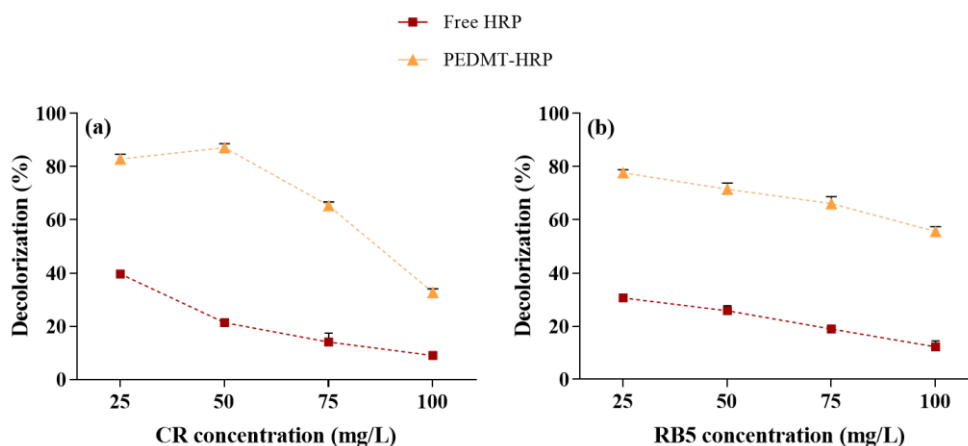
Figure 4.18. Effect of dye concentration on decolorization of (a) CR and (b) RB5 solutions

4.4.3. Decolorization microbead amount and enzyme concentration

Since enzymes have a finite lifetime, enzymatic decolorization reactions directly depend on the amount of added enzyme (Mohan et al., 2005). Figure 4.19 represents the dependence of decolorization on PEDMT-HRP's amount and free HRP's concentration, respectively. The results showed that the increase of PEDMT-HRP's amount from 10 to 50 mg and free HRP's solution volume from 50 to 150 µL resulted in a tremendous increase in the percentage of decolorization of CR (by 47% with PEDMT-HRP and 16% with free HRP) and RB5 (by 39% with PEDMT-HRP and 19% with free HRP). However, the further increase in free and immobilized enzyme amount did not significantly affect the decolorization ratio. Therefore, 50 mg of PEDMT-HRP and 150 µL of free HRP are assumed to be the optimum enzyme amount under experimental conditions.
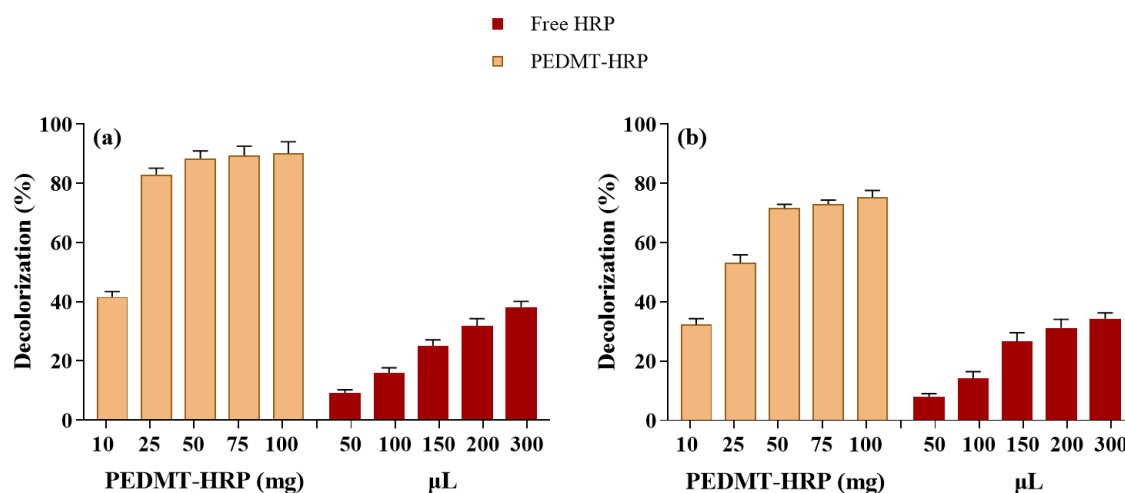
Figure 4.19. Effect of microbead amount and enzyme concentration on decolorization of (a) CR and (b) RB5 solutions

4.4.4. Decolorization H_2O_2 concentration

The H_2O_2 concentration dramatically affects the efficiency of the HRP enzyme (Jin et al., 2018). The dependence of CR and RB5 decolorization on H_2O_2 concentration is given in Figure 4.20. The highest CR and RB5 decolorization ratios with free HRP (36% for both dyes) and PEDMT-HRP (91% for CR, 81% for RB5) were obtained at 3% H_2O_2 concentration, while 1% H_2O_2 had the lowest efficiency. There was a rapid increase in the decolorization ratios with an increase in H_2O_2 concentration; however further increase resulted in the decrease of decolorization ratio. A similar optimum H_2O_2 concentration

(3%) was suggested by Kurtuldu et al. (2022), where HRP was adsorbed onto UiO-66-NH_2 and used in Methylene Blue and MO decolorization. The immobilized enzyme effectively decolorized both dyes over a broader H_2O_2 concentration range, demonstrating that PEDMT-HRP has greater tolerance to H_2O_2 than free HRP.
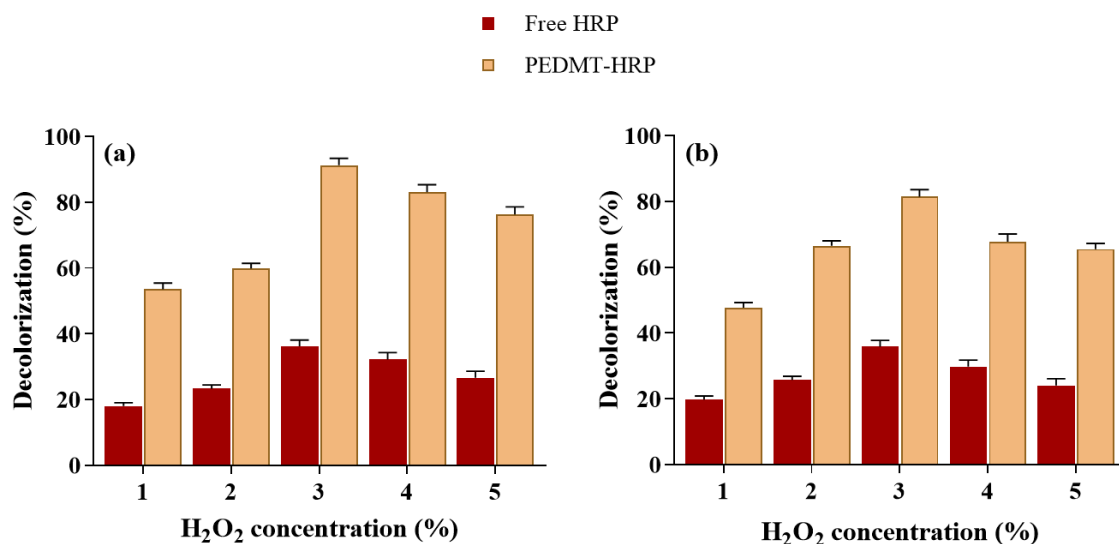
Figure 4.20. Effect of H_2O_2 concentration on decolorization of (a) CR and (b) RB5 solutions

4.4.5. Decolorization time

Determining the optimum contact time helps to achieve the best decolorization efficiency within the shortest period and, thus, reduces process consumption and cost. Figure 4.21 depicts the effect of contact time on CR and RB5 decolorization. According to the results, in the case of the free enzyme, the maximum decolorization was achieved after 120 minutes of reaction (31% for CR and 34% for RB5). The PEDMT-HRP, on the other hand, showed efficient color removal in 60 min but achieved its maximum efficiency after 120 min of incubation (83% for CR and 82% for RB5). The decolorization performance of both enzymes did not significantly change with an additional increase in time which might be due to the decrease in dye concentration. The same optimum reaction time (120 min) was reported by Karim et al. (2012), who cross-linked HRP onto the β-CD-chitosan complex and used it in the decolorization of dye mix (Cypress Green and Sultan Red). Farias et al. (2017) immobilized HRP into calcium alginate gel beads through encapsulation and applied in dye decolorization. They found that the optimum contact

time for Reactive Blue 221 and Reactive Blue 198 were 180 min and 240 min, respectively.
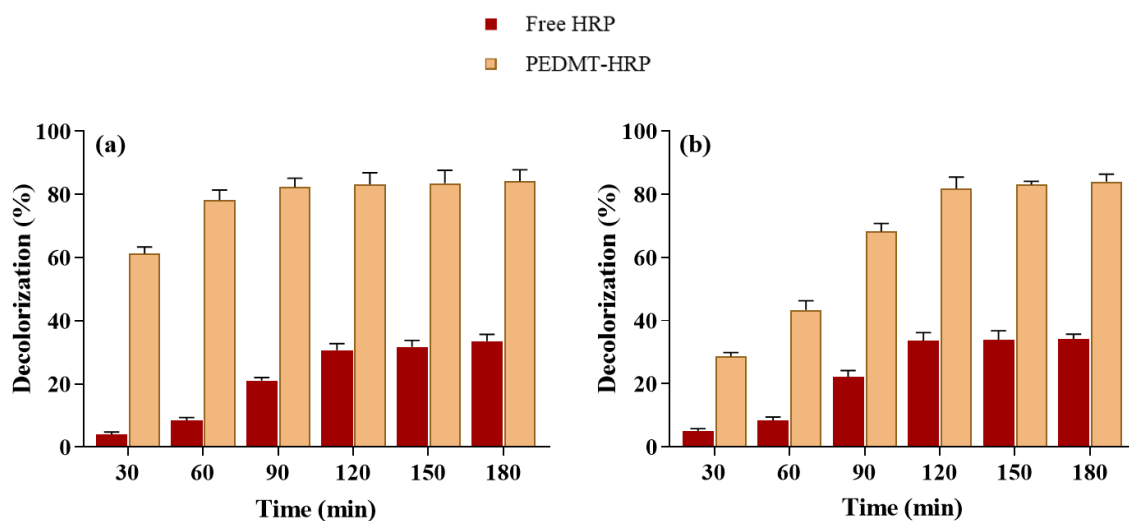
Figure 4.21. Effect of contact time on decolorization of (a) CR and (b) RB5 solutions

4.4.6. Reusability of PEDMT-HRP for decolorization

Reusability is an essential parameter of an immobilized enzyme, reducing the cost in applications (Jin et al., 2018). The reusability of PEDMT-HRP was evaluated in decolorization, and the results are presented in Figure 4.22. The immobilized enzyme saved 89% and 27% of its efficiency after three subsequent reactions with CR and RB5 solutions, respectively. PEDMT-HRP was reusable up to 10 and 5 cycles with CR and RB5 solutions, retaining 44% and 17% of initial efficiency, respectively. Gholami-Borujeni et al., 2011 encapsulated HRP into calcium alginate gel beads and tested its reusability with Acid Orange 7 and Acid Blue 25 dyes. The authors reported that the synthesized material could be reused for ten cycles with 10% remaining efficiency. Yapaoz and Attar (2020) published that HRP entrapped and cross-linked onto Na-alginate saved 74% of initial efficiency after ten reuse with Acid Yellow 11. The results proved that PEDMT-HRP displayed fairly good reusability compared to the literature, and it is a successful biocatalyst with reliable operational stability. The decrease in the decolorization ratio in the following cycles is probably due to the dye adsorption onto PEDMT-HRP, which could block the enzyme's active site.
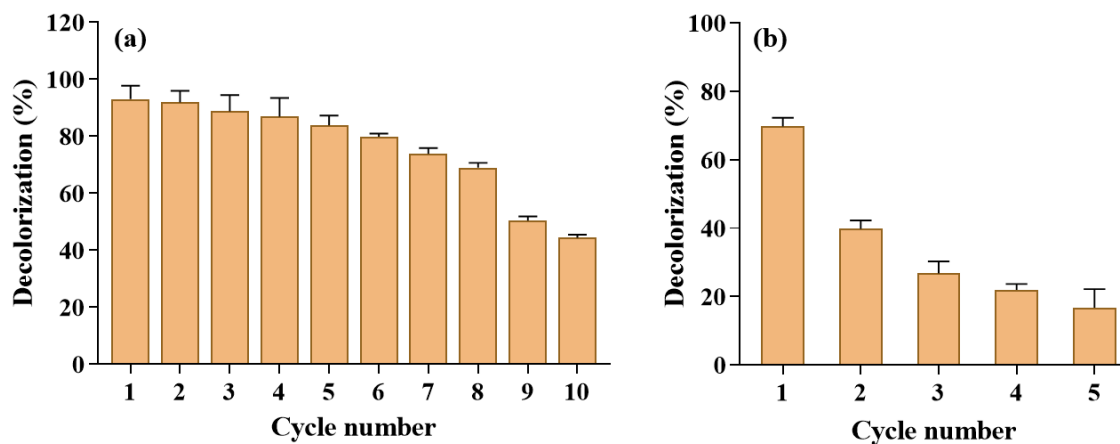
Figure 4.22. Reusability of PEDMT-HRP in decolorization of (a) CR and (b) RB5 solutions

4.4.7. HPLC studies

HPLC study was carried out to monitor the simultaneous decolorization process of the solution containing a mixture of CR and RB5 dyes. The maximum wavelengths of CR and RB5 were found and detected at 598 and 505 nm, respectively. Figure 4.23 shows the decolorization results of CR and RB5 by PEDMT-HRP at 50 mg/L dye concentration, 400 μL H_2O_2, 30 min contact time, 45 °C temperature, 15 mg for PEDMT-HRP and 400 μL for free HRP. It is worth noting that PEDMT-HRP achieved the almost complete decolorization of CR (98%) and half decolorization of RB5 (48%). In contrast, free HRP exhibited only 21% (CR) and 1% (RB5) of decolorization.
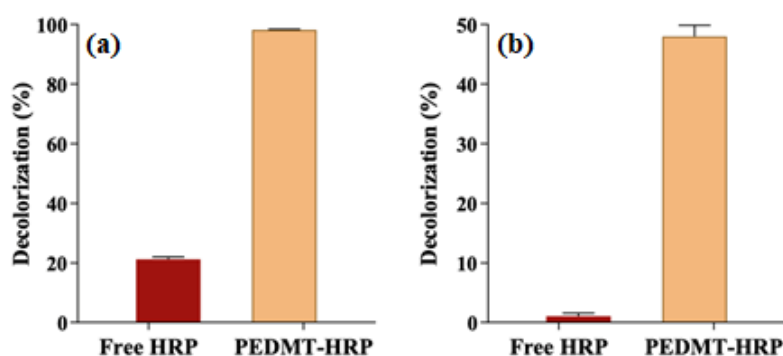
Figure 4.23. Decolorization ratio for (a) CR and (b) RB5 under optimum conditions

Figure 4.24 demonstrates the results of the study where CR and RB5 were decolorized at the same time in the same solution. The results revealed that PEDMT-HRP could simultaneously decolorize both dyes efficiently. A maximum decolorization ratio of 94% and 29%, respectively, with CR and RB5 was obtained by PEDMT-HRP, while free enzyme displayed only 4.5% of decolorization.
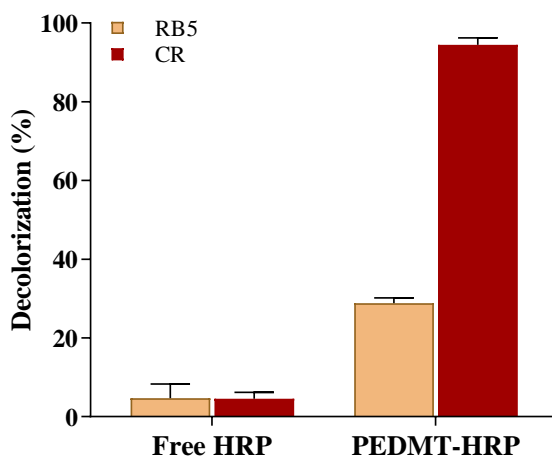
Figure 4.24. Simultaneous decolorization ratios of CR and RB5 under optimum conditions

5. CONCLUSION

This thesis investigated the potential of immobilizing HRP enzyme on polymeric microbeads and its use in dye decolorization. HRP was immobilized onto PEDMT microbeads by adsorption method. The efficiencies of free and immobilized HRP enzyme were compared by investigating the parameters affecting the immobilization. Then, the effectiveness of immobilized HRP in decolorization of CR and RB5 dyes was examined. The findings of the study are as follows:

- The PEDMT microbeads were synthesized through suspension polymerization by cross-linking MATrp monomers with EGDMA. After that, microbeads were characterized via FTIR, SEM-EDX and BET analysis.

- SEM images of PEDMT exhibited that microbeads have a highly porous and spherical structure with a diameter of approximately 150 μm.

- SEM-EDX analysis demonstrated that PEDMT contains carbon C, nitrogen N, and oxygen O elements. The PEDMT-HRP contains carbon C, nitrogen N, and oxygen O elements, but it included S and had a higher amount of N atoms.

- BET analysis demonstrated that microbeads have a pore volume of 1.94 cm^3 g^{-1}, a pore size of 9.99-55.3 A^0, and a surface area of 1103 m^2 g^{-1}. Nitrogen adsorption/desorption isotherms and pore diameter distribution graphs were built.

- Immobilization parameters such as immobilization yield, activity yield, and immobilization efficiency were determined and had a value of 84.86 ± 2.06%, 73.78 ± 5.91%, and 86.95 ± 6.92%, respectively.

- The optimum pH of the free HRP and PEDMT-HRP was found as pH 6.0.

- The optimum temperature of free HRP was assessed as 45 °C, and PEDMT-HRP's as 50 °C.

- The optimum H_2O_2 concentration for free HRP and PEDMT-HRP was 3% H_2O_2.

- The thermal stability of enzymes was estimated. After 3 h at 50 °C, free HRP saved 28%, and PEDMT-HRP saved 50% of its activity.

- The effect of metal ions on enzyme activity was determined. Ag^+, Cu^{2+}, and Fe^{3+} increased the activity of free HRP by 16%, 30%, and 45%, and PEDMT-HRP by 62%, 65%, and 93%, respectively. In the presence of other metal ions (Ca^{2+}, Co^{2+},

Mg^{2+}, Ni^{2+}, Sc^{3+}, Zn^{2+}, and Pb^{2+}), free HRP lost some of its activity, but PEDMT-HRP had an increased activity.

- The effect of Ca^{2+} and Fe^{3+} concentration on enzyme activity was determined. At 30 mM Ca^{2+} concentration, free HRP lost half of its activity, while PEDMT-HRP gained 80% of activity. 30 mM of Fe^{3+} increased the free enzyme's activity by 2.5 times, but the immobilized enzyme's activity by 7.5 times.

- Effect of organic solvents on enzyme activity was investigated. The enzymes were not inhibited only by two solvents: DMSO and ethanol. Other solvents (dichloromethane, toluene, diethyl ether, chloroform and benzene) decreased the activity of both free HRP and PEDMT-HRP.

- The storage stability of free HRP and PEDMT-HRP was investigated at room temperature. After 4 weeks, free HRP and PEDMT-HRP saved approximately 47% and 67% of their initial activity, respectively.

- The reusability of PEDMT-HRP was also tested. Reusing the PEDMT-HRP for 10 cycles was possible and it saved 55% of its initial activity.

- *Km* values of free and immobilized enzyme were detected as 3.66 mM and 0.76 mM, while *Vmax* values were 0.23 and 0,05 μmol/min, respectively.

- The use of PEDMT-HRP in the decolorization of CR and RB5 solutions was examined and compared with free HRP.

- The effect of pH on decolorization was studied. It was found that both free HRP and PEDMT-HRP showed the best decolorization at pH 6.0 with CR and RB5.

- The effect of dye concentration on the enzyme's decolorization ability was analyzed. The optimum dye concentration for free HRP and PEDMT-HRP for decolorization of CR and RB5 was 25 mg/L.

- The influence of the enzyme amount on dye decolorization was determined. 50 mg of PEDMT-HRP and 150 μL free HRP were the optimum enzyme amounts for decolorizing both dyes.

- The dependence of decolorization ratio to H_2O_2 concentration was investigated. The highest CR and RB5 decolorization ratios with free HRP and PEDMT-HRP were obtained at 3% H_2O_2 concentration.

- The effect of contact time on the decolorization ratio was investigated. According to the results, maximum CR and RB5 decolorization ratio by free HRP and PEDMT-HRP was achieved for 2 h.

- The reusability of PEDMT-HRP in decolorization reactions was evaluated. PEDMT-HRP preserved 44% of activity after 10 cycles with CR and 17% after 5 cycles with RB5.

- Decolorization of CR and RB5 solutions were followed with an HPLC analysis. PEDMT-HRP achieved the almost complete decolorization for CR (98%) and half decolorization for RB5 (48%), while free HRP exhibited 21% (CR) and 1% (RB5) decolorization. Also, CR and RB5 were decolorized simultaneously in the same solution. The results revealed that PEDMT-HRP could simultaneously decolorize both dyes with 94% (CR) and 29% (RB) efficiency. The free enzyme showed 4.5% decolorization ratio.

- The results obtained in this study proved that PEDMT is a resistant and durable support for the immobilization of enzymes. HRP was successfully immobilized onto PEDMT and stability and activity of PEDMT-HRP were higher than the free enzyme. Moreover, experiments showed that PEDMT-HRP has a high application potential in decolorizing azo dyes.

REFERENCES

Abbas, M., & Trari, M. (2015). Kinetic, equilibrium and thermodynamic study on the removal of Congo Red from aqueous solutions by adsorption onto apricot stone. *Process Safety and Environmental Protection*, 98, 424-436. https://doi.org/10.1016/j.psep.2015.09.015

Abdelrahman, T. & Neon, H. (2011). Wound dressings: principles and practice. *Surgery*, 29(10), 491–495.https://doi.org/10.1016/j.mpsur.2011.06.007

Abdulaal, W. H., Almulaiky, Y. Q., & El-Shishtawy, R. M. (2020). Encapsulation of HRP enzyme onto a magnetic Fe3O4 Np–PMMA film via casting with sustainable biocatalytic activity. *Catalysts*, 10(2), 181. doi:10.3390/catal10020181

Adnan, L. A., Sathishkumar, P., Yusoff, A. R. M., & Hadibarata, T. (2015). Metabolites characterisation of laccase mediated Reactive Black 5 biodegradation by fast growing ascomycete fungus Trichoderma atroviride F03. *International Biodeterioration & Biodegradation*, 104, 274-282. https://doi.org/10.1016/j.ibiod.2015.05.019

Aehle, W. (2004). Enzymes in industry: production and applications (Second. Enzymes in industry: production and applications (Second, completely revised edition)., (Ed. 2).

Afaq, S., & Iqbal, J. (2001). Immobilization and stabilization of papain on chelating sepharose: a metal chelate regenerable carrier. *Electronic Journal of Biotechnology*, 4(3), 1-2. DOI:10.2225/vol4-issue3-fulltext-1

Afkhami, A., & Moosavi, R. (2010). Adsorptive removal of Congo red, a carcinogenic textile dye, from aqueous solutions by maghemite nanoparticles. *Journal of hazardous materials*, 174(1-3), 398-403. doi:10.1016/j.jhazmat.2009.09.066

Aldhahri, M., Almulaiky, Y. Q., El-Shishtawy, R. M., Al-Shawafi, W. M., Salah, N., Alshahrie, A., & Alzahrani, H. A. (2021). Ultra-thin 2D CuO nanosheet for HRP immobilization supported by encapsulation in a polymer matrix: characterization and dye degradation. *Catalysis Letters*, 151(1), 232-246. https://doi.org/10.1007/s10562-020-03289-7

Ali, N., Uddin, S., Khan, A., Khan, S., Khan, S., Ali, N., & Bilal, M. (2020). Regenerable chitosan-bismuth cobalt selenide hybrid microspheres for mitigation of organic pollutants in an aqueous environment. *International Journal of Biological Macromolecules*, 161, 1305-1317. https://doi.org/10.1016/j.ijbiomac.2020.07.132

Al-Maqdi, K. A., Elmerhi, N., Athamneh, K., Bilal, M., Alzamly, A., Ashraf, S. S., & Shah, I. (2021). Challenges and Recent Advances in Enzyme-Mediated Wastewater Remediation—A Review. *Nanomaterials*, 11(11), 3124. https://doi.org/10.3390/nano11113124

Altikatoglu, M., Arioz, C., Basaran, Y., & Kuzu, H. (2009). Stabilization of horseradish peroxidase by covalent conjugation with dextran aldehyde against temperature and

pH changes. *Open Chemistry*, 7(3), 423-428. https://doi.org/10.2478/s11532-009-0041-z

Altikatoglu Yapaoz, M., & Attar, A. (2020). An accomplished procedure of horseradish peroxidase immobilization for removal of acid yellow 11 in aqueous solutions. *Water Science and Technology*, 81(12), 2664-2673. https://doi.org/10.2166/wst.2020.326

Alturkistani, H. A., Tashkandi, F. M., & Mohammedsaleh, Z. M. (2016). Histological stains: a literature review and case study. *Global journal of health science*, 8(3), 72. https://doi.org/10.5539/gjhs.v8n3p72

Alver, E., Bulut, M., Metin, A. Ü., & Çiftçi, H. (2017). One step effective removal of Congo Red in chitosan nanoparticles by encapsulation. *Spectrochimica Acta Part A: Molecular and Biomolecular Spectroscopy*, 171, 132-138. https://doi.org/10.1016/j.saa.2016.07.046

Amer, O. A., Ali, S. S., Azab, M., El-Shouny, W. A., Sun, J., & Mahmoud, Y. A. G. (2022). Exploring new marine bacterial species, Alcaligenes faecalis Alca F2018 valued for bioconversion of shrimp chitin to chitosan for concomitant biotechnological applications. *International Journal of Biological Macromolecules*, 196, 35-45. https://doi.org/10.1016/j.ijbiomac.2021.12.033

Arslan, M. (2011). Immobilization horseradish peroxidase on amine-functionalized glycidyl methacrylate-g-poly (ethylene terephthalate) fibers for use in azo dye decolorization. *Polymer bulletin*, 66(7), 865-879. https://doi.org/10.1007/s00289-010-0316-8

Barnard, A. (2012). The optimization of the extraction and purification of horseradish peroxidase from horseradish roots (Doctoral dissertation, Stellenbosch: Stellenbosch University).

Bayramoglu, G., Akbulut, A., & Arica, M. Y. (2021). Utilization of immobilized horseradish peroxidase for facilitated detoxification of a benzidine based azo dye. *Chemical Engineering: Research and Design*, 165, 435-444. https://doi.org/10.1016/j.cherd.2020.11.017

Bayramoglu, G., Altintas, B., & Yakup Arica, M. (2012). Cross-linking of horseradish peroxidase adsorbed on polycationic films: utilization for direct dye degradation. *Bioprocess and biosystems engineering*, 35(8), 1355-1365. https://doi.org/10.1007/s00449-012-0724-2

Bazrafshan, E., Kord Mostafapour, F., Rahdar, S., & Mahvi, A. H. (2015). Equilibrium and thermodynamics studies for decolorization of Reactive Black 5 (RB5) by adsorption onto MWCNTs. *Desalination and Water Treatment*, 54(8), 2241-2251. https://doi.org/10.1080/19443994.2014.895778

Bilal, M., Iqbal, H. M., Shah, S. Z. H., Hu, H., Wang, W., & Zhang, X. (2016). Horseradish peroxidase-assisted approach to decolorize and detoxify dye pollutants in a packed

bed bioreactor. *Journal of environmental management*, 183, 836-842. https://doi.org/10.1016/j.jenvman.2016.09.040

Bilal, M., Asgher, M., Iqbal, H. M., Hu, H., & Zhang, X. (2017a). Bio-based degradation of emerging endocrine-disrupting and dye-based pollutants using cross-linked enzyme aggregates. *Environmental Science and Pollution Research*, 24, 7035-7041.

Bilal, M., Rasheed, T., Iqbal, H. M., Hu, H., Wang, W., & Zhang, X. (2017b). Novel characteristics of horseradish peroxidase immobilized onto the polyvinyl alcohol-alginate beads and its methyl orange degradation potential. *International journal of biological macromolecules*, 105, 328-335. https://doi.org/10.1016/j.ijbiomac.2017.07.042

Bilal, M., Iqbal, H. M., Hu, H., Wang, W., & Zhang, X. (2017c). Enhanced bio-catalytic performance and dye degradation potential of chitosan-encapsulated horseradish peroxidase in a packed bed reactor system. *Science of the Total Environment*, 575, 1352-1360. https://doi.org/10.1016/j.scitotenv.2016.09.215

Bilal, M., Iqbal, H. M., Hu, H., Wang, W., & Zhang, X. (2017d). Development of horseradish peroxidase-based cross-linked enzyme aggregates and their environmental exploitation for bioremediation purposes. *Journal of environmental management*, 188, 137-143. https://doi.org/10.1016/j.jenvman.2016.12.015

Bilal, M., Rasheed, T., Iqbal, H. M., Hu, H., Wang, W., & Zhang, X. (2018). Horseradish peroxidase immobilization by copolymerization into cross-linked polyacrylamide gel and its dye degradation and detoxification potential. *International journal of biological macromolecules*, 113, 983-990. https://doi.org/10.1016/j.ijbiomac.2018.02.062

Bilal, M., Adeel, M., Rasheed, T., Zhao, Y., & Iqbal, H. M. (2019a). Emerging contaminants of high concern and their enzyme-assisted biodegradation–a review. *Environment international*, 124, 336-353. https://doi.org/10.1016/j.envint.2019.01.011

Bilal, M., Rasheed, T., Zhao, Y., and Iqbal, H. M. (2019b). Agarose-chitosan hydrogel-immobilized horseradish peroxidase with sustainable bio-catalytic and dye degradation properties. *International journal of biological macromolecules*, 124, 742-749. https://doi.org/10.1016/j.ijbiomac.2018.11.220

Bindu, V. U., Shanty, A. A., & Mohanan, P. V. (2018). Parameters affecting the improvement of properties and stabilities of immobilized α-amylase on chitosan-metal oxide composites. *Int. J. Biochem. Biophys*, 6, 44-57. DOI: 10.13189/ijbb.2018.060203

Bonnet, C., Andreescu, S., & Marty, J. L. (2003). Adsorption: an easy and efficient immobilisation of acetylcholinesterase on screen-printed electrodes. *Analytica Chimica Acta*, 481(2), 209-211. https://doi.org/10.1016/S0003-2670(03)00122-3

Borza, P., Benea, I. C., Bitcan, I., Todea, A., Muntean, S. G., & Peter, F. (2020). Enzymatic degradation of azo dyes using peroxidase immobilized onto commercial carriers with

epoxy groups. *Studia Universitatis Babes-Bolyai, Chemia*, 65(1). https://doi.org/10.24193/subbchem.2020.1.22

Borthakur, P., Boruah, P. K., Hussain, N., Silla, Y., & Das, M. R. (2017). Specific ion effect on the surface properties of Ag/reduced graphene oxide nanocomposite and its influence on photocatalytic efficiency towards azo dye degradation. *Applied Surface Science*, 423, 752-761. https://doi.org/10.1016/j.apsusc.2017.06.230

Boudrant, J., Woodley, J. M., & Fernandez-Lafuente, R. (2020). Parameters necessary to define an immobilized enzyme preparation. *Process Biochemistry*, 90, 66-80.

Brady, D., Jordaan, J., Simpson, C., Chetty, A., Arumugam, C., & Moolman, F. S. (2008). Spherezymes: A novel structured self-immobilisation enzyme technology. *Bmc Biotechnology*, 8(1), 1-11. https://doi.org/10.1186/1472-6750-8-8

Brady, D., & Jordaan, J. (2009). Advances in enzyme immobilisation. *Biotechnology letters*, 31, 1639-1650. https://doi.org/10.1007/s10529-009-0076-4

Brandão-Lima, L. C., Silva, F. C., Costa, P. V., Alves-Júnior, E. A., Viseras, C., Osajima, J. A., & Silva-Filho, E. C. (2021). Clay mineral minerals as a strategy for biomolecule incorporation: *Amino acids approach. Materials*, 15(1), 64. DOI:10.3390/ma15010064

Brena, B. M., & Batista-Viera, F. (2006). Immobilization of enzymes: a literature survey. *Immobilization of enzymes and cells*, 15-30.

Calleri, E., Ambrosini, S., Temporini, C., & Massolini, G. (2012). New monolithic chromatographic supports for macromolecules immobilization: challenges and opportunities. *Journal of pharmaceutical and biomedical analysis*, 69, 64-76. https://doi.org/10.1016/j.jpba.2012.01.032

Cao, L. (2005). Immobilised enzymes: science or art?. *Current opinion in chemical biology*, 9(2), 217-226. https://doi.org/10.1016/j.cbpa.2005.02.014

Cao, L. (2006). Carrier-bound immobilized enzymes: principles, application and design. John Wiley & Sons.

Cano, O. A., González, C. R., Paz, J. H., Madrid, P. A., Casillas, P. G., Hernández, A. M., & Pérez, C. M. (2017). Catalytic activity of palladium nanocubes/multiwalled carbon nanotubes structures for methyl orange dye removal. *Catalysis Today*, 282, 168-173. https://doi.org/10.1016/j.cattod.2016.06.053

Çelebi, S., İbibikcan, E., Kayahan, S. K., Yiĝitsoy, B., & Toppare, L. (2009). Immobilization of Invertase in Copolymer of 2, 5-Di (thiophen-2-yl)-1-p-Tolyl-1 H-Pyrrole with Pyrrole. *Journal of Macromolecular Science®, Part A: Pure and Applied Chemistry*, 46(8), 739-744. https://doi.org/10.1080/10601320903004434

Celebi, M., Kaya, M. A., Altikatoglu, M., & Yildirim, H. (2013). Enzymatic decolorization of anthraquinone and diazo dyes using horseradish peroxidase enzyme immobilized onto various polysulfone supports. *Applied biochemistry and biotechnology*, 171(3), 716-730. https://doi.org/10.1007/s12010-013-0377-x

Chakraborty, J. N. (2015). Dyeing with reactive dye. In Fundamentals and practices in colouration of textiles (pp. 83-98). *WPI Publishing*.

Chang, M., & Shih, Y. H. (2018). Synthesis and application of magnetic iron oxide nanoparticles on the removal of Reactive Black 5: Reaction mechanism, temperature and pH effects. *Journal of environmental management*, 224, 235-242. https://doi.org/10.1016/j.jenvman.2018.07.021

Chatterjee, S., Chatterjee, S., Chatterjee, B. P., & Guha, A. K. (2007). Adsorptive removal of congo red, a carcinogenic textile dye by chitosan hydrobeads: binding mechanism, equilibrium and kinetics. *Colloids and Surfaces A: Physicochemical and Engineering Aspects*, 299(1-3), 146-152. DOI:10.1016/j.colsurfa.2006.11.036

Chatterjee, S., Lee, M. W., & Woo, S. H. (2010). Adsorption of congo red by chitosan hydrogel beads impregnated with carbon nanotubes. *Bioresource technology*, 101(6), 1800-1806. doi:10.1016/j.biortech.2009.10.051

Chen, Y. Y., Yu, S. H., Jiang, H. F., Yao, Q. Z., Fu, S. Q., & Zhou, G. T. (2018). Performance and mechanism of simultaneous removal of Cd (II) and Congo red from aqueous solution by hierarchical vaterite spherulites. *Applied Surface Science*, 444, 224-234. https://doi.org/10.1016/j.apsusc.2018.03.081

Chinta, S. K. & VijayKumar, S. (2013). Technical facts & figures of reactive dyes used in textiles. *Int J Eng Manag Sci*, 4(3), 308-12.

Christie, R. (2014). Colour chemistry. *Royal society of chemistry*.

Cowan, D. A., & Fernandez-Lafuente, R. (2011). Enhancing the functional properties of thermophilic enzymes by chemical modification and immobilization. Enzyme and *Microbial Technology*, 49(4), 326-346. https://doi.org/10.1016/j.enzmictec.2011.06.023

Crestini, C., Melone, F., & Saladino, R. (2011). Novel multienzyme oxidative biocatalyst for lignin bioprocessing. *Bioorganic ve medicinal chemistry*, 19(16), 5071-5078. https://doi.org/10.1016/j.bmc.2011.05.058

Deng, H., Zhang, M., Cao, Y., & Lin, Y. (2019). Decolorization of Reactive Black 5 by Mesoporous Al2O3@ TiO2 Nanocomposites. *Environmental Progress & Sustainable Energy*, 38(s1), S230-S242. https://doi.org/10.1002/ep.12976

Demiray, E., Günan Yücel, H., Özkuzucu, H. E., Ertuğrul Karatay, S., Aksu, Z., & Dönmez, G. (2021). Synergistic effect of CTAB on Reactive Black 5 removal performance of

Candida tropicalis. *Bioremediation Journal*, 1-11. https://doi.org/10.1080/10889868.2021.1994521

Dizge, N., Aydiner, C., Demirbas, E., Kobya, M., & Kara, S. (2008). Adsorption of reactive dyes from aqueous solutions by fly ash: kinetic and equilibrium studies. *Journal of hazardous materials*, 150(3), 737-746. https://doi.org/10.1016/j.jhazmat.2007.05.027

Dursun, A. Y., Tepe, O., Uslu, G., Dursun, G., & Saatci, Y. (2013). Kinetics of Remazol Black B adsorption onto carbon prepared from sugar beet pulp. *Environmental Science and Pollution Research*, 20(4), 2472-2483. https://doi.org/10.1007/s11356-012-1133-4

El-Nahass, M. N., El-Keiy, M. M., & Ali, E. M. (2018). Immobilization of horseradish peroxidase into cubic mesoporous silicate, SBA-16 with high activity and enhanced stability. *International journal of biological macromolecules*, 116, 1304-1309. https://doi.org/10.1016/j.ijbiomac.2018.05.025

El Sikaily, A., Khaled, A., & El Nemr, A. (2012). Textile dyes xenobiotic and their harmful effect. Nonconventional textile waste water treatment (A. El Nemr Ed.), *Nova Science Publishers Inc.*, New York, USA, 31-64.

Eren, Z., & Acar, F. N. (2006). Adsorption of Reactive Black 5 from an aqueous solution: equilibrium and kinetic studies. *Desalination*, 194(1-3), 1-10. https://doi.org/10.1016/j.desal.2005.10.022

Eş, I., Vieira, J. D. G., & Amaral, A. C. (2015). Principles, techniques, and applications of biocatalyst immobilization for industrial application. *Applied microbiology and biotechnology*, 99, 2065-2082. DOI:10.1007/s00253-015-6390-y

Farhina, P., & Uzma, F. (2019). Use of Enzyme Technology for the Degradation of Harmful Xenobiotics (Aromatic Dye). *Indo Am. J. P. Sci*, 06(03), 6693-6699.

Farias, S., Mayer, D. A., de Oliveira, D., de Souza, S., & de Souza, A. A. U. (2017). Free and Ca-alginate beads immobilized horseradish peroxidase for the removal of reactive dyes: an experimental and modeling study. *Applied biochemistry and biotechnology*, 182(4), 1290-1306. https://doi.org/10.1007/s12010-017-2399-2

Faryadi, M., Rahimi, M., & Akbari, M. (2016). Process modeling and optimization of Rhodamine B dye ozonation in a novel microreactor equipped with high frequency ultrasound wave. *Korean Journal of Chemical Engineering*, 33, 922-933.

Fergusson, S. M., & Padhye, R. (2019). The effect of domestic laundry detergents on the light fastness of certain reactive dyes on 100% cotton. *Textile Research Journal*, 89(6), 1105-1112. DOI: 10.1177/0040517518760751

Flores-Rojas, G. G., López-Saucedo, F., Bucio, E., & Isoshima, T. (2017). Covalent immobilization of lysozyme in silicone rubber modified by easy chemical grafting. *MRS Communications*, 7(4), 904-912. https://doi.org/10.1557/mrc.2017.115

Foodprocessing-technology. "*CLEA Technologies*". Access: 20 February 2023. https://www.foodprocessing-technology.com/contractors/ingredients/clea/

Fraguas, L. F., Batista-Viera, F., & Carlsson, J. (2004). Preparation of high-density Concanavalin A adsorbent and its use for rapid, high-yield purification of peroxidase from horseradish roots. *Journal of Chromatography B*, 803(2), 237-241. https://doi.org/10.1016/j.jchromb.2003.12.023

Frid, P., Anisimov, S. V., & Popovic, N. (2007). Congo red and protein aggregation in neurodegenerative diseases. *Brain research reviews*, 53(1), 135-160. https://doi.org/10.1016/j.brainresrev.2006.08.001

Gajhede, M., Schuller, D. J., Henriksen, A., Smith, A. T., & Poulos, T. L. (1997). Crystal structure of horseradish peroxidase C at 2.15 Å resolution. *Nature structural biology*, 4(12), 1032-1038. DOI: 10.1038/nsb1297-1032

Garcia-Galan, C., Berenguer-Murcia, Á., Fernandez-Lafuente, R., & Rodrigues, R. C. (2011). Potential of different enzyme immobilization strategies to improve enzyme performance. *Advanced Synthesis & Catalysis*, 353(16), 2885-2904. https://doi.org/10.1002/adsc.201100534

Gholami-Borujeni, F., Mahvi, A. H., Naseri, S., Faramarzi, M. A., Nabizadeh, R., & Alimohammadi, M. (2011). Application of immobilized horseradish peroxidase for removal and detoxification of azo dye from aqueous solution. *Res J Chem Environ*, 15(2), 217-222.

Glover, BJ. (2004). Reactive Black 5. *SDCANZ International Symposium, Colouration*, 13–16.

Górecka, E., & Jastrzębska, M. (2011). Immobilization techniques and biopolymer carriers. *Biotechnology and food science*, 75(1), 65-86. https://doi.org/10.34658/bfs.2011.75.1.65-86

Gul, O. T., & Ocsoy, I. (2021). Co-Enzymes based nanoflowers incorporated-magnetic carbon nanotubes: A new generation nanocatalyst for superior removal of cationic and anionic dyes with great repeated use. *Environmental Technology & Innovation*, 24, 101992. https://doi.org/10.1016/j.eti.2021.101992

Hanefeld, U., Gardossi, L., & Magner, E. (2009). Understanding enzyme immobilisation. *Chemical Society Reviews*, 38(2), 453-468. DOI https://doi.org/10.1039/B711564B

Hamzeh, Y., Ashori, A., Azadeh, E., & Abdulkhani, A. (2012). Removal of Acid Orange 7 and Remazol Black 5 reactive dyes from aqueous solutions using a novel biosorbent. *Materials Science and Engineering: C*, 32(6), 1394-1400. https://doi.org/10.1016/j.msec.2012.04.015

Hartmann, M., & Kostrov, X. (2013). Immobilization of enzymes on porous silicas–benefits and challenges. *Chemical Society Reviews*, 42(15), 6277-6289. DOI https://doi.org/10.1039/C3CS60021A

Hassan, M. M. & Carr, C. M. (2018). A critical review on recent advancements of the removal of reactive dyes from dyehouse effluent by ion-exchange adsorbents. *Chemosphere*, 209, 201-219. https://doi.org/10.1016/j.chemosphere.2018.06.043

Hermanová, S., Zarevúcká, M., Bouša, D., Pumera, M., & Sofer, Z. (2015). Graphene oxide immobilized enzymes show high thermal and solvent stability. *Nanoscale*, 7(13), 5852-5858. DOI: 10.1039/C5NR00438A

Hoffmann, C., Pinelo, M., Woodley, J. M., & Daugaard, A. E. (2017). Development of a thiol-ene based screening platform for enzyme immobilization demonstrated using horseradish peroxidase. *Biotechnology progress*, 33(5), 1267-1277. https://doi.org/10.1002/btpr.2526

Hollmann, F., & Arends, I. W. (2012). Enzyme initiated radical polymerizations. *Polymers*, 4(1), 759-793. https://doi.org/10.3390/polym4010759

Horobin, R., & Kiernan, J. (Eds.). (2020). Conn's biological stains: a handbook of dyes, stains and fluorochromes for use in biology and medicine. *Taylor & Francis*.

Hunger, K. (Ed.). (2007). Industrial dyes: chemistry, properties, applications. John Wiley & Sons.

Hunger, K., Mischke, P., Rieper, W., Raue, R., Kunde, K., & Engel, A. (2000). Azo dyes. *Ullmann's encyclopedia of industrial chemistry*. https://doi.org/10.1002/14356007.a03_245

Husain, Q., & Ulber, R. (2011). Immobilized peroxidase as a valuable tool in the remediation of aromatic pollutants and xenobiotic compounds: a review. *Critical reviews in environmental science and technology*, 41(8), 770-804. https://doi.org/10.1080/10643380903299491

Imam, H. T., Marr, P. C., & Marr, A. C. (2021). Enzyme entrapment, biocatalyst immobilization without covalent attachment. *Green Chemistry*, 23(14), 4980-5005. DOI: 10.1039/D1GC01852C

Jafari, N., Soudi, M. R., & Kasra-Kermanshahi, R. (2014). Biodegradation perspectives of azo dyes by yeasts. Microbiology, 83(5), 484-497. DOI: 10.1134/S0026261714050130

Jafari, A. J., Kakavandi, B., Kalantary, R. R., Gharibi, H., Asadi, A., Azari, A., & Takdastan, A. (2016). Application of mesoporous magnetic carbon composite for reactive dyes removal: Process optimization using response surface methodology. *Korean Journal of Chemical Engineering*, 33(10), 2878-2890. https://doi.org/10.1007/s11814-016-0155-x

Jalali Sarvestani, M. R., & Doroudi, Z. (2020). Removal of reactive black 5 from waste waters by adsorption: a comprehensive review. *Journal of Water and Environmental Nanotechnology*, 5(2), 180-190. https://doi.org/10.22090/jwent.2020.02.008

Jalandoni-Buan, A. C., Decena-Soliven, A. L. A., Cao, E. P., Barraquio, V. L., & Barraquio, W. L. (2010). Characterization and identification of Congo red decolorizing bacteria from monocultures and consortia. *Philipp. J. Sci*, 139(1), 71-78.

Jankowska, K., Zdarta, J., Grzywaczyk, A., Degórska, O., Kijeńska-Gawrońska, E., Pinelo, M., & Jesionowski, T. (2021). Horseradish peroxidase immobilised onto electrospun fibres and its application in decolourisation of dyes from model sea water. *Process Biochemistry*, 102, 10-21. https://doi.org/10.1016/j.procbio.2020.11.015

Janović, B. S., Mićić Vićovac, M. L., Vujčić, Z. M., & Vujčić, M. T. (2017). Tailor-made biocatalysts based on scarcely studied acidic horseradish peroxidase for biodegradation of reactive dyes. *Environmental Science and Pollution Research*, 24(4), 3923-3933. https://doi.org/10.1007/s11356-016-8100-4

Jiang, Y., Tang, W., Gao, J., Zhou, L., & He, Y. (2014). Immobilization of horseradish peroxidase in phospholipid-templated titania and its applications in phenolic compounds and dye removal. *Enzyme and microbial technology*, 55, 1-6. https://doi.org/10.1016/j.enzmictec.2013.11.005

Jin, X., Li, S., Long, N., & Zhang, R. (2018). A robust and stable nano-biocatalyst by co-immobilization of chloroperoxidase and horseradish peroxidase for the decolorization of azo dyes. *Journal of Chemical Technology ve Biotechnology*, 93(2), 489-497. https://doi.org/10.1002/jctb.5379

Jun, L. Y., Yon, L. S., Mubarak, N. M., Bing, C. H., Pan, S., Danquah, M. K., & Khalid, M. (2019). An overview of immobilized enzyme technologies for dye and phenolic removal from wastewater. *Journal of Environmental Chemical Engineering*, 7(2), 102961. https://doi.org/10.1016/j.jece.2019.102961

Kamal, T., Khan, S. B., & Asiri, A. M. (2016). Synthesis of zero-valent Cu nanoparticles in the chitosan coating layer on cellulose microfibers: evaluation of azo dyes catalytic reduction. *Cellulose*, 23(3), 1911-1923. https://doi.org/10.1007/s10570-016-0919-9

Karim, Z., Adnan, R., & Husain, Q. (2012). A β-cyclodextrin–chitosan complex as the immobilization matrix for horseradish peroxidase and its application for the removal of azo dyes from textile effluent. *International Biodeterioration ve Biodegradation*, 72, 10-17. https://doi.org/10.1016/j.ibiod.2012.04.008

Kawakita, H. (2012). Metal recovery using polyphenols prepared by enzymatic reactions of horseradish peroxidase. *Science and Technology*, 2(1), 25-29. DOI: 10.5923/j.scit.20120201.05

Kawaoka, A., Kawamoto, T., Ohta, H., Sekine, M., Takano, M., & Shinmyo, A. (1994). Wound-induced expression of horseradish peroxidase. *Plant Cell Reports*, 13(3), 149-154.

Kaykıoğlu, G., & Debik, E. (2006). Color removal from textile wastewater with anaerobic treatment processes. *Sigma*, 4.

Keshta, B. E., Gemeay, A. H., & Khamis, A. A. (2022). Impacts of horseradish peroxidase immobilization onto functionalized superparamagnetic iron oxide nanoparticles as a biocatalyst for dye degradation. *Environmental Science and Pollution Research*, 29(5), 6633-6645. https://doi.org/10.1007/s11356-021-16119-z

Kotwal, S. M., & Shankar, V. (2009). Immobilized invertase. *Biotechnology Advances*, 27(4), 311-322. https://doi.org/10.1016/j.biotechadv.2009.01.009

Krajewska, B. (2004). Application of chitin-and chitosan-based materials for enzyme immobilizations: a review. *Enzyme and microbial technology*, 35(2-3), 126-139. https://doi.org/10.1016/j.enzmictec.2003.12.013

Krishnamoorthi, S., Banerjee, A., & Roychoudhury, A. (2015). Immobilized enzyme technology: potentiality and prospects. *J Enzymol Metabol*, 1(1), 010-104.

Kumar, S., Dwevedi, A., & Kayastha, A. M. (2009). Immobilization of soybean (Glycine max) urease on alginate and chitosan beads showing improved stability: Analytical applications. *Journal of Molecular Catalysis B: Enzymatic*, 58(1-4), 138-145. https://doi.org/10.1016/j.molcatb.2008.12.006

Kurtuldu, A., Eşgin, H., Yetim, N. K., & Semerci, F. (2022). Immobilization Horseradish Peroxidase onto UiO-66-NH2 for Biodegradation of Organic Dyes. *Journal of Inorganic and Organometallic Polymers and Materials*, 1-9. https://doi.org/10.1007/s10904-022-02310-3

Kyzas, G. Z., Deliyanni, E. A., & Matis, K. A. (2014). Graphene oxide and its application as an adsorbent for wastewater treatment. *Journal of Chemical Technology & Biotechnology*, 89(2), 196-205. 10.1002/jctb.4220

Lai, Y. C., & Lin, S. C. (2005). Application of immobilized horseradish peroxidase for the removal of p-chlorophenol from aqueous solution. *Process Biochemistry*, 40(3-4), 1167-1174. https://doi.org/10.1016/j.procbio.2004.04.009

Lewis, D. M. (2011). The chemistry of reactive dyes and their application processes. In Handbook of textile and industrial dyeing (pp. 303-364). *Woodhead Publishing*. https://doi.org/10.1533/9780857093974.2.301

Li, S. F., Zhai, X. J., Zhang, C., Mo, H. L., & Zang, S. Q. (2020). Enzyme immobilization in highly ordered macro–microporous metal–organic frameworks for rapid biodegradation of hazardous dyes. *Inorganic Chemistry Frontiers*, 7(17), 3146-3153. https://doi.org/10.1039/D0QI00489H

Lima-Ramos, J., Neto, W., & Woodley, J. M. (2014). Engineering of biocatalysts and biocatalytic processes. *Topics in Catalysis*, 57, 301-320. https://doi.org/10.1007/s11244-013-0185-0

Liu, Y., & Chen, J. Y. (2016). Enzyme immobilization on cellulose matrixes. *Journal of Bioactive and Compatible Polymers*, 31(6), 553-567. https://doi.org/10.1177/0883911516637377

Liu, D. M., Chen, J., & Shi, Y. P. (2018). Advances on methods and easy separated support materials for enzymes immobilization. *TrAC Trends in Analytical Chemistry*, 102, 332-342. https://doi.org/10.1016/j.trac.2018.03.011

Lopes, L. A., Dias, L. P., da Costa, H. P. S., da Silva Neto, J. X., Morais, E. G., de Oliveira, J. T. A., & de Sousa, D. D. O. B. (2021). Immobilization of a peroxidase from Moringa oleifera Lam. roots (MoPOX) on chitosan beads enhanced the decolorization of textile dyes. *Process Biochemistry*, 110, 129-141. https://doi.org/10.1016/j.procbio.2021.07.022

Magner, E. (2013). Immobilisation of enzymes on mesoporous silicate materials. *Chemical Society Reviews*, 42(15), 6213-6222. DOI https://doi.org/10.1039/C2CS35450K

Mahapatra, N. N. (2016). Textile dyes. CRC press.

Majumdar, R., Shaikh, W. A., Chakraborty, S., & Chowdhury, S. (2022). A review on microbial potential of toxic azo dyes bioremediation in aquatic system. *Microbial Biodegradation and Bioremediation*, 241-261. https://doi.org/10.1016/B978-0-323-85455-9.00018-7

Miandad, R., Kumar, R., Barakat, M. A., Basheer, C., Aburiazaiza, A. S., Nizami, A. S., & Rehan, M. (2018). Untapped conversion of plastic waste char into carbon-metal LDOs for the adsorption of Congo red. *Journal of colloid and interface science*, 511, 402-410. https://doi.org/10.1016/j.jcis.2017.10.029

Michels, J., & Büntzow, M. (2010). Assessment of Congo red as a fluorescence marker for the exoskeleton of small crustaceans and the cuticle of polychaetes. *Journal of Microscopy*, 238(2), 95-101. https://doi.org/10.1111/j.1365-2818.2009.03360.x

Mohamed, S. A., Elaraby, N. M., Abdel-Aty, A. M., Shaban, E., Abu-Saied, M. A., Kenawy, E. R., & El-Naggar, M. E. (2021). Improvement of enzymatic properties and decolorization of azo dye: Immobilization of horseradish peroxidase on cationic maize starch. *Biocatalysis and Agricultural Biotechnology*, 38, 102208. https://doi.org/10.1016/j.bcab.2021.102208

Mohan, S. V., Prasad, K. K., Rao, N. C., & Sarma, P. N. (2005). Acid azo dye degradation by free and immobilized horseradish peroxidase (HRP) catalyzed process. *Chemosphere*, 58(8), 1097-1105. https://doi.org/10.1016/j.chemosphere.2004.09.070

Munagapati, V. S., & Kim, D. S. (2016). Adsorption of anionic azo dye Congo Red from aqueous solution by Cationic Modified Orange Peel Powder. *Journal of Molecular Liquids*, 220, 540-548. https://doi.org/10.1016/j.molliq.2016.04.119

Nadaroglu, H., Kalkan, E., Celebi, N., Tasgin, E., & Dakovic, A. (2015). Removal of reactive black 5 from wastewater using natural clinoptilolite modified with apolaccase. *Clay Minerals*, 50(1), 65-76. https://doi.org/10.1180/claymin.2015.050.1.07

Namal, O. Ö. (2017). Tekstil endüstrisi atıksularının arıtımında kullanılan proseslerin araştırılması. *Nevşehir Bilim ve Teknoloji Dergisi*, 6, 388-396. https://doi.org/10.17100/nevbiltek.322169

Nakarani, M., & Kayastha, A. M. (2007). Kinetics and diffusion studies in urease-alginate biocatalyst beads. *Advances in Traditional Medicine*, 7(1), 79-84. https://doi.org/10.3742/OPEM.2007.7.1.079

Naseem, K., Farooqi, Z. H., Begum, R., & Irfan, A. (2018). Removal of Congo red dye from aqueous medium by its catalytic reduction using sodium borohydride in the presence of various inorganic nano-catalysts: a review. *Journal of cleaner production*, 187, 296-307. https://doi.org/10.1016/j.jclepro.2018.03.209

Neto, S. A., Forti, J. C., Zucolotto, V., Ciancaglini, P., & De Andrade, A. R. (2011). The kinetic behavior of dehydrogenase enzymes in solution and immobilized onto nanostructured carbon platforms. *Process Biochemistry*, 46(12), 2347-2352. https://doi.org/10.1016/j.procbio.2011.09.019

Nisha, S., Karthick, S. A., & Gobi, N. (2012). A review on methods, application and properties of immobilized enzyme. *Chemical Science Review and Letters*, 1(3), 148-155.

Nguyen, H. H., & Kim, M. (2017). An overview of techniques in enzyme immobilization. *Applied Science and Convergence Technology*, 26(6), 157-163. https://doi.org/10.5757/ASCT.2017.26.6.157

Noma, S. A. A., Ulu, A., Acet, Ö., Sanz, R., Sanz-Pérez, E. S., Odabaşı, M., & Ateş, B. (2020). Comparative study of ASNase immobilization on tannic acid-modified magnetic Fe 3 O 4/SBA-15 nanoparticles to enhance stability and reusability. *New Journal of Chemistry*, 44(11), 4440-4451.

Oladoye, P. O., Bamigboye, O. M., Ogunbiyi, O. D., & Akano, M. T. (2022). Toxicity and decontamination strategies of Congo red dye. *Groundwater for Sustainable Development*, 100844. https://doi.org/10.1016/j.gsd.2022.100844

Onder, S., Celebi, M., Altikatoglu, M., Hatipoglu, A., & Kuzu, H. (2011). Decolorization of naphthol blue black using the horseradish peroxidase. *Applied Biochemistry and Biotechnology*, 163, 433-443.

Osman, B., Özer, E. T., Demirbel, E., Güçer, Ş., & Beşirli, N. (2013). Synthesis and characterization of L-tryptophan containing microbeads for removal of dimethyl phthalate from aqueous phase. *Separation and Purification Technology*, 109, 40-47. https://doi.org/10.1016/j.seppur.2013.02.025

Öz, S., Karaçelik, A. A., Çimen, A., Dede, B., Dumitriu, C. Ş., Aşikuzun, E., & Kiranşan, M. *Scientific Researches*, 2021.

Öztop, H. N., Hepokur, C., & Saraydin, D. (2010). Poly (acrylamide/maleic acid)–sepiolite composite hydrogels for immobilization of invertase. *Polymer bulletin*, 64(1), 27-40. https://doi.org/10.1007/s00289-009-0131-2

Patel, M., & Day, B. J. (1999). Metalloporphyrin class of therapeutic catalytic antioxidants. *Trends in pharmacological sciences*, 20(9), 359-364. https://doi.org/10.1016/S0165-6147(99)01336-X

Petri, A., Gambicorti, T., & Salvadori, P. (2004). Covalent immobilization of chloroperoxidase on silica gel and properties of the immobilized biocatalyst. *Journal of Molecular Catalysis B: Enzymatic*, 27(2-3), 103-106. https://doi.org/10.1016/j.molcatb.2003.10.001

Pierre, S. J., Thies, J. C., Dureault, A., Cameron, N. R., Van Hest, J. C., Carette, N., & Weberskirch, R. (2006). Covalent enzyme immobilization onto photopolymerized highly porous monoliths. *Advanced Materials*, 18(14), 1822-1826. https://doi.org/10.1002/adma.200600293

Pirillo, S., Rueda, E. H., & Ferreira, M. L. (2012). Supported biocatalysts for Alizarin and Eriochrome Blue Black R degradation using hydrogen peroxide. *Chemical engineering journal*, 204, 65-71. http://dx.doi.org/10.1016/j.cej.2012.07.057

Poslu, A. H., Osman, B., Kaya, Y., KOZ, Ö., & Koz, G. (2022). L-(+)-Tryptophan methyl ester derived polymeric microbeads as an efficient heterogeneous catalyst for green synthesis of 2-amino-4-(nitromethyl)-4H-chromene-3-carbonitriles. *Turkish Journal of Chemistry*, 46(5), 1642-1650.

Preethi, S., Anumary, A., Ashokkumar, M., & Thanikaivelan, P. (2013). Probing horseradish peroxidase catalyzed degradation of azo dye from tannery wastewater. *SpringerPlus*, 2(1), 1-8. https://doi.org/10.1186/2193-1801-2-341

Purkait, M. K., Maiti, A., Dasgupta, S., & De, S. (2007). Removal of congo red using activated carbon and its regeneration. *Journal of Hazardous Materials*, 145(1-2), 287-295. DOI:10.1016/j.jhazmat.2006.11.021

Qiu, Y., Zheng, Z., Zhou, Z., & Sheng, G. D. (2009). Effectiveness and mechanisms of dye adsorption on a straw-based biochar. *Bioresource technology*, 100(21), 5348-5351. https://doi.org/10.1016/j.biortech.2009.05.054

Quilles Junior, J. C., Ferrarezi, A. L., Borges, J. P., Brito, R. R., Gomes, E., Da Silva, R., & Boscolo, M. (2016). Hydrophobic adsorption in ionic medium improves the catalytic properties of lipases applied in the triacylglycerol hydrolysis by synergism. *Bioprocess and biosystems engineering*, 39, 1933-1943. https://doi.org/10.1007/s00449-016-1667-9

Qureshi, U. A., Khatri, Z., Ahmed, F., Khatri, M., & Kim, I. S. (2017). Electrospun zein nanofiber as a green and recyclable adsorbent for the removal of reactive black 5 from the aqueous phase. *ACS Sustainable Chemistry & Engineering*, 5(5), 4340-4351. https://doi.org/10.1021/acssuschemeng.7b00402

Rathi, B. S., & Kumar, P. S. (2022). Sustainable approach on the biodegradation of azo dyes: A short review. *Current Opinion in Green and Sustainable Chemistry*, 33, 100578. https://doi.org/10.1016/j.cogsc.2021.100578

Raval, N. P., Shah, P. U., & Shah, N. K. (2016). Adsorptive amputation of hazardous azo dye Congo red from wastewater: a critical review. *Environmental Science and Pollution Research*, 23(15), 14810-14853. https://doi.org/10.1007/s11356-016-6970-0

Rennke, H. G., & Venkatachalam, M. A. (1979). Chemical modification of horseradish peroxidase. Preparation and characterization of tracer enzymes with different isoelectric points. *Journal of Histochemistry & Cytochemistry*, 27(10), 1352-1353.

Romhányi, G. (1971). Selective differentiation between amyloid and connective tissue structures based on the collagen specific topo-optical staining reaction with Congo red. *Virchows Archiv A*, *354*(3), 209-222.

Sambamurthy, K. (2006). Pharmaceutical biotechnology. *New Age International*.

Sarika, D., Kumar, P. S. S. A., Arshad, S., & Sukumaran, M. K. (2015). Purification and evaluation of horseradish peroxidase activity. *International Journal of Current Microbiology and Applied Sciences*, 4(7), 367-375.

Sarkar, A. K., Pal, A., Ghorai, S., Mandre, N. R., & Pal, S. (2014). Efficient removal of malachite green dye using biodegradable graft copolymer derived from amylopectin and poly (acrylic acid). *Carbohydrate polymers*, 111, 108-115. doi:10.1016/j.carbpol.2014.04.042

Sarsik, B., Özsan, N., & Şen, S. (2009). Renal Amiloidoz Tanısında Tioflavin T'nin Önemi. *Turkish Journal of Pathology*, 25(2).

Sassolas, A., Blum, L. J., & Leca-Bouvier, B. D. (2012). Immobilization strategies to develop enzymatic biosensors. *Biotechnology advances*, 30(3), 489-511. https://doi.org/10.1016/j.biotechadv.2011.09.003

Satar, R., & Husain, Q. (2009). Applications of Celite-adsorbed white radish (Raphanus sativus) peroxidase in batch process and continuous reactor for the degradation of

reactive dyes. *Biochemical Engineering Journal*, 46(2), 96-104. https://doi.org/10.1016/j.bej.2009.04.012

Šekuljica, N. Ž., Jovanović, J. R., Jakovetić Tanasković, S. M., Ognjanović, N. D., Gazikalović, I. V., Knežević-Jugović, Z. D., & Mijin, D. Ž. (2020). Immobilization of horseradish peroxidase onto Purolite® A109 and its anthraquinone dye biodegradation and detoxification potential. *Biotechnology Progress*, 36(4), e2991. https://doi.org/10.1002/btpr.2991

Šekuljica, N. Ž., Prlainović, N. Ž., Jovanović, J. R., Stefanović, A. B., Grbavčić, S. Ž., Mijin, D. Ž., & Knežević-Jugović, Z. D. (2016a). Immobilization of horseradish peroxidase onto kaolin by glutaraldehyde method and its application in decolorization of anthraquinone dye. *Hemijska industrija*, 70(2), 217-224. https://doi.org/10.2298/HEMIND150220028S

Šekuljica, N. Ž., Prlainović, N. Ž., Jovanović, J. R., Stefanović, A. B., Djokić, V. R., Mijin, D. Ž., & Knežević-Jugović, Z. D. (2016b). Immobilization of horseradish peroxidase onto kaolin. *Bioprocess and Biosystems Engineering*, 39(3), 461-472. https://doi.org/10.1007/s00449-015-1529-x

Shakerian, F., Zhao, J., & Li, S. P. (2020). Recent development in the application of immobilized oxidative enzymes for bioremediation of hazardous micropollutants–A review. *Chemosphere*, 239, 124716. https://doi.org/10.1016/j.chemosphere.2019.124716

Sharma, B., Dangi, A. K., & Shukla, P. (2018). Contemporary enzyme based technologies for bioremediation: a review. *Journal of environmental management*, 210, 10-22. https://doi.org/10.1016/j.jenvman.2017.12.075

Sharma, K., Sharma, P., Dhiman, S. K., Chadha, P., & Saini, H. S. (2022). Biochemical, genotoxic, histological and ultrastructural effects on liver and gills of fresh water fish Channa punctatus exposed to textile industry intermediate 2 ABS. *Chemosphere*, 287, 132103. https://doi.org/10.1016/j.chemosphere.2021.132103

Sheldon, R. A. (2007). Enzyme immobilization: the quest for optimum performance. *Advanced Synthesis & Catalysis*, 349(8-9), 1289-1307. https://doi.org/10.1002/adsc.200700082

Sim, Y. K., Jung, H., Kim, S. H., Park, J. W., Park, W. J., & Jun, C. H. (2018). A one-step method for covalent bond immobilization of biomolecules on silica operated in aqueous solution. *Chemical Science*, 9(41), 7981-7985. https://doi.org/10.1039/C8SC02565G

Sirisha, V. L., Jain, A., & Jain, A. (2016). Enzyme immobilization: an overview on methods, support material, and applications of immobilized enzymes. *Advances in food and nutrition research*, 79, 179-211. https://doi.org/10.1016/bs.afnr.2016.07.004

Song, W., Liu, Y., Qian, L., Niu, L., Xiao, L., Hou, Y., & Fan, X. (2016). Hyperbranched polymeric ionic liquid with imidazolium backbones for highly efficient removal of anionic dyes. *Chemical Engineering Journal*, 287, 482-491. https://doi.org/10.1016/j.cej.2015.11.039

Steensma, D. P. (2001). "Congo" red: out of Africa?. *Archives of pathology & laboratory medicine*, 125(2), 250-252. https://doi.org/10.5858/2001-125-0250-CR

Sun, W., Zhang, C., Chen, J., Zhang, B., Zhang, H., Zhang, Y. & Chen, L. (2017a). Accelerating biodegradation of a monoazo dye Acid Orange 7 by using its endogenous electron donors. *Journal of hazardous materials*, 324; 739-743. https://doi.org/10.1016/j.jhazmat.2016.11.052

Sun, H., Jin, X., Long, N., & Zhang, R. (2017b). Improved biodegradation of synthetic azo dye by horseradish peroxidase cross-linked on nano-composite support. *International journal of biological macromolecules*, 95, 1049-1055. https://doi.org/10.1016/j.ijbiomac.2016.10.093

Sun, H., Jin, X., Jiang, F., & Zhang, R. (2018). Immobilization of horseradish peroxidase on ZnO nanowires/macroporous SiO2 composites for the complete decolorization of anthraquinone dyes. *Biotechnology and applied biochemistry*, 65(2), 220-229. https://doi.org/10.1002/bab.1559

Sun, H., Jin, X., Long, N., & Zhang, R. (2017). Improved biodegradation of synthetic azo dye by horseradish peroxidase cross-linked on nano-composite support. *International journal of biological macromolecules*, 95, 1049-1055. http://dx.doi.org/10.1016/j.ijbiomac.2016.10.093

Swan, N. B., & Zaini, M. A. A. (2019). Adsorption of malachite green and congo red dyes from water: recent progress and future outlook. *Ecological Chemistry and Engineering*, 26(1), 119-132. DOI: 10.1515/eces-2019-0009

Tavares, T. S., da Rocha, E. P., Esteves Nogueira, F. G., Torres, J. A., Silva, M. C., Kuca, K., & Ramalho, T. C. (2020). Δ-FeOOH as support for immobilization peroxidase: optimization via a chemometric approach. *Molecules*, 25(2), 259. DOI:10.3390/molecules25020259

Tran, D. N., & Balkus Jr, K. J. (2011). Perspective of recent progress in immobilization of enzymes. *Acs Catalysis*, 1(8), 956-968. https://doi.org/10.1021/cs200124a

Ulu, A., Noma, S. A. A., Koytepe, S., & Ates, B. (2018). Magnetic Fe3O4@ MCM-41 core–shell nanoparticles functionalized with thiol silane for efficient l-asparaginase immobilization. *Artificial cells, nanomedicine, and biotechnology*, 46(sup2), 1035-1045. https://doi.org/10.1080/21691401.2018.1478422

Uludağ, Y. (2000). İmmobilize glukoamilaz ile maltodekstrinden glukoz üretimi. Gebze İleri teknoloji Üniversitesi Fen Bilimleri Enstitüsü.

Umpuch, C., & Sakaew, S. (2015). Adsorption characteristics of reactive black 5 onto chitosan-intercalated montmorillonite. *Desalination and water treatment*, 53(11), 2962-2969. doi: 10.1080/19443994.2013.867541

Urrea, D. A. M., Gimenez, A. V. F., Rodriguez, Y. E., & Contreras, E. M. (2021). Immobilization of horseradish peroxidase in Ca-alginate beads: Evaluation of the enzyme leakage on the overall removal of an azo-dye and mathematical modeling. *Process Safety and Environmental Protection*, 156, 134-143. https://doi.org/10.1016/j.psep.2021.10.006

Valderrama, B., Ayala, M., & Vazquez-Duhalt, R. (2002). Suicide inactivation of peroxidases and the challenge of engineering more robust enzymes. *Chemistry & biology*, 9(5), 555-565. https://doi.org/10.1016/S1074-5521(02)00149-7

Varamini, M., Zamani, H., Hamedani, H., Namdari, S., & Rastegari, B. (2021). Immobilization of horseradish peroxidase on lysine-functionalized gum Arabic-coated Fe3O4 nanoparticles for cholesterol determination. *Preparative Biochemistry & Biotechnology*, 1-11. https://doi.org/10.1080/10826068.2021.1992780

Veitch, N. C. (2004). Horseradish peroxidase: a modern view of a classic enzyme. *Phytochemistry*, 65(3), 249-259. https://doi.org/10.1016/j.phytochem.2003.10.022

Veitch, N. C., & Smith, A. T. (2000). Horseradish peroxidase. https://doi.org/10.1016/S0898-8838(00)51002-2

Vineh, M. B., Saboury, A. A., Poostchi, A. A., Rashidi, A. M., & Parivar, K. (2018). Stability and activity improvement of horseradish peroxidase by covalent immobilization on functionalized reduced graphene oxide and biodegradation of high phenol concentration. *International journal of biological macromolecules*, 106, 1314-1322. https://doi.org/10.1016/j.ijbiomac.2017.08.133

Vineh, M. B., Saboury, A. A., Poostchi, A. A., & Ghasemi, A. (2020). Biodegradation of phenol and dyes with horseradish peroxidase covalently immobilized on functionalized RGO-SiO2 nanocomposite. *International Journal of Biological Macromolecules*, 164, 4403-4414. https://doi.org/10.1016/j.ijbiomac.2020.09.045

Vimonses, V., Lei, S., Jin, B., Chow, C. W., & Saint, C. (2009). Kinetic study and equilibrium isotherm analysis of Congo Red adsorption by clay materials. *Chemical Engineering Journal*, 148(2-3), 354-364. DOI:10.1016/j.cej.2008.09.009

Waheed, A., Mansha, M., Kazi, I. W., & Ullah, N. (2019). Synthesis of a novel 3, 5-diacrylamidobenzoic acid based hyper-cross-linked resin for the efficient adsorption of Congo Red and Rhodamine B. *Journal of hazardous materials*, 369, 528-538. https://doi.org/10.1016/j.jhazmat.2019.02.058

Wang, Q., Wang, X., & Shi, C. (2018). LDH nanoflower lantern derived from ZIF-67 and its application for adsorptive removal of organics from water. *Industrial & Engineering Chemistry Research*, 57(37), 12478-12484. https://doi.org/10.1021/acs.iecr.8b01324

Wang, Y. J., Xu, K. Z., Ma, H., Liao, X. R., Guo, G., Tian, F., & Guan, Z. B. (2020). Recombinant horseradish peroxidase C1A immobilized on hydrogel matrix for dye decolorization and its mechanism on acid blue 129 decolorization. *Applied Biochemistry and Biotechnology*, 192(3), 861-880. https://doi.org/10.1007/s12010-020-03377-9

Wang, M., Wang, X., Guo, C., Zhao, T., & Li, W. (2020). A feasible method applied to one-bath process of wool/acrylic blended fabrics with novel heterocyclic reactive dyes and application properties of dyed textiles. *Polymers*, 12(2), 285. https://doi.org/10.3390/polym12020285

Wong, J. K. H., Tan, H. K., Lau, S. Y., Yap, P. S., & Danquah, M. K. (2019). Potential and challenges of enzyme incorporated nanotechnology in dye wastewater treatment: A review. *Journal of environmental chemical engineering*, 7(4), 103261. https://doi.org/10.1016/j.jece.2019.103261

Wu, W., He, Q., & Jiang, C. (2008). Magnetic iron oxide nanoparticles: synthesis and surface functionalization strategies. *Nanoscale research letters*, 3, 397-415. https://doi.org/10.1007/s11671-008-9174-9

Wu, X. C., Zhang, Y., Wu, C. Y., & Wu, H. X. (2012). Preparation and characterization of magnetic Fe3O4/CRGO nanocomposites for enzyme immobilization. *Transactions of Nonferrous Metals Society of China*, 22, s162-s168. https://doi.org/10.1016/S1003-6326(12)61703-8

Xu, R. K., Xiao, S. C., Yuan, J. H., & Zhao, A. Z. (2011). Adsorption of methyl violet from aqueous solutions by the biochars derived from crop residues. *Bioresource technology*, 102(22), 10293-10298. https://doi.org/10.1016/j.biortech.2011.08.089

Yakupova, E. I., Bobyleva, L. G., Vikhlyantsev, I. M., & Bobylev, A. G. (2019). Congo Red and amyloids: history and relationship. *Bioscience reports*, 39(1). https://doi.org/10.1042/BSR20181415

Zaini, M. A. A., Cher, T. Y., Zakaria, M., Kamaruddin, M. J., Mohd. Setapar, S. H., & Che Yunus, M. A. (2014). Palm oil mill effluent sludge ash as adsorbent for methylene blue dye removal. *Desalination and Water Treatment*, 52(19-21), 3654-3662. doi:10.1080/19443994.2013.854041

Zare, K., Sadegh, H., Shahryari-Ghoshekandi, R., Maazinejad, B., Ali, V., Tyagi, I., ... & Gupta, V. K. (2015). Enhanced removal of toxic Congo red dye using multi walled carbon nanotubes: kinetic, equilibrium studies and its comparison with other adsorbents. *Journal of Molecular Liquids*, 212, 266-271. https://doi.org/10.1016/j.molliq.2015.09.027

Zeng, L. X., Chen, Y. F., Zhang, Q. Y., Kang, Y., & Luo, J. W. (2014). Adsorption of Congo red by cross-linked chitosan resins. *Desalination and Water Treatment*, 52(40-42), 7733-7742. doi:10.1080/19443994.2013.833879

Zdarta, J., Meyer, A. S., Jesionowski, T., & Pinelo, M. (2018). Developments in support materials for immobilization of oxidoreductases: *A comprehensive review. Advances in colloid and interface science*, 258, 1-20. https://doi.org/10.1016/j.cis.2018.07.004

Zhang, B., Weng, Y., Xu, H., & Mao, Z. (2012). Enzyme immobilization for biodiesel production. *Applied microbiology and biotechnology*, 93, 61-70. https://doi.org/10.1007/s00253-011-3672-x

Zhu, B., Mizoguchi, T., Kojima, T., & Nakano, H. (2015). Ultra-high-throughput screening of an in vitro-synthesized horseradish peroxidase displayed on microbeads using cell sorter. *PLoS One*, 10(5), e0127479. DOI:10.1371/journal.pone.0127479

RESUME

Name Surname:	Altynay Zhumabekova
Place and Date of Birth:	Kazakhstan, Atyrau 07/03/1999
Foreign Languages:	Kazakh, English, Turkish, Rushian
High School:	Nazarbayev Intellectual School of Chemistry and Biology in Atyrau, 2016
Bachelor's:	L. N. Gumilyov Eurasian National University, 2020
Master's:	Bursa Uludag University, 2023
Work Experience:	Chemistry teacher at Nazarbayev Intellectual School of Chemistry and Biology in Atyrau
Contact (e-mail):	altynay99@mail.ru
Publications:	-